

TEMPERATURE MODELING AND CONTROL ALGORITHM FOR HIGH
VOLTAGE UNDERGROUND CABLES

by

Ansovinus Akumawah Nche

A thesis submitted to the faculty of
The University of North Carolina at Charlotte
in partial fulfillment of the requirements
for the degree of Master of Science in
Applied Energy and Electromechanical Systems

Charlotte

2017

Approved by:

Dr. Maciej Noras

Dr. Barry Sherlock

Dr. Valentina Cecchi

©2017
Ansovinus Akumawah Nche
ALL RIGHTS RESERVED

ABSTRACT

ANSOVINUS AKUMAWAH NCHE. Temperature modeling and control algorithm for high voltage underground cables. (Under the direction of Dr. Maciej Noras)

The use of underground cables in transmission and distribution of electric energy is growing. The most commonly installed is the cross-linked polyethylene known as XLPE as an insulator. The XLPE insulation has excellent dielectric properties. However, the XLPE insulator can lose properties prematurely under excessive thermal stress. XLPE cables are designed to operate at 90 °C and 105 °C for emergencies. Temperature limits the current carrying capacity of this cable. This is due to the maximum temperature of the insulating material. Beyond the maximum insulation temperatures, the XPLE insulation ages and consequently breakdown.

Thermal stress occurs in the cable is due to the copper losses from the load current and core conductor. These losses occurred in the form of heat. It can be investigated by performing a heating cycle test. The test is implemented by circling enough current through a cable to generate heat to a specific temperature value for a given period. In this thesis, a heat cycle test will be investigated and a model and an algorithm to control the load current to produce a specific conductor temperature given jacket temperature, ambient temperature, bonding, load current, and cable surrounding as inputs will be developed.

Keywords: high-voltage cable, XLPE cable, type test, load cycling, heat cycle test, ampacity.

ACKNOWLEDGMENTS

I would first like to thank my thesis advisor Dr. Noras Maciej of the Electrical Engineering Technology Department at the University of North Carolina at Charlotte. The door to Prof. Dr. Barry Sherlock office was always open whenever I had a question about my research. He consistently allowed this paper to be my work but steered me in the right the direction whenever he thought I needed it. Dr. Sharer Debora for all her technical assistance and encouragement she gave me.

I would like to extend my sincerest thanks to Dr. Sheriff Kamel and Dr. Cory Liu of Southwire for their valuable input for my thesis. Without their help, it would have been exceedingly difficult to complete my thesis.

I will also like to acknowledge Dr. Tom Zhao and Paul Knapper at Electrical Power Research Institute (EPRI) for their valuable resources.

I am also grateful to Luis, Alzarrio, Davda, and all other friends in the University. Finally, I wish to thank my parents Mr. Awah Peter and Christina Kyen, my cousin Lorrain, my friend Isidore, Raymond, and brother in law Daniel for their love and support throughout my studies. Moreover, to my sisters and brother for their love and support

Table of Contents

List of Figures	viii
List of Tables	x
List of Abbreviations	xi
CHAPTER 1: INTRODUCTION	1
1.1. Research Statement	3
1.2. The Objective	3
1.3. Research Question	3
1.4. Research Motivation	4
CHAPTER 2: XLPE CABLE	5
2.1. Structure of XLPE Cable	5
2.1.1. Conductor	6
2.1.2. Conductor Screen	7
2.1.3. Insulation	7
2.1.4. Insulation Screen	8
2.1.5. Metallic Screen	8
2.1.6. The Jacket	8
2.2. XLPE Cable Benefits and Challenges	8
2.2.1. Benefits	9
2.2.2. Challenges	9

CHAPTER 3:	AMPACITY	11
3.1.	The IEC 60287 and Nether-McGrath method.....	12
3.1.1.	Calculation of Losses	16
3.1.2.	Thermal Resistances.....	21
CHAPTER 4:	LOAD CYCLE HEAT TEST	26
4.1.	System Specifications.....	27
4.2.	Test sample specification.....	27
4.3.	Experimental setup.....	29
4.3.1.	Thermocouples Installation.....	31
4.4.	Heat cycle sample test	35
4.4.1.	Safety Requirements.....	35
4.4.2.	Test procedure.....	36
CHAPTER 5:	CABLE TESTING AND RESULTS.....	39
5.1.	Measured Results	39
5.2.	Gathering and calculation of ampacity data.....	45
5.3.	Transient Ampacity Analysis.....	52
5.4.	Modeling	56
5.5.	Model Results.....	60
5.6.	Measured vs. Model Results	64
5.6.1.	Cable temperature profile @ 1530A step-load current	64

CHAPTER 6: CONCLUSIONS	66
REFERENCES.....	67
APPENDIX A: Ampacity Calculation	69
APPENDIX B-2: ASD power Load Cycle Test System spec	75
APPENDIX C-1: Sample Cable Specification	76
APPENDIX C-2: Sample Cable Specification	77
APPENDIX D-1: Thermocouple Specification	78
APPENDIX E: Data logger Specification	79
APPENDIX F: Cable termination specification	80
APPENDIX G: 1530A at 19 hours Data	81
APPENDIX H: 2030A at 24 hours Data	83
APPENDIX I: 2030A at 1 day 2 hours Data	85
APPENDIX J: MATLAB Code	87

List of Figures

Figure 1: (a) XLPE Cable layers	6
Figure 2: (b) Conductor construction	7
Figure 3: Extruded underground Cable Thermal to Electrical equivalent circuit	13
Figure 4: Extruded underground cable electrical equivalent circuit	14
Figure 5: Sample cable looped as secondary	27
Figure 6: XLPE Cable Sample.....	28
Figure 7: Experimental Equipment components layout	30
Figure 8: Thermocouple installation location A; (a) 12 o'clock conductor drilling; (b) 6 o'clock conductor drilling	32
Figure 9: Cross-section A-A; Thermocouples installation positions	33
Figure 10: Conductor thermocouple installation.....	33
Figure 11: Jacket thermocouple installation	34
Figure 12: Complete Thermocouple installation location A.....	34
Figure 13: Cable joint temperature measurement	35
Figure 14: Load cycle heat test operator screen.....	38
Figure 15: Cable profile @ 1530A load current for 112 hours.....	40
Figure 16: Cable profile @ 2030A load current for 15 hours.....	42
Figure 17 Cable profile @ 2030A variable load current for 1 day 2 hours	43
Figure 18: Cable profile @ 1530A load current for 9 hours with insulated cable	44
Figure 19: Conductor temperature model with current as input	57

Figure 20: Insulation temperature model with current as input	57
Figure 21: Jacket temperature model with current as input	58
Figure 22: XLPE Cable model with current as input	58
Figure 23: Conductor PID temperature control	59
Figure 24: 1530A current step input response (temperature profile)	60
Figure 25: 2030A Pulse current input response	61
Figure 26: 60-degree desired conductor temperature response with PID control.....	62
Figure 27: 60-degree desired conductor temperature response with PID control and disturbance verification.	63
Figure 28: Cable temperature profile @ 1530A step-load current; (a) Measured result;(b) Model result	64
Figure 29: Cable temperature profile @ 2030A step load current; (a) Measured result;(b) Model result	65

List of Tables

Table 1: Skin and proximity effect constants EPRI Green Book [1].	20
Table 2: Duct Thermal Resistance Constants from EPRI Green Book 2007[1].....	23
Table 3: Thermal Resistivity of Common Cable Materials from EPRI Green Book 2007[1]	23
Table 4: Typical Soil Thermal Resistivity from EPRI Green Book 2007[1]	24
Table 5: Specific heat capacity and density of some common cable layers	54
Table 6: PID Controller tuned parameters	62

List of Abbreviations

$\Delta\theta$	temperature rise in the cable
W_d	dielectric losses
θ_a	ambient temperature
θ_c	conductor temperature
I	load current
R_{ac}	AC resistance of the conductor
T_1	thermal resistance of the insulation
T_2	thermal resistance of the shield/sheath
T_3	thermal resistance of the jacket
T_4	thermal resistance between cable surface and ambient
λ	Loss factor of screen
n	number of cables
$\tan\delta$	dissipation factors
U_o	voltage to earth
C	capacitance of the cable
ϵ	relative permittivity of the insulation
Di	external diameter of the insulation (excluding screen)
dc	diameter of the conductor, including screen
ρ	electrical resistivity of metal in ohm/m
R_{dc}	dc resistance at the conductor operating temperature θ (Ω/m)
y_s	skin effect factor
y_p	proximity effect factor
f	supply frequency (Hz)

k_s	skin factor constant
k_p	proximity factor constant
s	distance between conductor axes
d_c	diameter of the conductor
X_{sl}	reactance per unit length of the sheath or screen per unit length of cable
R_{sl}	resistance of the screen per unit length of cable at its maximum operating
R_{S0}	resistance of the cable screen at 20 °C [Ω/m].
θ_{sc}	cable screen operating temperature (90 °C)
ρ_i	thermal resistivity of material
D_c	diameter over conductor
T_i	insulation thickness
D_{oi}	diameter over insulation
t_3	thickness of jacket
D'_{oj}	outer diameter of the jacket
D'_{ij}	internal diameter of the jacket
h	heat transfer coefficient of air
L	Sample cable length
A	cross-sectional area of metal
$\theta_{c,(I,t)}$	conductor temperature as a function of time and load current
$\theta_{ins,(I,t)}$	insulation temperature as a function of time and load current
$\theta_{jac,(I,t)}$	jacket temperature as a function of time and load current
V_c	volume of the conductor length
C_{p_c}	specific heat of copper
ρ_c	density of copper

V_i	volume of the whole cable insulation length
C_{p_i}	specific heat of insulation
ρ_i	density of insulation
C_{p_c}	specific heat of copper
ρ_s	density of sheath material
C_{p_j}	specific heat of jacket
ρ_j	density of jacket

CHAPTER 1: INTRODUCTION

There are two main ways of transporting electrical energy. One is the overhead transmission, and the other is the underground transmission. The overhead transmission uses wires while underground uses cables. Overhead transmission wires can be noticeable from their high structures, and wire. Unlike underground transmission cable, there are buried under the ground and cannot be seen. Underground cable installations are more expensive than overhead wires. Urbanization does not like the fact of having high tower structures and high voltage wire running beside homes and businesses. Underground cables have a lower forced outage rate than overhead wire, but the outage durations are typically much longer. For these reasons, there is a high demand for underground cable projects. However, underground cable has a high dielectric loss; this loss is present any time the cable is energized, and it reduces the amount of power that can be transferred on the cable. Hence, power transfer levels for underground cable are lower than those for overhead wires. This is because the XLPE insulation has a temperature limit of 90 °C under normal load conditions.

There are four kinds of underground cables system; pipe-type cable, self-contained cable, cross-linked polyethylene or ethylene-propylene (XLPE/EPR), and gas insulated lines. Each of the cables used in these cable systems has four main parts, which are the conductor, the semiconducting shield, insulation, and the outer layers (shielding and sheath). The insulation is the one component of a cable that distinguishes the different

kinds of underground cable systems. For XLPE/EPR insulation, the insulation material is extruded over the conductor shield. More detail on XLPE cables will be coming in chapter two of this document. For impregnated paper cables, individual paper or laminated paper polypropylene (LPP) tapes are helically wrapped around the conductor. For gas cables, rigid epoxy spacers and gaseous (SF₆ or nitrogen/SF₆ mixtures) are used to provide the insulation between the tubular conductor and the tubular enclosure[1]. In this paper, the investigated sample is an XLPE. Studies have shown that XLPE insulation for high voltage and extra high voltage cables last for about forty years[1-3]. However; XLPE cable suffers from thermal and electric stresses while in use.

In most high-voltage cable designs, the operating current is lower than its rated values[4]. One of the restraining factors on the amount of current that can be transferred through a high voltage XLPE cable is the maximum operating temperature. Although there are other limiting factors, the most significant limitation is the maximum operating temperature on the dielectric. The reason is, heat energy generated at the core of the cable is transferred to the surface, and the heat around the cable also tries to move back to the core. In between the core and the surface is the XLPE insulation. Consequently, with heat generated on both sides, the cable operating temperature increases and as a result its current carrying capacity reduces. The operating temperature of XLPE cables dielectric material according to IEEE and IEC is 90 °C and 105 °C for emergency [4, 5]. Beyond these temperatures, degradation processes begin to occur on the XLPE material. Studies have shown that XLPE cable has a long-life expectancy. Unfortunately, the life expectancy can be drastically shortened due to thermal stress.

1.1. Research Statement

High voltage cables are essential components of today's energy transmission networks. They are also an important element of the electric power systems in modern cities. There are millions of miles of high voltage cables installed in the US and around the world[1], these cables are mostly XLPE. Studies have shown that long electrical life characterizes XLPE insulation for high voltage and extra high voltage cables; however, there are other insulation types been used (impregnated paper and EPR). To keep the reliability and long-life of an XLPE cable, it is critical for these cables to maintenance a low thermal and electric stress.

There are many methods of testing a cable before and after it is installed; however, these methods do not predict the age or remaining live of a cable. Since cable experiences temperature variation depending on how much current is pushed through it, the monitoring of the cable temperature can show deterioration and aging.

1.2. The Objective

The aim of this master thesis is to develop a model and an algorithm to control the load current of an underground cable to produce a specific conductor temperature given the jacket temperature, ambient temperature, bonding, load history, and cable surrounding.

1.3. Research Question

How can the load current and temperature of an underground power cable be predicted based on the jacket surface temperature, given the thermal properties of the cable and its surroundings?

1.4. Research Motivation

Due to the increase in demand and the competitive deregulated electricity market, the cable industry is being pushed to their design limit, and utilities are being forced to maximize the use of their assets (cable). According to IEEE and IEC reports[5-7], one of the common modes of high voltage unground cable failure generates from high thermal stress. Thermal stress occurs in cables due to the copper losses from load current, installation technique, bonding technique, nearby circuit, soil temperature and ambient.

Designing an underground cable network requires the understanding of its thermal and other problems. The current rating of cable depends on the, operating temperature of the conductor, the dielectric losses, sheath, bonding system and its surrounding environment. With that being said, as the cable temperature rises, thermal energy is transferred to the local environment. On the other hand, if the local environment temperature is higher than the cable; the cable will absorb heat. For this reason, the rating must, therefore, be evaluated, this evaluation balance between heat generated in the cable core and then the transfer of this heat to the local environment as well as the heat produced by the local environment to the cable core. This evaluation will determine the critical point at which the temperature limit on the cable might be exceeded. High voltage cables are rated according to some specifications; the most straightforward is the ampacity; which is the maximum continuous or the steady state AC load current that the cable conductor can carry without exceeding the specified temperature limit.

CHAPTER 2: XLPE CABLE

Cross-linked Polyethylene, also denoted as XLPE, is an insulating material that is created through both heat and high pressure. The first cross-linking methods emerged in the 1930s [1]. In general, polyethylene has some excellent electrical properties, with its low dielectric losses it is a suitable insulating material for high voltage. The construction of an XLPE cable is explained below.

2.1. Structure of XLPE Cable

A typical XLPE Cable is constructed as shown in Figure 1 (a) of a conductor either (copper or aluminum), insulated with the cross-linked polyethylene (XLPE), shield wires, and then shielded with metallic screen (corrugated and seamless aluminum or copper wires with open helix copper tape as a binder). Then it is covered with PVC or polyethylene for anticorrosion (HDPE, LLDPE, MDPE).

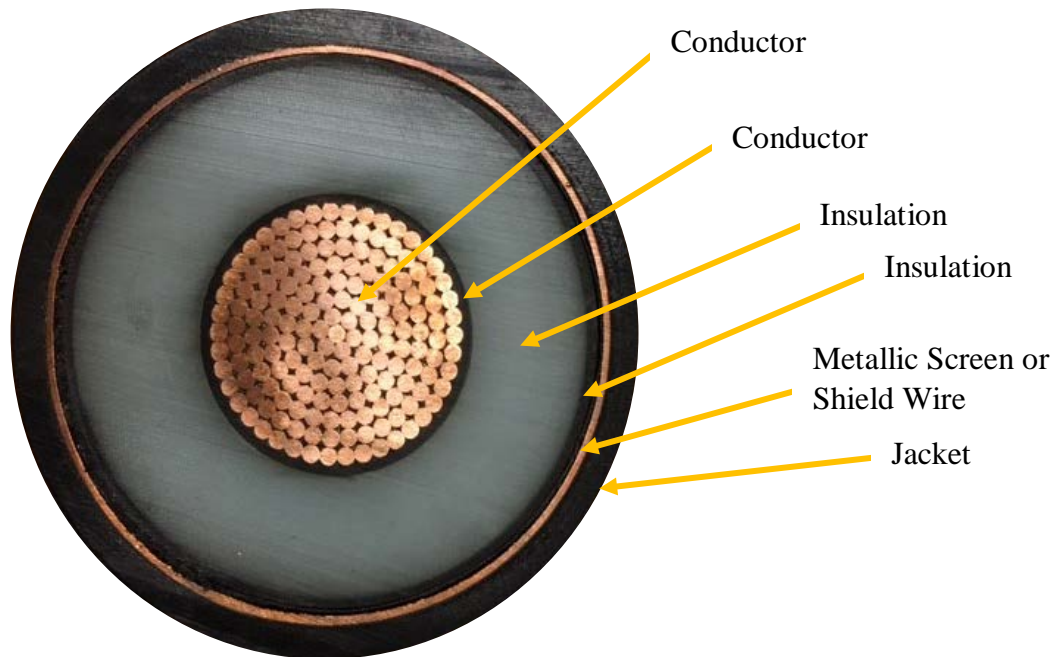


Figure 1: (a) XLPE Cable layers

2.1.1. Conductor

The conductor is the part of the cable that carries the current. It is the most important layer in the cable. This conductor consists of annealed copper or hard aluminum stranded wires; there are classified into three major types: concentric, compacted circular and segmental compacted circular see Figure 1 (b). The concentric design is when the wires are wound up concentrically; the compacted circular conductor consists of segments wound up and then compacted. Normally the segmental compacted circular conductor has four segments to prevent the increase of A.C. resistance caused by skin effect when the conductors cross-sectional is less than 630 mm^2 ; the compacted circular is applied [1].

Conductor Construction

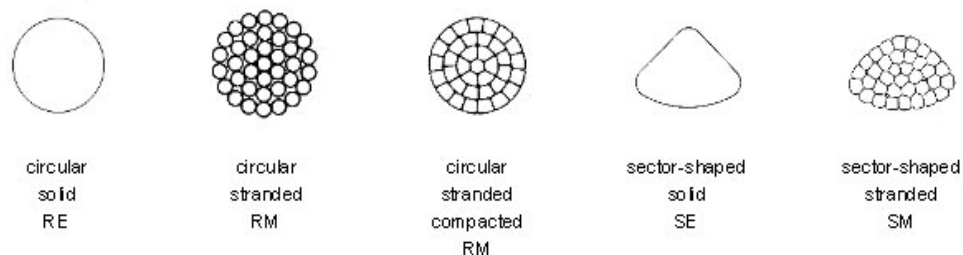


Figure 2: (b) Conductor construction

2.1.2. Conductor Screen

The conductor screen is a semiconducting polyethylene compound extruded around the conductor. This semi-conducting compound minimizes the electrical stresses in the conductor. These are due to the stranded configuration of the conductor. The semi-conducting material used for conductor screen has no deleterious effect on the conductor[1]. In some cable designs, an additional layer of a semi-conducting tape is applied as a separator between the conductor and the semiconductor.

2.1.3. Insulation

The insulation is the layer of the cable that electrically insulates and protect the conductor. The thickness of the insulation defines the maximum rated AC or DC voltage and impulse voltage of the cable. Also, the insulation should be able to withstand switching over-voltage during transients. The insulation material is an extruded cross-linked polyethylene (XLPE) produced from a polyethylene under high pressure and temperature with organic peroxides as additives. Using heat and pressure, the extrusion process is carried out under strictly controlled atmospheric conditions. The individual molecular chain to link with one another which in turn cause the material to change from a

thermoplastic to a flexible material[1]. Hence, the XLPE material will still be thermoplastic, but now it will also be polymerized and crosslinked, which gives it flexibility.

2.1.4. Insulation Screen

The insulation screen is the semi-conducting layer over the insulation. Just like the conductor, this semi-conducting compound is extruded concentrically and circularly to minimize the possibility of ionization on the outer surface of the dielectric (insulation)[5-7]. The conductor-screen, the insulation, and the insulation screen are extruded simultaneously in one process to ensure that the screen and XLPE are intimately bonded together and free from all possibilities of voids between these layers. Voids in XLPE cables causes partial discharge and eventually lead to higher voltage stress on the insulation.

2.1.5. Metallic Screen

This layer of the cable consists of shield wire, and it is the short circuit current carrying component. The metallic screen can be a copper wire with open helix copper tape as a binder or a lead alloy sheath it can also be a corrugated aluminum sheath[5-7]. The cross-sectional area of this metallic screen/shield wires is design to satisfy the phase to earth fault level in the network.

2.1.6. The Jacket

The jacket is the protective layer of the cable; it protects the metallic sheath and all other underlying layers from physical abuse, sunlight, flame, or chemical corrosion. The jacket is a nonconductive material made of PVC or PE (HDPE, LDPE, MDPE).

2.2. XLPE Cable Benefits and Challenges

2.2.1. Benefits

The benefits of an XLPE cable compared to other high voltage insulating material from EPRI green book [1] are:

The increase in the operating temperature of 70 °C for PE to 90 °C for XLPE

The increase in the emergency operating temperature (105 °C).

The increase in short circuit temperature of 250 °C.

2.2.2. Challenges

The challenges of XLPE cable are concentrated in the manufacturing process of the XLPE insulation according to the EPRI green book [1]. Some of these challenges are:

- The high crosslinking temperature increases the insulation contraction strain that acts at accessories.
- The residual core temperature at the end of the CV process locks the take-up reel curvature into the insulation. A heat straightening process is required immediately prior to the assembly of the accessories.
- The increased risk of impurities and voids in the insulation requires increased process control and sample testing.
- The crosslinking process requires a synchronized CV (continuous vulcanizing) line; this is a large machine requiring significant capital investment.
- The crosslinking process is comparatively slow and reduces factory output.
- The crosslinking process is a chemical reaction that increases dependence on high standards in material and manufacturing quality control.
- The CV tubes in VCV (vertical continuous vulcanizing) and in CCV (catenary continuous vulcanizing) lines require periodic cleaning to remove acetophenone, which condenses on the surface as fat.

- The pressure applied to the cable in the extruder and CV tube increases the risk of the melt flowing through the conductor between the wires (“fall-in”).

CHAPTER 3: AMPACITY

According to EPRI Green Book 2006[1], ampacity or current rating, of a cable is one of the most important concepts for the cable engineer to understand. Ampacity is a term given by Del Mar in 1951 to the current-carrying capacity of a cable[8]. There are two major standards (IEEE & IEC) These two standards have three standardized ampacity rating: steady state, transient (or emergency) and short-circuit. In this chapter, we will be talking about the steady state ampacity ratings. The ampacity calculation in this chapter and further sections in this paper will be based on a 1957 paper by J. H. Neher and M. H. McGrath (Neher and McGrath 1957)[9]. Also, the work by CIGRE documented an ampacity procedure in the International Electrotechnical Commission (IEC) standard (IEC-60287 and IEC- 60853), which provides a step-wise approach to calculating ampacity based upon cable construction. Both methods based their ampacity calculations on the following parameters:

- The load current and load cycle
- Conductor size, construction and material type (Copper and Aluminum)
- Dielectric loss in the insulation
- Current-dependent losses in the conductor, metallic shields (screens), sheath
- Thermal resistances of conductor, insulation, sheaths and jacket, filling medium, conduit, and the various earth layers

- Thermal capacitances of conductor, insulation, sheaths and jacket, filling medium of the thermal circuit
- Mutual-heating effects of other cables and other heat sources
- Ambient earth temperature

3.1. The IEC 60287 and Nether-McGrath method

The calculation procedures in this section follow the IEC 60287 approach, with roots in Neher-McGrath including the use of the loss factor method to account for daily load cycles. This approach based its calculation on the idea of the thermal, electrical analogy of a cable; it subdivides the cable into layers. This technique replaced the generated heat sources with the current sources, the thermal resistances with electrical resistances and the thermal capacitances with electrical capacitances. Figure 2 shows the correspondence between the cable insulation components and electrical equivalent circuit for steady state calculation.

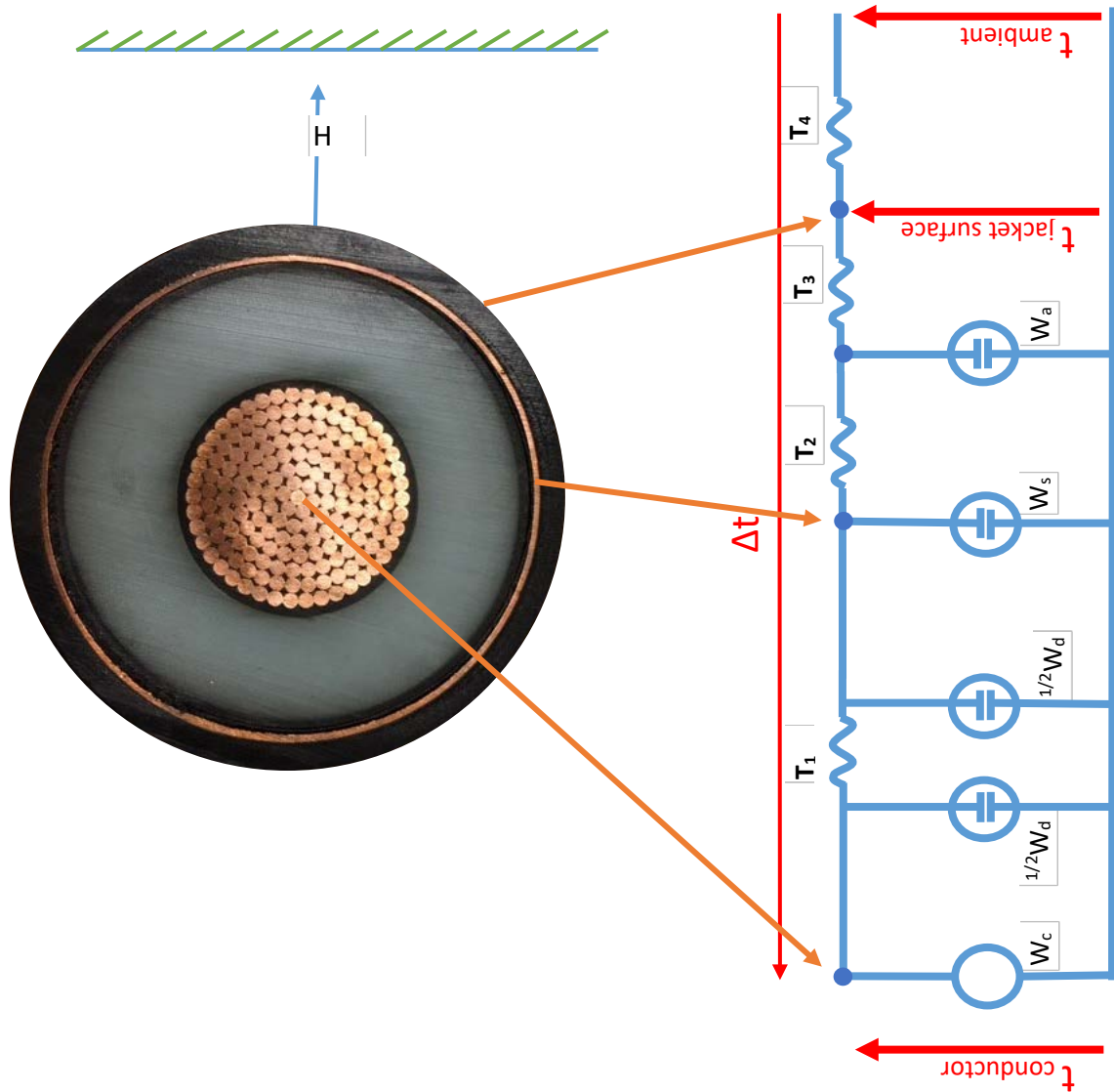


Figure 3: Extruded underground Cable Thermal to Electrical equivalent circuit

Calculation principles

The ampacity as explained above is the solution to the heat transfer problem in a cable at a rate which allows the conductor temperature to reach but not exceed the maximum allowable temperature of the insulation. The heat in a cable is generated from ohmic losses in the conductor, the shield/sheath wire, and in the other metallic layers. The “steady-state” ampacity is the rating of the cable under normal operation.

To determine the ampacity according to IEC 660287 and Neher-McGrath[9, 10], using the electric circuit in Figure 3 every node in the circuit is analog to the temperature the boundary between the layers. Hence, from the circuit, the potential difference between the terminals of the circuits and the innermost current source represents the temperature rise of the core (conductor) of the cable with respect to the ambient temperature[8]. From the circuit shown in Figure 3, the temperature of the cable's core (conductor) is the ambient temperature plus the difference in temperature between the core conductor and the surrounding.

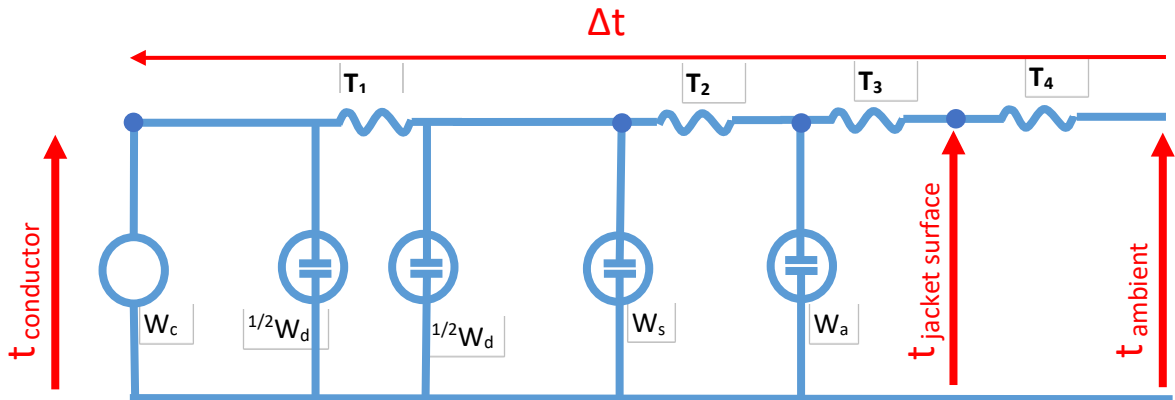


Figure 4: Extruded underground cable electrical equivalent circuit

According to IEC 660287 and Neher-McGrath[9, 10], the procedure to calculate ampacity of an underground cable is summarized as follows:

1. Select a cable construction and conductor size that are anticipated to meet the ampacity requirements for the expected installation conditions.
2. Refer to industry standards (IEC, AEIC) or manufacturer's limits for the maximum allowable conductor temperature for the cable insulation material. Determine the temperature rise over ambient earth temperature that will give this value $\Delta t =$

$$t_{conductor} - t_{ambient}.$$

3. Calculate dielectric loss.
4. Calculate the electrical resistances of each current carrying component of the system for the expected operating temperature of that component.
5. Calculate the thermal resistance of each component of the system, including the earth.
6. Calculate the temperature rise due to dielectric loss flowing through the thermal resistances, and subtract that number from the total available temperature rise.
7. Solve the Ohm's law equivalent of the core conductor, to determine the ampacity that achieves the allowable temperature rise.
8. If calculated ampacity is too high or too low, make adjustments in conductor size and installation parameters, and repeat these steps as necessary to achieve the desired ampacity.

From IEC 660287 and Neher-McGrath[9, 10], the ampacity of an underground AC cable is derived from the expression for the temperature rise of the cable conductor above ambient temperature using the circuit in Figure 3:

$$\Delta t = (W_c + .5W_d)T_1 + (W_c + W_d + W_s)nT_2 + (W_c + W_d + W_s + W_a)n(T_3 + T_4)(I)$$

$$W_c = I^2 R_{ac} \quad (2)$$

$$W_d = \omega C U_o^2 \tan \delta \quad (3)$$

$$W_s = \lambda_1 W_c \quad (4)$$

$$W_a = \lambda_2 W_c \quad (5)$$

Equation 2 to 5 in 1

$$\Delta t = (I^2 R_{ac} + .5W_d)T_1 + [I^2 R_{ac}(1 + \lambda_1) + W_d]nT_2 + [I^2 R_{ac}(1 + \lambda_1 + \lambda_2) + W_d]n(T_3 + T_4) \quad (6)$$

$$\Delta \theta = \theta_c - \theta_a$$

$$\theta_c = \Delta \theta + \theta_a$$

$$I = \sqrt{\frac{\Delta\theta - W_d[0.5T_1 + n(T_2 + T_3 + T_4)]}{R_{ac}[T_1 + n(1 + \lambda_1)T_2 + n(1 + \lambda_1 + \lambda_2)(T_3 + T_4)]}} \quad (7)$$

Where:

Δt is the temperature rise in the cable

W_d is the dielectric losses

θ_a is the ambient temperature

I is the load current

R_{ac} is the AC electrical resistance of the conductor

T_1 is the thermal resistance of the insulation

T_2 is the thermal resistance of the shield/sheath

T_3 is the thermal resistance of the jacket

T_4 is the thermal resistance between cable surface and ambient

λ is the Loss factor of screen

n is the number of cables

Note: the detail of this formula and its parameters will be explained below.

3.1.1. Calculation of Losses

Just like any other electric component with heat properties, cable is one of the electric components that has heat losses. The heat losses in the cable are due to the Ohmic (I^2R) losses and the losses in the dielectric due to charging and discharging of the cable capacitance. This section describes the losses in a cable and how it affects the ampacity at steady state.

3.1.1.1. Dielectric Losses

A high voltage power cable is known to be a large capacitor. Energy is supplied through the conductor by current flow to charge and discharge the capacitor at a power frequency of 50 or 60 Hz. Dielectric losses are generated on a per-meter basis and increase the radial heat generated in the cable, ultimately reducing typical ampacity[1]. The dielectric loss is expressed as:

$$W_d = \omega C U_o^2 \tan \delta \quad [W/m]$$

Where:

$$\omega = 2\pi f$$

$\tan \delta$ = the dissipation factor

U_o = the voltage to earth

C = the capacitance of the cable

$$C = \frac{\epsilon}{18 \ln D_i/d_c} 10^{-9} \quad [F/m] \quad (8)$$

Where:

ϵ = the relative permittivity of the insulation;

D_i = the external diameter of the insulation (excluding screen) [mm];

d_c = the diameter of conductor, including screen [mm].

3.1.1.2. AC resistance of conductor

The biggest energy losses in a power cable are the copper losses. These losses occur in the conductor and the shield wires. They are also known as ohmic (I^2R) losses. Ohmic losses arise from the flow of current through an electrical resistance, such as conductor currents and induced currents in short-circuited cable sheaths or other parallel conductors having a return path[1]. The AC resistance of cable consists of three components; DC resistance, the skin effect, and the proximity effect. The DC resistance is expressed as a function of the

cross-sectional area, length and the electrical resistivity of the material. It can be calculated per unit length of the cable based on IEC 60287-1 clause 2.1 [10] as:

$$R_{dc20} = \frac{1.02 \times 10^6 \times \rho_{20}}{A} [1 + \alpha_{20}(\theta - 20)] \quad [\Omega/m] \quad (9)$$

Where:

ρ = electrical resistivity of metal in ohm/m at 20°C

For copper conductors, = 1.7241×10^{-8}

For aluminum conductors, = 2.8264×10^{-8}

A = cross-sectional area of metal in mm²

α_{20} = the temperature coefficient of the conductor material per K at 20°C.

For copper conductors, = 3.93×10^3

For aluminum conductors, = 4.03×10^3

Θ = the conductor operating temperature (°C)

3.1.1.2.1. AC Skin (y_s) and Proximity (y_p) Effects

There is an unequal current distribution in an AC current carrying conductor; this is due to the magnetic field induced by the flow of electrical current. As a result, losses in the conductor are affected by self and mutual inductance[1]. The self-inductance causes the current to concentrate near the conductor surface, and the result is called “conductor skin effect.” The magnetic field of neighboring conductors affects the distribution of current across the conductor called “conductor proximity effect”[1].

The AC resistance of a power cable is defined as:

$$R_{ac} = R_{DC}(1 + y_s + y_p) \quad (10)$$

Where:

R_{dc} = the DC resistance at the conductor operating temperature θ (Ω/m)

y_s = the skin effect factor

y_p = the proximity effect factor

The skin effect factor is computed as:

$$y_s = \frac{x_s^4}{192+0.8 \times x_s^4} \quad (11)$$

Where:

$$x_s = \sqrt{\left(\frac{8\pi f}{R_{dc}} 10^{-7} \cdot k_s\right)} \quad (12)$$

R_{dc} = the DC resistance at the conductor operating temperature θ (Ω / m)

f = the supply frequency (Hz)

k_s = a constant (see Table 1 below)

Note equation 11 above is only accurate provided $x_s \leq 2.8$

The proximity effect factor of a cable varies depending on the conductor geometry. In a case where the conductor is round, the proximity effect factor is.

$$y_s = \frac{x_p^4}{192+0.8 \times x_p^4} \left(\frac{d_c}{s}\right)^2 \times 2.9 \quad (13)$$

Where:

$$x_p = \sqrt{\left(\frac{8\pi f}{R_{dc}} 10^{-7} \cdot k_p\right)} \quad (14)$$

R_{dc} = the dc resistance at the conductor operating temperature θ (Ω / m)

f = the supply frequency (Hz)

k_p = a constant (see Table 1 below)

s = the distance between conductor axes (mm)

d_c = the diameter of the conductor (mm)

Note equation 13 above is only accurate provided when $x_p \leq 2.8$

Table 1: Skin and proximity effect constants EPRI Green Book [1].

Type of conductor	Dried and impregnated?	K_s	K_p
Copper			
Round, stranded	Yes	1	0.8
Round, stranded	No	1	1
Round, 4 segmental	-	0.435	0.37
Sector-shaped	Yes	1	0.8
Sector-shaped	No	1	1
Aluminum			
Round, stranded	Either	1	1
Round, 4 segment	Either	0.28	0.37
Round, 5 segment	Either	0.19	0.37
Round, 6 segment	Either	0.12	0.37

3.1.1.3. Loss factor for the screen (λ)

The loss factor for the screen according to IEC 60287-1-1 section 2.2 is defined as (λ_1), this loss consists of the circulating current (λ_1') and eddy current (λ_1'')[10].

$$\lambda_1 = \lambda_1' + \lambda_1'' \quad (15)$$

Where:

$$\lambda_1' = \frac{R_{sl}}{R_{ac}} \frac{1}{1 + \left(\frac{R_{sl}}{X_{sl}}\right)^2} \quad (16)$$

$$X_{sl} = 2\omega \cdot 10^{-7} \ln \frac{2s}{d} \quad (17)$$

Where:

X_{sl} = the reactance per unit length of the sheath or screen per unit length of cable [Ω/m]

$$\omega = 2\pi f \text{ [rad/s]}$$

s = the distance between conductor axes in the electrical section being considered [mm]

d = the mean diameter of the sheath [mm]

$\lambda_1'' = 0$. The eddy-current loss is ignored according to IEC 60287-1-1 section 2.3.1 [10]

R_{sl} is the resistance of the screen per unit length of cable at its maximum operating temperature [Ω/m].

$$R_{sl} = R_{s0} [1 + \alpha_{20}(\theta_{sc} - 20)] \quad [\Omega/m] \quad (18)$$

Where:

R_{s0} is the resistance of the cable screen at 20 °C [Ω/m].

θ_{sc} = the cable screen operating temperature (°C)

3.1.2. Thermal Resistances

Thermal resistance is a heat property of mediums that limit the transfer of heat. The thermal resistance for the different layers of the cable is expressed as follow.

3.1.2.1. Thermal resistance of the insulator

The thermal resistance of the insulator is the thermal resistance between the conductor and the sheath. According to IEC 60287-2-1[10], this resistance is express as

$$T_1 = 0.00522\rho_i G \quad \text{or} \quad T_1 = \frac{\rho_i}{2\pi} \ln\left(\frac{D_{oi}}{D_c}\right) \quad \left[\frac{^\circ C}{W} \right] \quad (19)$$

And,

$$G = \ln(D_c + 3T_i) - 0.86 \ln(D_c) + 0.05 \quad (20)$$

Where:

G = the geometric factor according to IEC 60287

ρ_i = the thermal resistivity of insulation [$K.m/W$]

D_c = the diameter over conductor [mm]

T_i = the insulation thickness [mm]

D_{oi} = the diameter over insulation [mm]

3.1.2.2. Thermal resistance of the sheath T_2

The power cable in this investigation did not contain an armour. However, it did have a sheath. From EPRI green book 2007 [1], studies have shown that metallic shields and sheaths, steel casings and pipes, and metallic conduits have negligible thermal resistances. Therefore, the thermal resistance of the metallic shield and sheaths is considered to be zero in the experiment.

$$T_2 = 0 \quad \left[\frac{^{\circ}C}{W} \right] \quad (21)$$

3.1.2.3. Thermal resistance of the jacket T_3

The thermal resistance of the jacket is the resistance between the sheath and the cable surface.

$$T_3 = \frac{\rho_J}{2\pi} \ln \left(1 + \frac{2t_3}{D'_{ij}} \right) \quad \text{or} \quad T_3 = \frac{\rho_J}{2\pi} \ln \left(\frac{D'_{oj}}{D'_{ij}} \right) \quad \left[\frac{^{\circ}C}{W} \right] \quad (22)$$

Where:

ρ_J = the thermal resistivity of jacket material [$K.m/W$]

t_3 = the thickness of jacket [mm]

D'_{oj} = the outer diameter of the jacket [mm]

D'_{ij} = the internal diameter of the jacket [mm]

3.1.2.4. Thermal resistance of the surrounding T_4

The thermal resistance of a cable surrounding depends on where the cable is installed. If the cable is installed in a duct system, the thermal resistance of the surrounding consists of three parts. T'_4 , the thermal resistance of the air space between the cable surface and the duct's internal surface; T''_4 ; the thermal resistance of the duct itself; and T'''_4 ; the external thermal resistance of the duct.

$$T_4 = T'_4 + T''_4 + T'''_4 \quad (23)$$

3.1.2.4.1. Thermal resistance between cable surface and duct inner surface T'_4

$$T'_4 = \frac{U}{1+0.1(V+Y\theta_m)D_e} \quad [^{\circ}\text{C}\cdot\text{m}/\text{W}] \quad (24)$$

Where:

D_e = the external diameter of the cable [mm]

θ_m = the mean temperature of the medium filling the space between cable and duct (air, or nitrogen gas, or dielectric liquid). An assumed value should be used initially and the calculation repeated with a modified value if necessary [$^{\circ}\text{C}$]

U, V, and Y as defined in Table 2.

Table 2: Duct Thermal Resistance Constants from EPRI Green Book 2007[1]

Configuration	U	V	Y
Fiber Duct (PVC or PE) in Concrete	5.2	0.91	0.010
Asbestos Cement in Concrete	5.2	1.1	0.011
Earthenware Ducts	1.87	0.28	0.0036

Table 3: Thermal Resistivity of Common Cable Materials from EPRI Green Book 2007[1]

Material	Range($^{\circ}\text{C}\cdot\text{m}/\text{W}$)	Typical ($^{\circ}\text{C}\cdot\text{m}/\text{W}$)
XLPE	3.5-4.0	3.5
EPR	4.5-5.0	4.5
PVC	4.0-4.5	4.0

3.1.2.4.2. Thermal resistance of the duct T''_4

$$T''_4 = \frac{\rho_T}{2\pi} \ln \left(1 + \frac{D_o}{D_d} \right) \quad (25)$$

Where:

D_o = the outside diameter of the duct [mm]

D_d = the inside diameter of the duct [mm]

ρ_T = the thermal resistivity of duct material [$^{\circ}\text{Cm/W}$]

3.1.2.4.3. The external thermal resistance of the duct

$$T'''_4 = \frac{\rho_T}{2\pi} \ln \left(\frac{4H}{D_o} \right) \quad (26)$$

Where:

ρ_T = the thermal resistivity of the soil see table 4 [$^{\circ}\text{Cm/W}$]

D_o = the outside diameter of the duct [mm]

H = the placement depth [mm]

Table 4: Typical Soil Thermal Resistivity from EPRI Green Book 2007[1]

Soil Type	Thermal Resistivity	
	5% Moisture ($^{\circ}\text{Cm/W}$)	0% Moisture ($^{\circ}\text{Cm/W}$)
Fluidized Thermal Backfill	0.4	0.75
Concrete	0.6	0.8
Stone Screenings	0.4	1.0
Thermal Sand	0.5	1.0
Uniform Sand	0.7	2.0
Clay	1.0	2.5
Lake Bottom	1.0 (50% moisture)	>3.0
Seabed (typical)	0.7 (100% moisture)	>3.0
Highly Organic Soil	>3.0	>6.0

In this investigation, the cable was in the air with a length of 15.25m. The thermal resistance of air in natural or free convection is:

$$T_{air} = \frac{1}{h \times A_{air}} \quad [^{\circ}\text{C}/\text{W}]$$

h = heat transfer coefficient of air [10 w/m²°C]

L = Sample cable length 15.25m

$$A_{air} = \frac{L^2}{4\pi}$$

CHAPTER 4: LOAD CYCLE HEAT TEST

Load cycle heat test is a test designed to raise and control the temperature of a closed loop solid dielectric cable and other closed loop electrical conductor. The load cycle heat test aims to simulate the current loading conditions in an electrical circuit (Cable). The heating in this kind of test is achieved by using the test loop as the secondary winding of a current transformer. The secondary loop of the current transformer should have a low inductive resistance. In a power cable heat test, the cable is used as a secondary loop of the current transformer as shown in Figure 4 below. A small current is passed through the primary winding of the current transformer, and the current is induced to the secondary of the transformer which is the test object. Since the ratio of the secondary is one, a higher current then flows through the cable and generates energy in the form of I^2R . See Equation 2 in section 3.1.2 about ohmic losses.

The current transformers shown in Figure 4 below operate on a low voltage but high current. Typically load cycle heat test require the test sample to have a high voltage applied to it simultaneously with the heating current. If a high voltage is applied to the test sample during the test cycle, the high voltage will prevent the direct measurement of the conductor temperature during the test.



Figure 5: Sample cable looped as secondary

4.1. System Specifications

The test equipment used in this investigation was manufactured by Automation System & Diagnostics (ASD). The equipment is designed to raise and control current induced in a loop of a sample cable or any other conductor sample. This test equipment is an automated PC-based Load Cycle Test System. The specifications of the ASD power load cycle test system are:

- Primary Winding: 480 VAC, 1 PH, 60 Hz
- Secondary Winding: 12 VAC, 4000 Amps, one turn
- Current transformer window is 10" x 10"
- Two current transformers installed on a platform with caster wheels
- Transformer platform dimensions are 16" x 24" and can be wheeled around or forklift/crane lifetable.

More detail on the ASD cable test system can be found in Appendix B

4.2. Test sample specification

The sample cable is an XLPE cable manufactured by ABB Huntersville plant acquired by Southwire in 2015 and continued with the manufacturing of cables. The XLPE cable was delivered on a cable drum, and a 50ft sample was cut from the drum. Figure 5 shows the XLPE cable drum and the 50ft sample on the floor.



Figure 6: XLPE Cable Sample.

The cable sample shown in Figure 5 is 138 kV XLPE power cable with copper conductor. It has a transitional wall of 850 MIL XLPE copper neutrals with Copper Composite Laminate Sheath. The jacket is Polyethylene with Extruded Semi-Conductive Outer Layer[[11](#), [12](#)].

- Nominal voltage 138 kV
- Max. voltage 145 kV

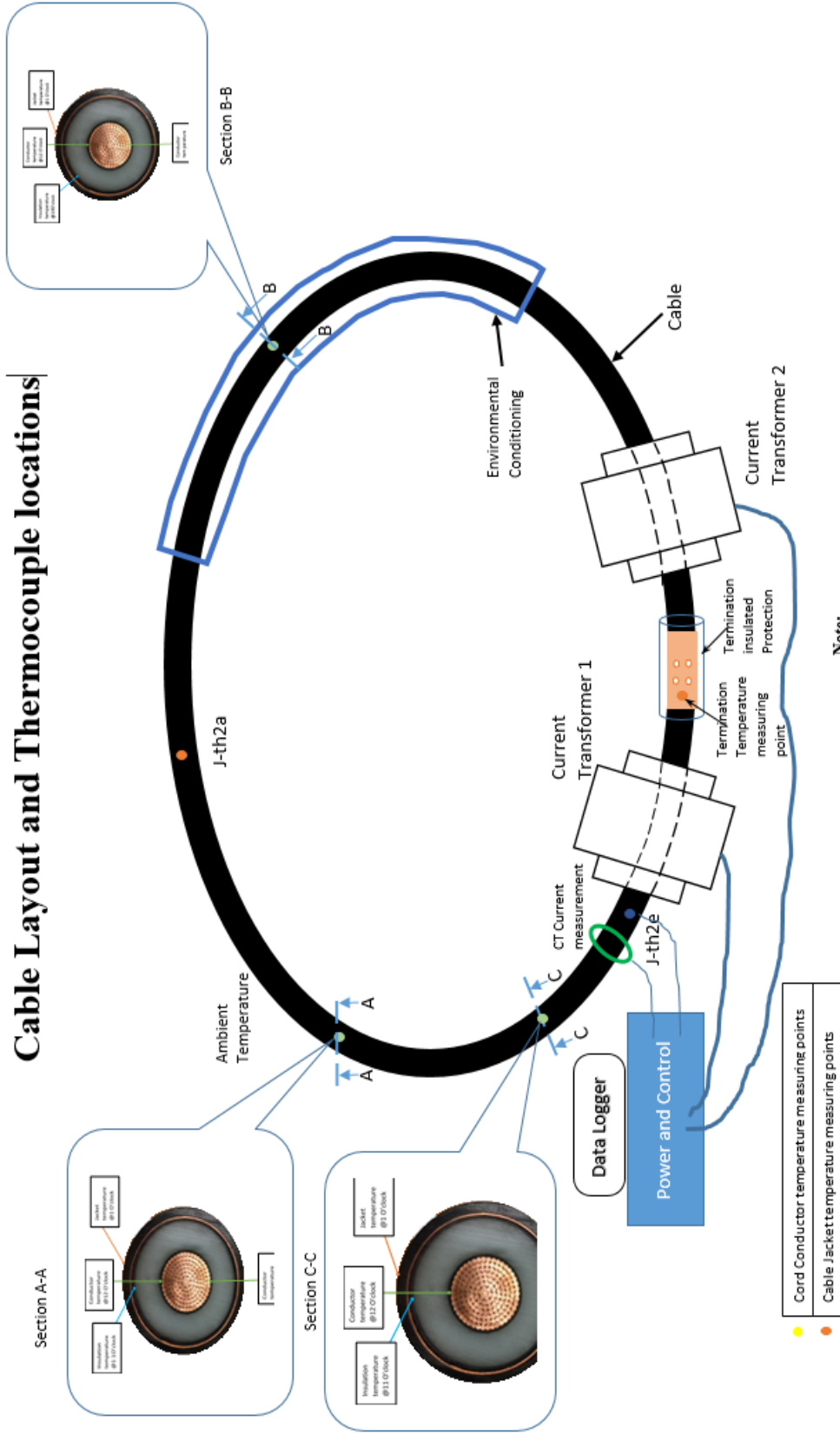
- Relative permittivity 2.3
- XLPE loss factor 0.05%
- Cable length 15.25 m
- Conductor size 1000 mm²
- Conductor diameter 40.9 mm
- Insulation thickness 15.011 mm
- Diameter over insulation 86.4 mm
- Cross-section of shield 180 kcmil
- Diameter over sheath 96.2 mm
- Overall jacket dia. 104.3 mm
- Capacitance 56.3 pF/ft

The complete specification of the cable can be found in Appendix C. The test sample was installed in the EPIC Flex power lab.

4.3. Experimental setup

The setup for this experiment was prepared following all the safety requirements for a high current and temperature test assemblies. The current transformers, measuring components were installed following the layout is shown in Figure 6 below.

Cable Layout and Thermocouple locations



Note:
 Thermocouples installed on top the cable jacket: J-th2a and J-th2e.
 The thermocouple sensors used in the system are K type (-50°C to 200°C)
 Data logger: 8 input, 24-bit resolution (USB TC)

The environmental Conditioning allows us to change the temperature around the cable jacket for that section of the cable. This allows us to mimic the different climate and temperature around the cable in the different seasons or period of the year.

Figure 7: Experimental Equipment components layout

The layout in Figure 6 shows the positions and locations of the different component and measuring equipment use in this experiment. The components and measuring equipment on this layout are the sample test cable, an ASD power loads cycle test system, a data logger (USB-TC), and thermocouples (TP-01).

The specification of the sample cable is listed above in section 4.1.1. The 50 feet sample cable is connected as a loop through two current transformers of the ASD power load cycle test system. The data logger is an eight input, 24-bit resolution logger (USB-TC). It means the data logger can measure eight temperature inputs and store the data. A brief detail of the logger will be explained later in the report, and the specification is in Appendix E. The thermocouple used in the experiment is the K type with a temperature range $-40\text{ }^{\circ}\text{C}$ to $250\text{ }^{\circ}\text{C}$. The set-up had a total of 19 thermocouples connected in locations shown in Figure 6. The locations were chosen to have the acquired result. The temperature was the key data for this investigation, so the installation is critical to the experiment. The locations and installation of the thermocouples will be explained in section 4.3.1 below.

4.3.1. Thermocouples Installation

The test cable sample in Figure 6 and 7 has 19 K-type thermocouples which were installed in 9 different locations. The thermocouple placement was chosen to obtain the acquired results and to get the temperature changes in the test sample and its various layers. As shown in Figure 6, a total of 19 thermocouples used for temperature measurement, one was used to measure the ambient temperature, and the others were used to measure the temperature of the sample cable. The thermocouples on the cable sample were installed in four different locations, three of the locations namely A, B, and C were used to measure the temperature of the conductor, insulation, and jacket to see if there is any significant

variation in temperature. This includes installing thermocouples both at the top and bottom of the cable sample. Figure 7 (a) shows top drilling of the cable sample at location A, and Figure 7 (b) shows bottom drilling. The depth of the drilling was all the way to the conductor. Another hole was drilled to the depth of the insulation to measure the insulation temperature.

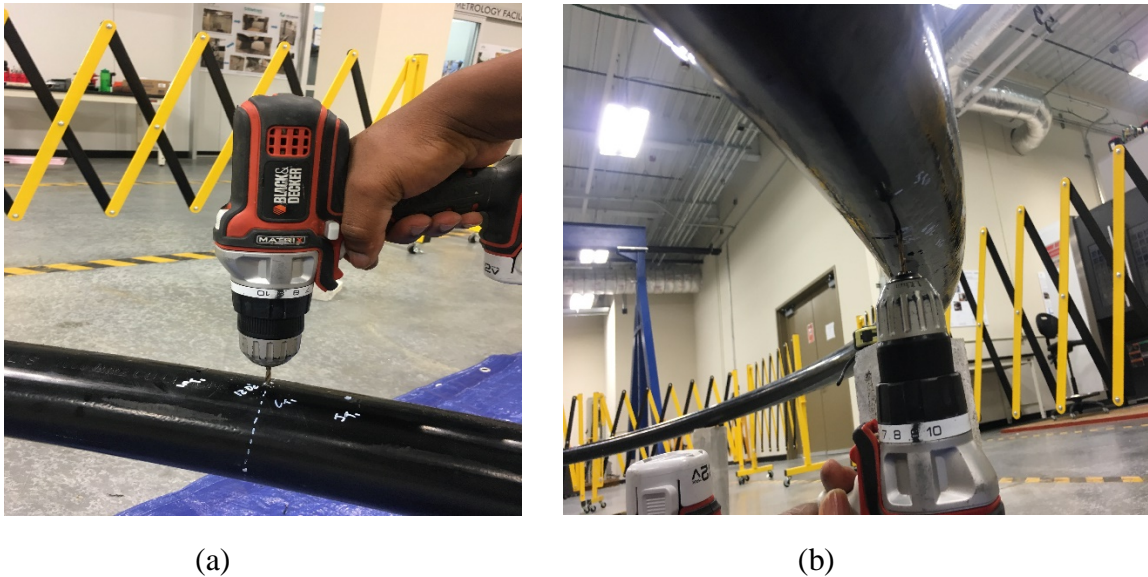


Figure 8: Thermocouple installation location A; (a) 12 o'clock conductor drilling; (b) 6 o'clock conductor drilling

After all the drilling at the different location had been completed, insertion was made with 2 mm drill bit. Figure 8 shows the cross-section A-A of location A. to measure the conductor temperature thermocouples were inserted into the cable so that it contacts conducting part and a high-temperature silicon sealant was used to secured in position. See Figure 9. For measuring the surface, temperature thermocouple was placed on the cable surface and was seal with high-temperature silicone and tape. See Figure 10, and Figure 11 show the complete installation of Section A

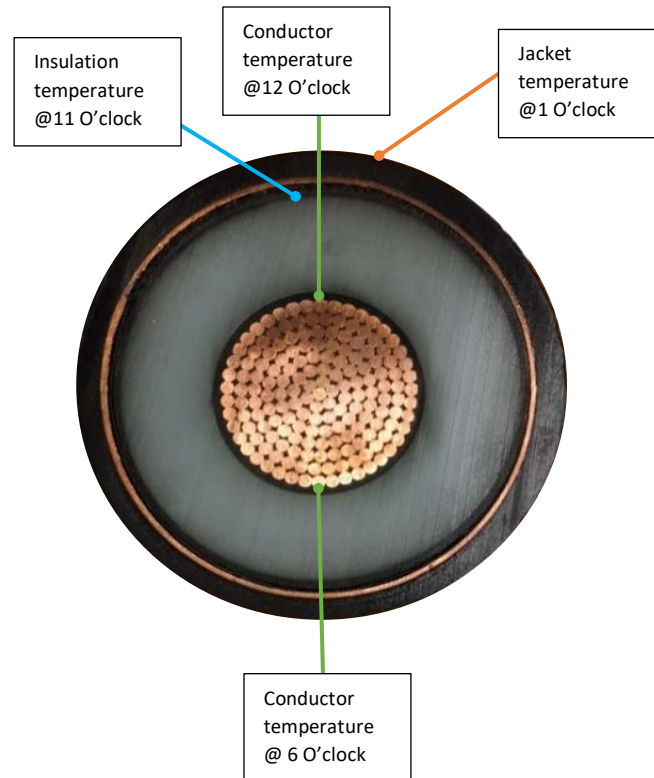


Figure 9: Cross-section A-A; Thermocouples installation positions



Figure 10: Conductor thermocouple installation

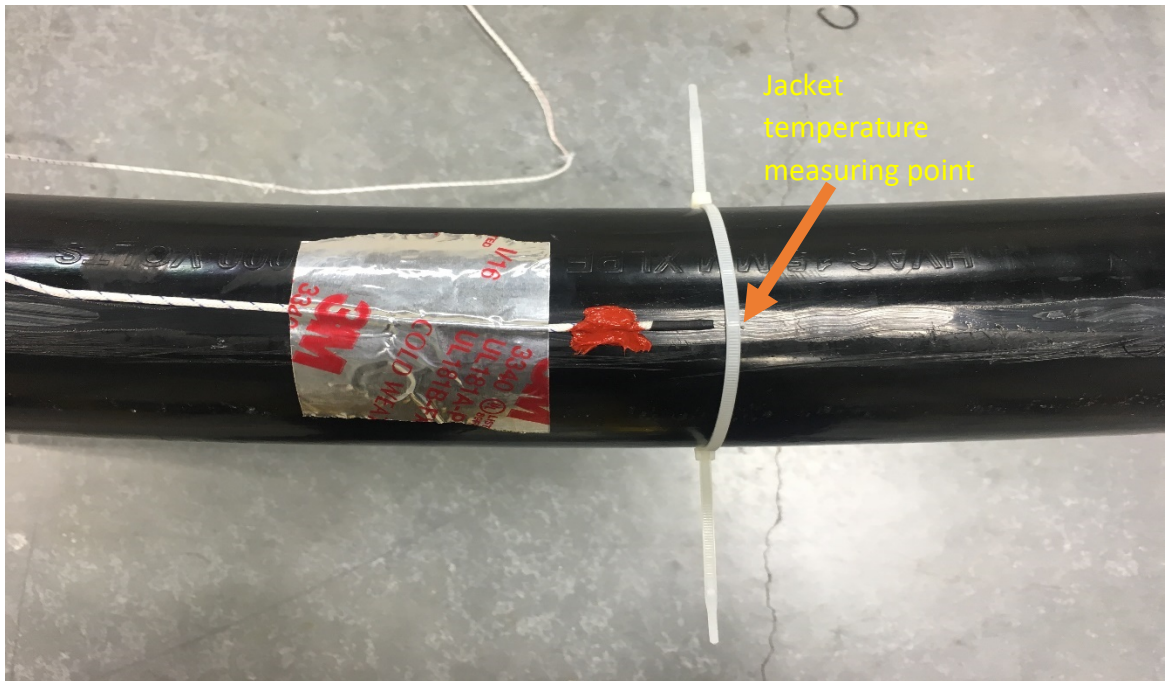


Figure 11: Jacket thermocouple installation

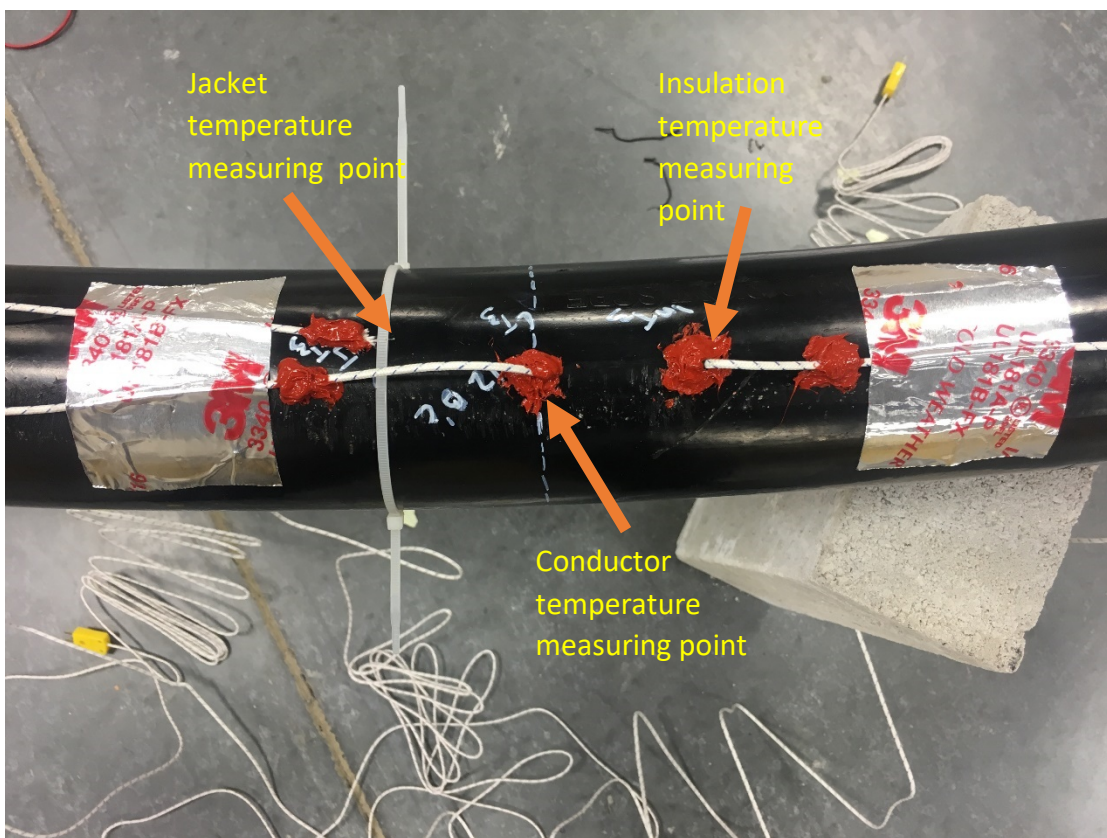


Figure 12: Complete Thermocouple installation location A

The same installation and measuring points were done in locations B and C as shown in Figure 11. The temperature at the cable joint was measured, and Figure 12 show the measuring point. The joint was made of two cable terminations, the specification of these terminations can be found in Appendix F

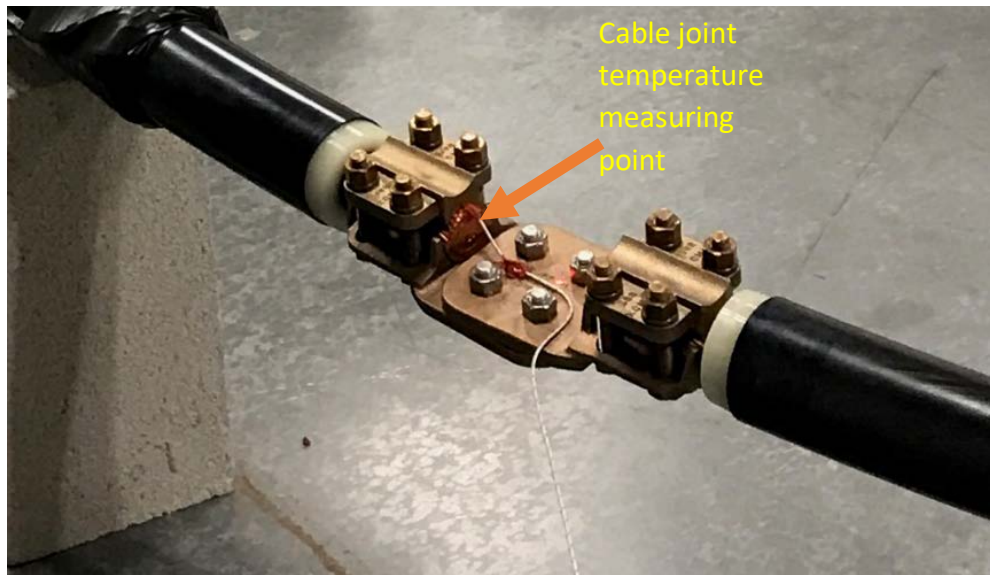


Figure 13: Cable joint temperature measurement

After installation, all the thermocouples were tested to make sure it is functioning properly and accurately. The cable sample was then tested; the detail is explained in the next section.

4.4. Heat cycle sample test

4.4.1. Safety Requirements

As it is known safety is the first thing in a high current/ voltage lab. Considering the level of current involved in this test setup, it is, therefore, necessary to comply with the safety requirements of the lab. The safety measures for the load cycle heat test are:

1. At least two people should be present at this lab at all time.

2. Test setup and all test equipment shall be clearly marked with warning signs to prevent unauthorized personnel from entering test area.
3. There shall be indicator lights displaying the operational status of the test equipment. Red color indicating the test circuit is active and green indicating test circuit is inactive. This light should be visible at any location in the lab.
4. The test installations controls and test circuits shall be clearly marked.
5. Entrances shall be provided with a warning sign “No unauthorized persons beyond this point.” The setup shall have an interlock in case an unauthorized person find themselves close to the marked area.
6. An emergency switch-off facility shall be provided both inside and outside the test area to cut-off the electricity in case a situation arises that could compromise the safety of personnel or cause damage to testing equipment.
7. There should be means provided to prevent unauthorized turning on of the test circuit.
8. There shall also be interlocks to prevent automatic energization of the test circuit when the mains power is resumed after a power failure.

4.4.2. Test procedure

After making sure the safety requirements are in place, the general requirement for operation of test station should be implemented

1. The operation of the test equipment should only be performed a person who was trained on the equipment’s use.
2. Operating manual of the test devices should be provided to the operator. This should contain adequate information on how to conduct the test safely.

3. The test installations used shall be inspected prior to the operation.
4. An authorized person shall inspect all the safety devices at suitable intervals of time and record all these inspections shall be maintained.
5. Only authorized and trained persons may work with test installations.
6. All personnel involved shall be instructed in the safety requirements, safety rules and school instructions applicable for their work.
7. A written record of the training provided to the operators should be maintained
8. Test areas should only be entered by authorized personnel and any other persons who have received adequate safety training.

From the safety requirements and the current level of this setup, the operator station is located outside the test area. The system is remotely operated using a laptop. Figure 13 shows the operator screen

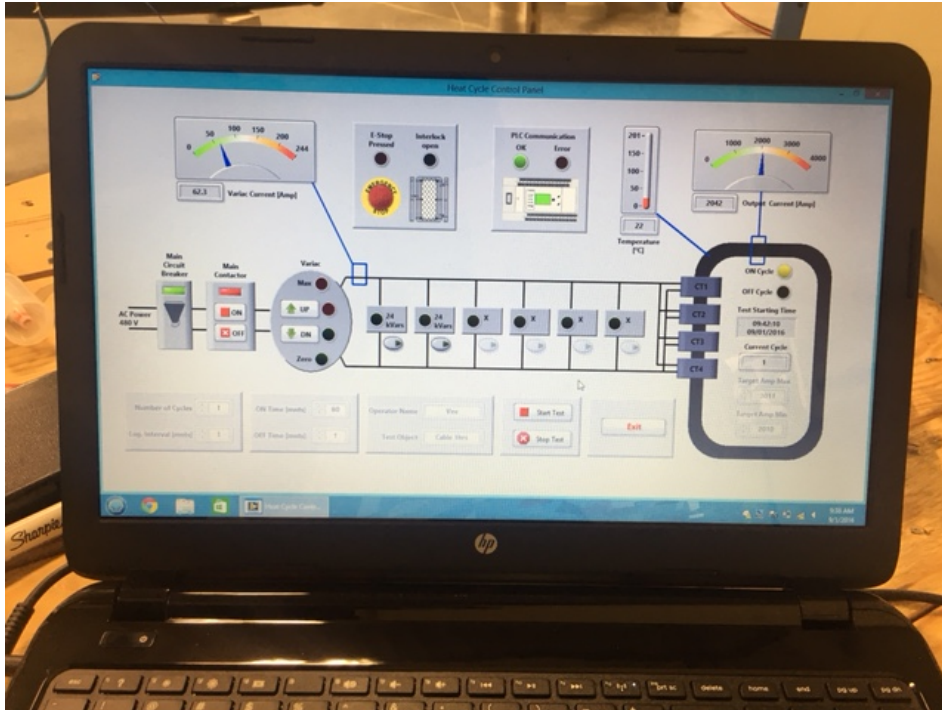


Figure 14: Load cycle heat test operator screen

Heat cycle test takes an extended period, for this reason, it is mostly run unsupervised. The test area shall be barricaded. These barriers shall have wheelable around the test area, and they shall also have lifting hooks. Emergency doors, gates shall be able to be opened from the inside of the test area.

CHAPTER 5: CABLE TESTING AND RESULTS

In this chapter, the ampacity according to IEC 60287[8] will be calculated, and the results are compared with the measured results. From the measured and calculated values, a model will be designed to predict the conductor temperature given a load current and cable location. Also, the model will be able to predict the load current from the desired conductor temperature. The calculations for this experiment were performed taking into consideration the cable was installed in the air, and other calculations were done with the cable insulated in an insulated duct and an icy environment around a section of the cable. The environmental conditioning section shown in Figure 6 is used to simulate the cable surrounding conditions

5.1. Measured Results

The measured result of the first experiment was performed with a load current at approximately 1530A for a duration of 19 hours. The sample cable was placed in air, the data collected from the data logger are shown in Appendix G, and the graph in Figure 14 shows the results.

The result in Figure 14 represents the data collected at measuring point A on the cable sample. The light blue curve represents the conductor temperature; gray, the insulation temperature; yellow, the jacket temperature; orange, the load current; and blue, the ambient temperature. The current was on for approx. 11.5 hours and was turned off for 7.5 hours. The conductor, insulation, and jacket temperature rose and became steady after eight hours of running at about 58.6, 45.2, and 41. °C respectively.

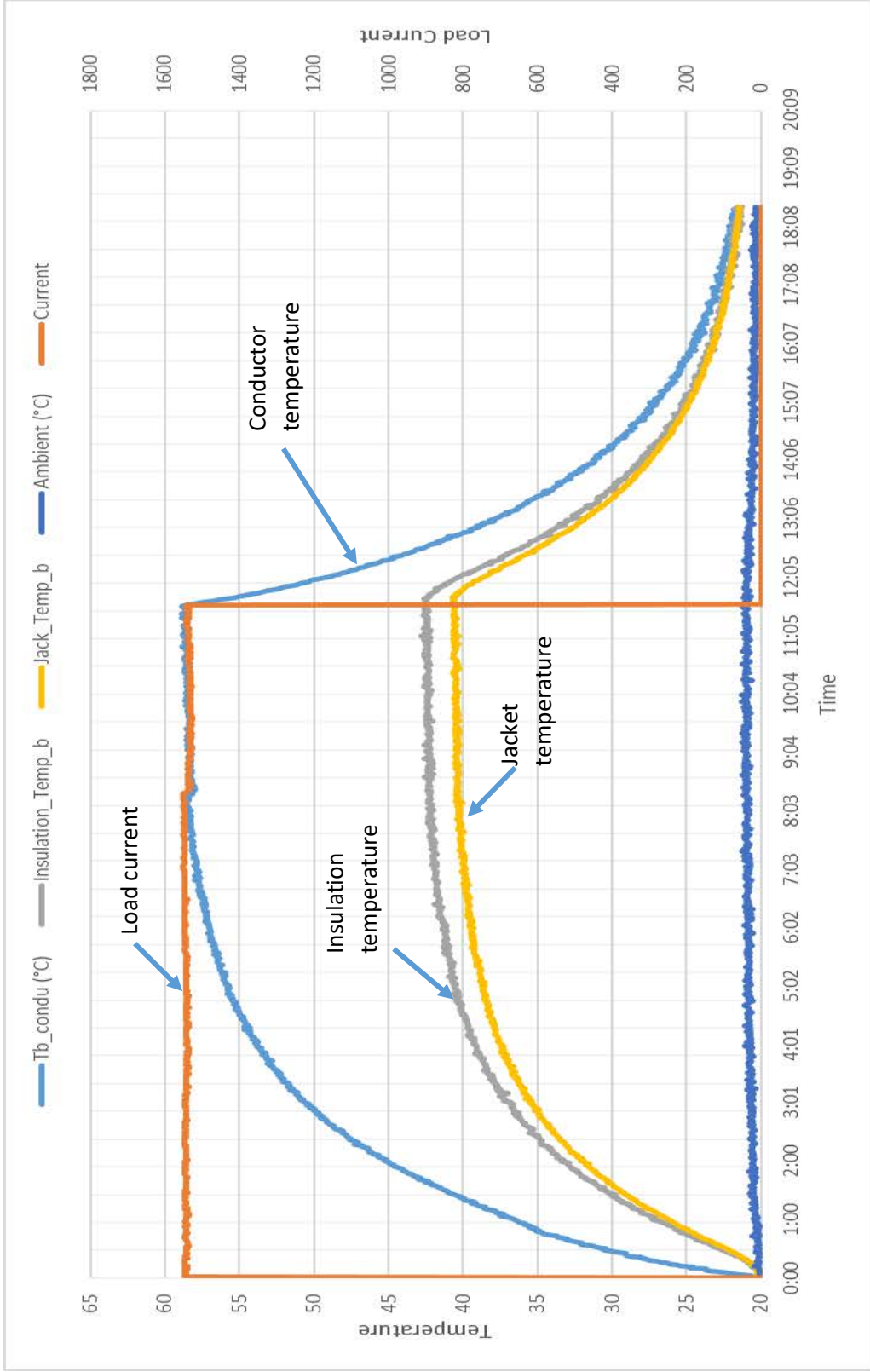


Figure 15: Cable profile @ 1530A load current for 112 hours

The second experiment was carried out with a load current of, 2030 A for 24 hours. The collected result is shown in Figure 15 and logs data in Appendix H. From the results in Figure 15; the current was turned on for 15 hours and off for 9 hours. The following temperature reading was obtained from the conductor, insulation, jacket, and ambient at point B. The blue curve represents the load current; light blue represents the conductor temperature; orange, the insulation; gray, the jacket; and yellow, the ambient temperature. The conductor temperature reaches 90.5 °C at 13 hours while the insulation, jacket, and ambient are at 58.6, 54.9, and 20.9 degrees respectively. The cable took 9 hours after the current was cut off to cool down to ambient temperature.

A third test was done with a variable load current of 2030A for three cycles. For each cycle, the current was on for four hours and was off for next four hours. The curves in Figure 16 show the results and the data are in Appendix I.

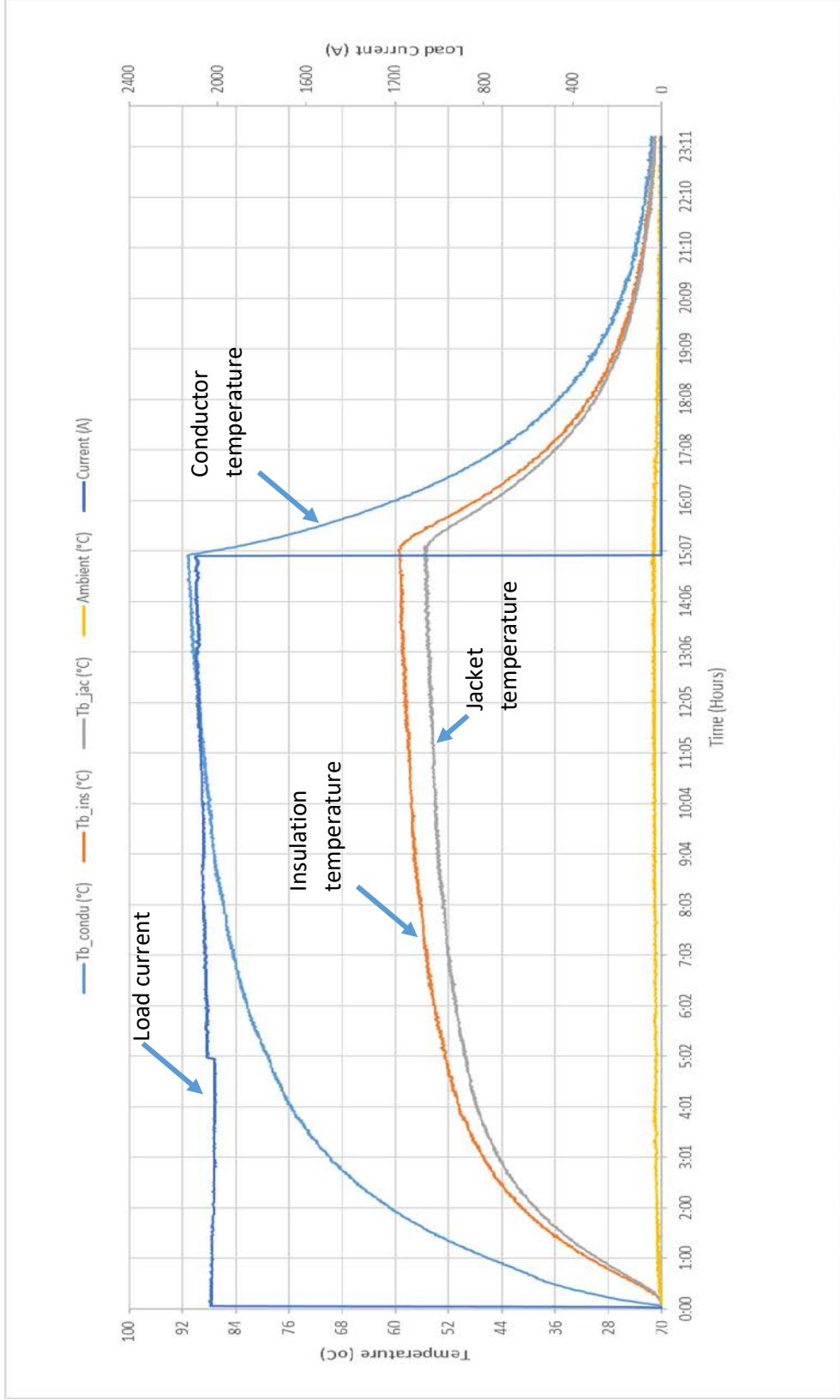


Figure 16: Cable profile @ 2030A load current for 15 hours

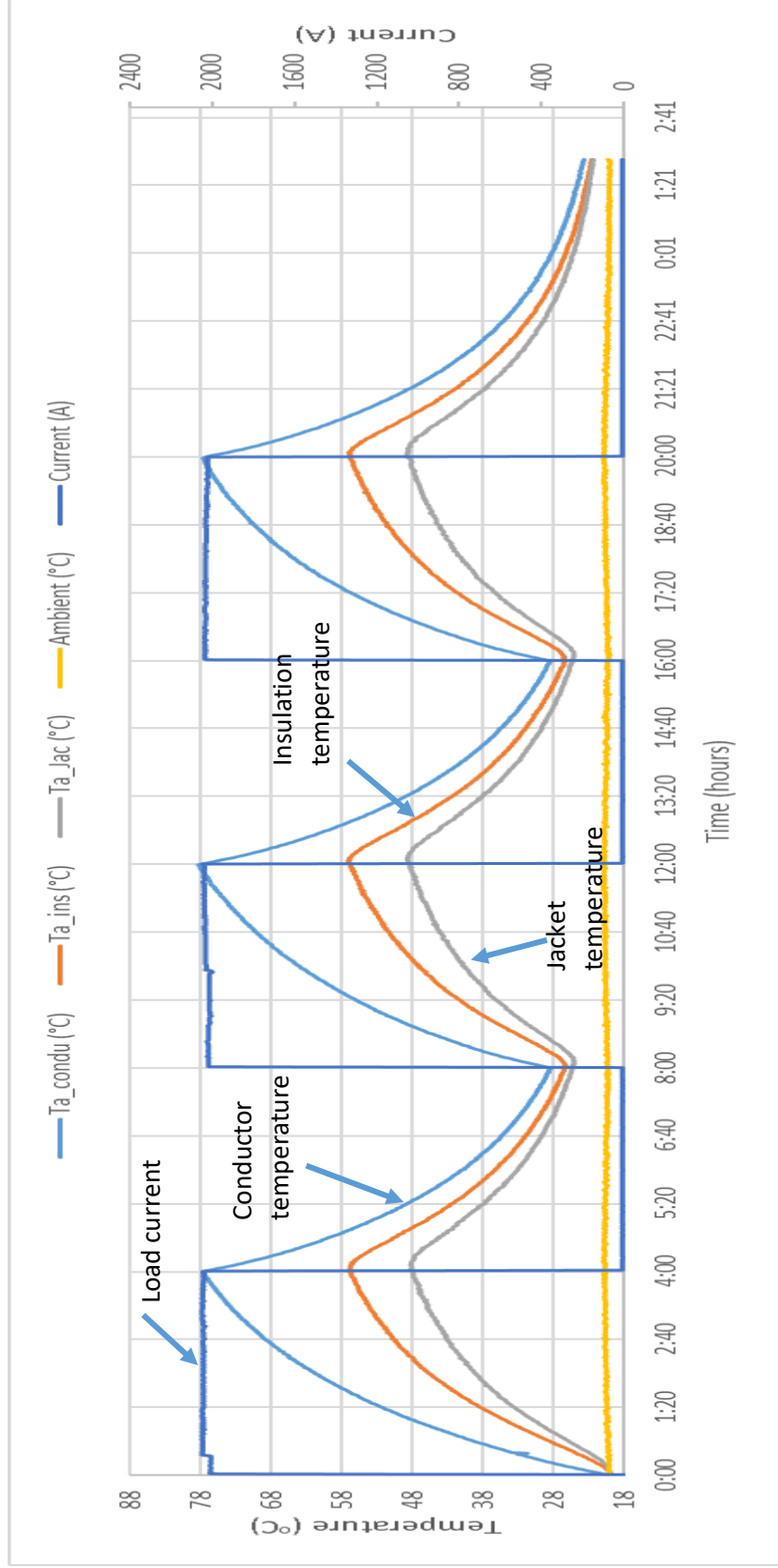


Figure 17 Cable profile @ 2030A variable load current for 1 day 2 hours

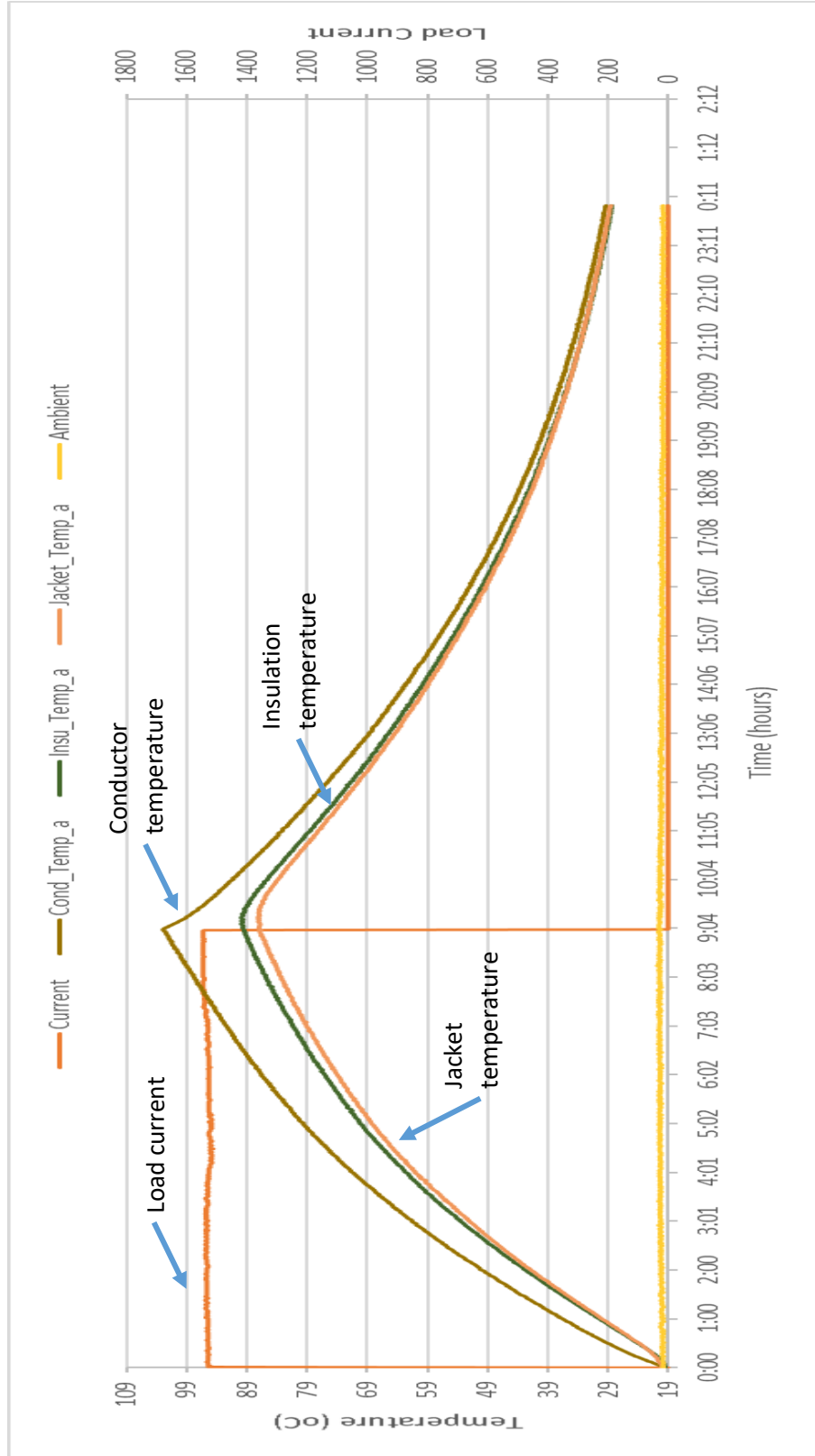


Figure 18: Cable profile @ 1530A load current for 9 hours with insulated cable

5.2. Gathering and calculation of ampacity data

From the cable specification in section 4.2 above and other physical data, the cable ampacity at steady state is computed using the approach in section 0 above:

1. Dielectric losses

From equation 3

$$W_d = \omega C U_o^2 \tan \delta \quad [W/m]$$

Where:

$$\omega = 2\pi f \text{ (} f = 60 \text{ Hz)} = 2\pi 60 \text{ rad/s}$$

$$\tan \delta = 0.004$$

$$U_o = \frac{138}{\sqrt{3}} 10^3 = 79.67 \times 10^3 \text{ v}$$

C = the capacitance of the cable

$$C = \frac{\epsilon}{18 \ln^{Di}/d_c} 10^{-9} = \frac{2.3}{18 \ln(86.4/40.9)} 10^{-9} = 1.708 \times 10^{-10} \text{ [F/m]}$$

$$W_d = \omega C U_o^2 \tan \delta$$

$$W_d = 2\pi 60 \times 1.708 \times 10^{-10} \times (79.67 \times 10^3)^2 \times 0.004 = 1.63 [W/m]$$

2. DC resistance

From equation 9, the DC resistance is

$$R_{dc20} = \frac{1.02 \times 10^6 \times \rho_{20}}{A} [1 + \alpha_{90}(\theta - 20)] \quad [\Omega/m]$$

$$\begin{aligned} R_{dc20} &= \frac{1.02 \times 10^6 \times 1.7241 \times 10^{-8} \times 15.25}{1000} [1 + 3.93 \times 10^{-3} (90 - 20)] \\ &= \mathbf{3.42 \ 10^{-4} \ [\Omega/m]} \end{aligned}$$

Where:

A = cross-sectional area of metal in mm^2

ρ = electrical resistivity of metal in ohm/m at 20°C

For copper conductors, = 1.7241×10^{-8}

α_{20} = the temperature coefficient of the conductor material per K at 20°C.

For copper conductors, = 3.93×10^{-3}

For aluminum conductors, = 4.03×10^{-3}

θ = the conductor operating temperature = 90°C)

The AC resistance from equation 10

$$R_{ac} = R_{DC}(1 + y_s + y_p)$$

Where:

R_{DC} = the dc resistance at the conductor operating temperature θ (Ω/m)

y_s = the skin effect factor (see below)

y_p = the proximity effect factor (see below)

The skin effect factor is computed as:

$$y_s = \frac{x_s^4}{192 + 0.8 \times x_s^4}$$

Where:

$$x_s = \sqrt{\left(\frac{8\pi f}{R_{dc}} 10^{-7} \cdot k_s\right)}$$

$$x_s = \sqrt{\left(\frac{8\pi f}{3.42 \cdot 10^{-4}} 10^{-7} \times 1\right)} = \mathbf{0.664}$$

R_{dc} = the dc resistance at the conductor operating temperature θ (Ω / m)

f = 60 Hz

k_s = a constant (see Table 1 above)

$$y_s = \frac{0.664^4}{192 + 0.8 \times 0.664^4} = \mathbf{0.0010}$$

The proximity effect factor of a cable varies depending on the conductor geometry. In a case, while the conductor is round, the proximity effect factor is.

$$y_p = \frac{x_p^4}{192 + 0.8 \times x_p^4} \left(\frac{d_c}{s} \right)^2 \times 2.9$$

Where:

$$x_p = \sqrt{\left(\frac{8\pi f}{R_{dc}} 10^{-7} \cdot k_p \right)}$$

$$x_p = \sqrt{\left(\frac{8\pi f}{R_{dc}} 10^{-7} \cdot k_p \right)} = \mathbf{0.6641}$$

R_{dc} = the dc resistance at the conductor operating temperature θ (Ω / m)

f = 60 Hz

k_p = (see Table 1 below)

s = 55.9 mm

d_c = 102.5 mm

$$y_p = \frac{0.6641^4}{192 + 0.8 \times 0.6641^4} \left(\frac{40.8}{55.9} \right)^2 \times 2.9 = \mathbf{0.0016}$$

The AC resistance from equation 10

$$R_{ac} = R_{DC}(1 + y_s + y_p)$$

$$R_{ac} = 3.42 \cdot 10^{-4} (1 + 0.0010 + 0.0016) = \mathbf{3.43 \cdot 10^{-4} \Omega}$$

Loss factor for screen (λ)

The loss factor for the screen according to IEC 60287-1-1 section 2.2 is defined as (λ_1), this loss consists of the circulating current (λ_1') and eddy current (λ_1'')[8].

$$\lambda_1 = \lambda_1' + \lambda_1''$$

Where:

$$\lambda_1' = \frac{R_{sl}}{R_{ac}} \frac{1}{1 + \left(\frac{R_{sl}}{X_{sl}}\right)^2}$$

$$X_{sl} = 2\omega \cdot 10^{-7} \ln \frac{2s}{d}$$

$$X_{sl} = 2\omega \cdot 10^{-7} \ln \frac{2 \times 55.9}{104.3} = \mathbf{5.977 \times 10^{-6} [\Omega]}$$

Where:

$$\omega = 2\pi f [\text{rad/s}]$$

$$s = 55.9 \text{ mm}$$

$$d = 104.3 \text{ mm}$$

$\lambda_1'' = 0$. The eddy-current loss is ignored according to IEC 60287-1-1 section 2.3.1 [8]

R_{sl} is the resistance of the screen per unit length of cable at its maximum operating temperature [Ω/m].

$$R_{sl} = R_{S0} [1 + \alpha_{20}(\theta_{sc} - 20)] L \quad [\Omega]$$

$$R_{sl} = \frac{1.02 \times 10^6 \times 1.7241 \times 10^{-8} \times 15.25}{1400} [1 + 3.93 \times 10^{-3} (90 - 20)] = \mathbf{2.433 \times 10^{-4} [\Omega]}$$

Where:

R_{S0} is the resistance of the cable screen at 20 °C [Ω/m].

$$\theta_{sc} = 90 \text{ °C}$$

$$\lambda_1' = \frac{R_{sl}}{R_{ac}} \frac{1}{1 + \left(\frac{R_{sl}}{X_{sl}}\right)^2} = \frac{2.433 \times 10^{-4}}{3.43 \times 10^{-4}} \frac{1}{1 + \left(\frac{2.433 \times 10^{-4}}{5.977 \times 10^{-6}}\right)^2} = \mathbf{4.28 \times 10^{-4}}$$

$$\lambda_1 = \lambda_1' + \lambda_1''$$

$$\lambda_1 = 4.28 \times 10^{-4} + 0 = \mathbf{4.28 \times 10^{-4}}$$

Thermal Resistances

Thermal resistance is a heat property or mediums that limit the transfer of heat. The thermal resistance for the different layers of the cable is expressed as follow.

Thermal resistance of the insulator

The thermal resistance of the insulator is the thermal resistance between the conductor and the sheath. According to IEC 60287-2-1[8], this resistance is express as

$$T_1 = \frac{\rho_i}{2\pi L} \ln\left(\frac{D_{oi}}{D_c}\right) = \frac{3.5}{2\pi \times 15.25} \ln\left(\frac{86.4}{40.9}\right) = \mathbf{0.0273} \left[\frac{^{\circ}C}{W} \right]$$

Where:

$$\rho_i = 3.5 \text{ Km/W}$$

$$D_c = 40.9 \text{ mm}$$

$$T_i = 15.01 \text{ mm}$$

$$D_{oi} = 86.4 \text{ mm}$$

Thermal resistance of the sheath T2

The power cable in this investigation did not contain an armour. However, it did have a sheath. From EPRI green book 2007 [1], studies have shown that metallic shields and sheaths, steel casings and pipes, and metallic conduits have negligible thermal resistances.

Therefore, the thermal resistance of the metallic shield and sheaths is considered to be zero in the experiment.

$$T_2 = \mathbf{0} \left[\frac{^{\circ}C}{W} \right]$$

Thermal resistance of the jacket T₃

The thermal resistance of the jacket is the resistance between the sheath and the jacket surface.

$$T_3 = \frac{\rho_J}{2\pi} \ln \left(1 + \frac{2t_3}{D'_{ij}} \right) \quad \text{or}$$

$$T_3 = \frac{\rho_J}{2\pi L} \ln \left(\frac{D'_{oj}}{D'_{ij}} \right) = \frac{3.5}{2\pi \times 15.25} \ln \left(\frac{104.3}{96.2} \right) = \mathbf{0.0030} \left[\frac{^\circ\text{C}}{\text{W}} \right]$$

Where:

$$\rho_J = 3.5 \text{ Km/W}$$

$$D'_{oj} = 104.3 \text{ mm}$$

$$D'_{ij} = 96.2 \text{ mm}$$

Thermal resistance of the surrounding T₄

The thermal resistance of a cable surrounding depends on where the cable is installed. If the cable is installed in a duct system (commonly install method in the US), the thermal resistance of the surrounding consists three parts. Namely T'₄, the thermal resistance of the air space between the cable surface and the duct's internal surface; T''₄; the thermal resistance of the duct itself; and T'''₄; the external thermal resistance of the duct.

$$T_4 = T'_4 + T''_4 + T'''_4$$

Thermal resistance between cable surface and duct inner surface T'₄

$$T'_4 = \frac{U}{1 + 0.1(V + Y\theta_m)D_e} \quad \left[\frac{^\circ\text{C}\cdot\text{m}}{\text{W}} \right]$$

Where:

D_e = the external diameter of the cable [mm]

θ_m = the mean temperature of the medium filling the space between cable and duct. An assumed value should be used initially and the calculation repeated with a modified value if necessary [°C]

U, V, and Y as defined in Table 2.

In this investigation, the cable was in air with a length of 15.25m

$$T_{air} = \frac{1}{h \times A_{air}} \quad [^{\circ}\text{C}/\text{W}]$$

$$h = 10 \text{ w/m}^2\text{ }^{\circ}\text{C}$$

$$L = 15.25\text{m}$$

$$A_{air} = \frac{L^2}{4\pi}$$

$$T_{air} = \frac{1}{10 \times \frac{15.25^2}{4\pi}} = \mathbf{0.0054} [^{\circ}\text{C}/\text{W}]$$

From the above calculations, the temperature rise in the sample cable is then computed as using equation 6:

$$\Delta\theta = (I^2 R_{ac} + .5W_d)T_1 + [I^2 R_{ac}(1 + \lambda_1) + W_d]nT_2 \\ + [I^2 R_{ac}(1 + \lambda_1 + \lambda_2) + W_d]n(T_3 + T_4)$$

For a load current of 1530A, the temperature rise in the cable sample is:

$$\Delta\theta = (1530^2 \times 3.43 \times 10^{-4} + .5 \times 1.65)0.0273 + [1530^2 \times 3.43 \times 10^{-4}(1 + 4.28 \times 10^{-4}) + 1.65](0.003 + 0.0054) = \mathbf{39.5}$$

The temperature rise at 1530 load current is

$$\Delta\theta = \mathbf{39.5}$$

$$\Delta\theta = \theta_c - \theta_a$$

The conductor temperature at steady state for a load current of 1530A is computed as shown below. In this case, the ambient temperature is assumed to be 20 degree

$$\theta_c = \theta_a + \Delta\theta$$

$$\theta_a = 20$$

$$\theta_c = \theta_a + \Delta\theta$$

$$\theta_c = 20 + 39.5 = 59.5$$

$$\theta_c = \mathbf{59.5} \text{ } ^\circ\mathbf{C}$$

5.3. Transient Ampacity Analysis

The transient ampacity analysis of an XLPE cable involves calculation of the cable response to arbitrary, dynamic excitations. Transient behavior, in general, is defined as a process' variables changes in time before it reaches its steady state. In an XLPE cable, this results in the calculation of the cable current as a function of conductor's temperature and time, or computation of the cable conductor's temperature as a function of current and time. In the transient analysis of a cable, the calculations take both the thermal resistance and capacitance of the different cable layers and its environment into consideration, while steady-state calculations ignore this thermal capacitance and consider only the thermal resistance. From the equivalent electrical circuit of a cable in Figure 3 above in section 3.1.1, the transient behavior of a cable can be analyzed based on the RC electrical network consisting of a current source, resistors, and capacitors. This represents the heat generation in the cable, due to the thermal resistances and thermal capacitances of the different cable and earth layers. In a cable system, the heat generated is due to RI^2 losses. Studies from EPRI green book [1] show that a quicker solution for transient ampacity analysis can be obtained by utilizing a two- or three-section R-C model for the cable system and an analytic expression in the form of the exponential function, which describes the temperature response of the earth to a step-change in load.

$$\theta_{c,(I,t)} = \Delta\theta_c - \Delta\theta_c \times e^{-t/R_T C_T} + \theta_{ci} \quad [^\circ\text{C}]$$

$$\theta_{c,(I,t)} = \Delta\theta_c \left(1 - e^{-t/R_T C_T}\right) + \theta_{ci} \quad [^\circ\text{C}]$$

The rise in temperature from equation six is given as

$$\Delta\theta_c = (I^2R_{ac} + .5W_d)T_1 + [I^2R_{ac}(1 + \lambda_1 + \lambda_2) + W_d](T_3 + T_4)$$

Equation 6 in 28

$$\theta_{c,(I,t)} = (I^2R_{ac} + .5W_d)T_1 + [I^2R_{ac}(1 + \lambda_1 + \lambda_2) + W_d](T_3 + T_4) \left(1 - e^{-t/R_T C_T}\right) + \theta_{ci} \quad (27)$$

Hence,

$$\theta_{ins,(I,t)} = [\theta_c - (I^2R_{ac} + .5W_d)T_1] \left(1 - e^{-t/R_T C_T}\right) + \theta_{ci} \quad [^\circ C]$$

$$\theta_{ins,(I,t)} = [I^2R_{ac}(1 + \lambda_1 + \lambda_2) + W_d](T_3 + T_4) \left(1 - e^{-t/R_T C_T}\right) + \theta_{ci} \quad [^\circ C] \quad (28)$$

Hence,

$$\theta_{jac,(I,t)} = [\theta_c - [I^2R_{ac}(1 + \lambda_1 + \lambda_2) + W_d](T_3 + T_4)] \left(1 - e^{-t/R_T C_T}\right) + \theta_{ci} \quad [^\circ C]$$

$$\theta_{jac,(I,t)} = (I^2R_{ac} + .5W_d)T_1 \times \left(1 - e^{-t/R_T C_T}\right) + \theta_{ci} \quad [^\circ C] \quad (29)$$

Where:

$\theta_{c,(I,t)}$ = the conductor temperature as a function of time and load current

$\theta_{ins,(I,t)}$ = the insulation temperature as a function of time and load current

$\theta_{jac,(I,t)}$ = the jacket temperature as a function of time and load current

$\Delta\theta_c$ = the temperature rise in the cable

θ_{ci} = initial conductor temperature

$R_T C_T$ = cable time constant [minutes]

The computation of thermal resistances in the transient analysis is the same as a steady state; see section 3.1.3 and 5.2 above. The thermal capacitances for each layer of the cable is the volume of the layer times the specific heat capacity and the density of the

layer[1, 11, 12]. Table 5 shows the specific heat capacity and density of some common cable layers.

$$C_{Th} = V \times C_p \times \rho$$

Table 5: Specific heat capacity and density of some common cable layers

Layers		Specific heat capacity [J/kg. °C]	Density [kg/m ³]
Conductor	Copper	390	8900
	Aluminum		
XLPE		2.4e ⁶	922
PVC		2.4e ⁶	962

Thermal capacitance of the conductor

$$C_{Th_c} = V_c \times C_{p_c} \times \rho_c \quad [J / ^\circ C] \quad (30)$$

Where:

V_c = the volume of the conductor length [m³]

$$V_c = A \times L$$

A = area of the conductor [m²]

L = length of the conductor [m]

C_{p_c} = the specific heat of copper [J/kg.oC]

ρ_c = the density of copper [kg/m³]

Thermal capacitance of insulation

$$C_{Th_i} = V_i \times C_{p_i} \times \rho_i \quad [J / ^\circ C] \quad (31)$$

Where:

V_i = the volume of the whole cable insulation length [m³]

$$V_i = \frac{\pi L}{4} (D_{oi}^2 - D_{ii}^2)$$

D_{oi} = the outer diameter of the insulation [m]

D_{ii} = the internal diameter of the insulation [m]

L = length of the cable [m]

C_{p_i} = the specific heat of insulation [J/kg.°C]

ρ_i = the density of insulation [kg/m³]

Thermal capacitance of the sheath

$$C_{Th_s} = V_s \times C_{p_s} \times \rho_s \quad [J/^\circ C] \quad (32)$$

Where:

V_c = the volume of the whole cable sample length [m³]

$$V_c = A \times L$$

A = area of the sheath [m²]

L = length of the sheath [m]

C_{p_c} = the specific heat of copper [J/kg.°C]

ρ_s = the density of sheath material (copper) [kg/m³]

Thermal capacitance of insulation

$$C_{Th_i} = V_i \times C_{p_i} \times \rho_i \quad [J/^\circ C] \quad (33)$$

Where:

V_i = the volume of the whole cable insulation length [m³]

$$V_i = \frac{\pi L}{4} (D'_{oj}{}^2 - D'_{ij}{}^2)$$

D'_{oj} = the outer diameter of the jacket [m]

D'_{ij} = the internal diameter of the jacket [m]

L = length of the cable [m]

C_{p_j} = the specific heat of jacket [J/kg.°C]

ρ_j = the density of jacket [kg/m³]

5.4. Modeling

Using physical parameters and the formulas above, a transient cable model was developed. All the computation was done in MATLAB, and the model was designed in Simulink. The model was developed by transforming the conductor temperature equation (equation (27)) as a function of time and load current (time domain) to the frequency domain. This transformation was accomplished using the Laplace transform. The system was designed with the current fed through the conductor. The Laplace transformation of an exponential function given below is[13]:

$$f_t = k \left(1 - e^{-t/\tau} \right) \rightarrow F_s = \frac{K}{\tau s + 1} \quad (34)$$

Where:

K is the gain

τ is the time constant (RC)

s is the frequency domain variable

As mention above, the model was developed, the cable system was then modeled in Simulink. Figures 18, 19, 20, and 21 show the model of the conductor, insulation, and jacket respectively. Figures 18, 19, and 20 represent the Laplace transformation of equation 27, 28, and 29 respectively. Figure 21 is the combination of all the layers of the cable (conductor, insulation, and jacket). Figure 18 is a Simulink circuit of a cable conductor. This diagram has a current input and a conductor temperature as an output. The response

of the circuit is shown in Figure 23 below. This circuit is developed from a Laplace transform of equation 27.

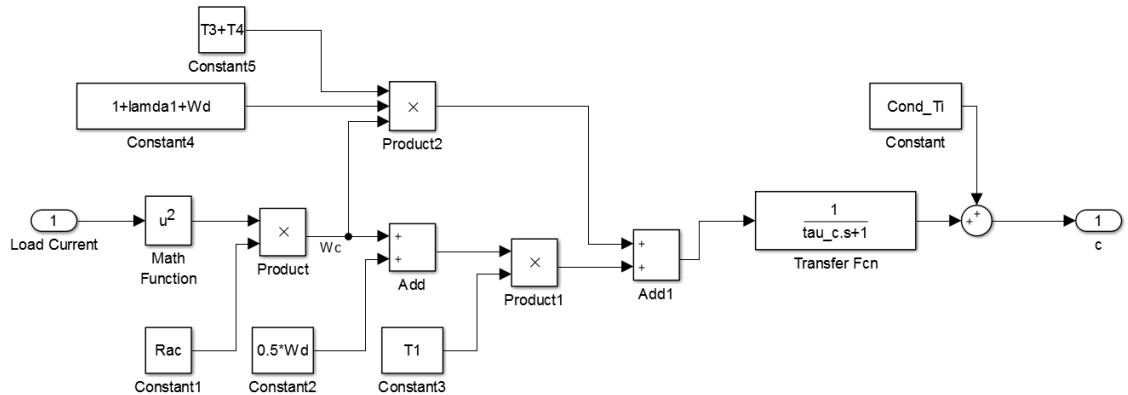


Figure 19: Conductor temperature model with current as input

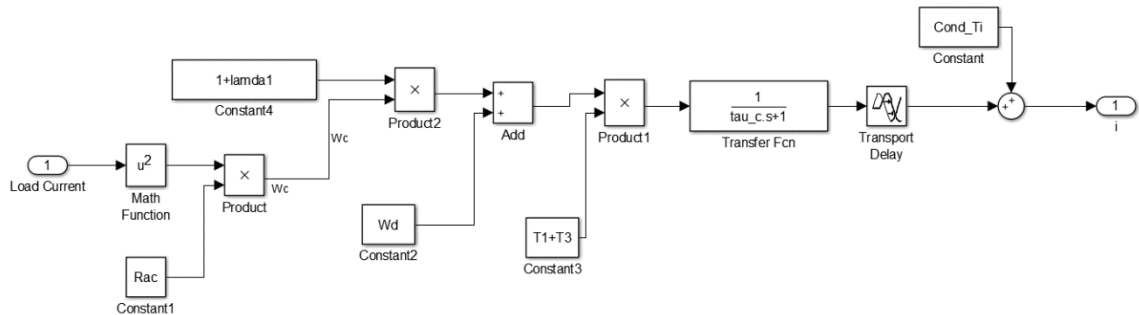


Figure 20: Insulation temperature model with current as input

Figure 19 represent the insulation model. This model has a current input, and the output, in this case, is the temperature of the top surface of the insulation. This circuit is developed from the Laplace transform of equation 28. Figure 20 represent the jacket model. This circuit modeled the temperature at the surface of the jacket given the load current as the input. This diagram is developed from a Laplace transform of equation 29.

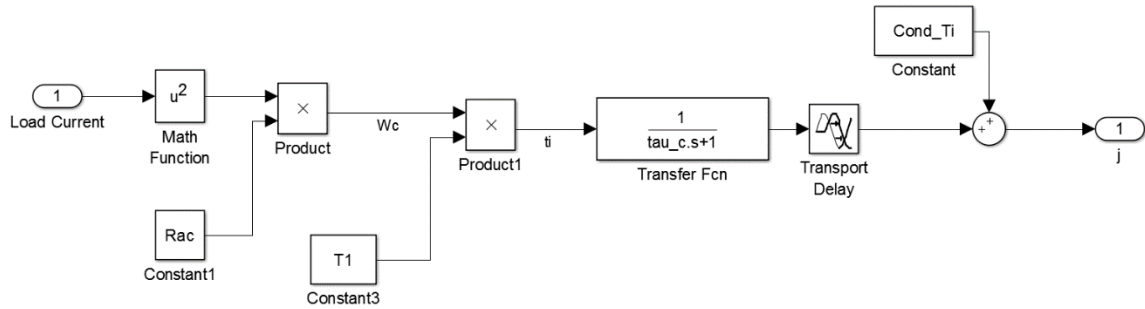


Figure 21: Jacket temperature model with current as input

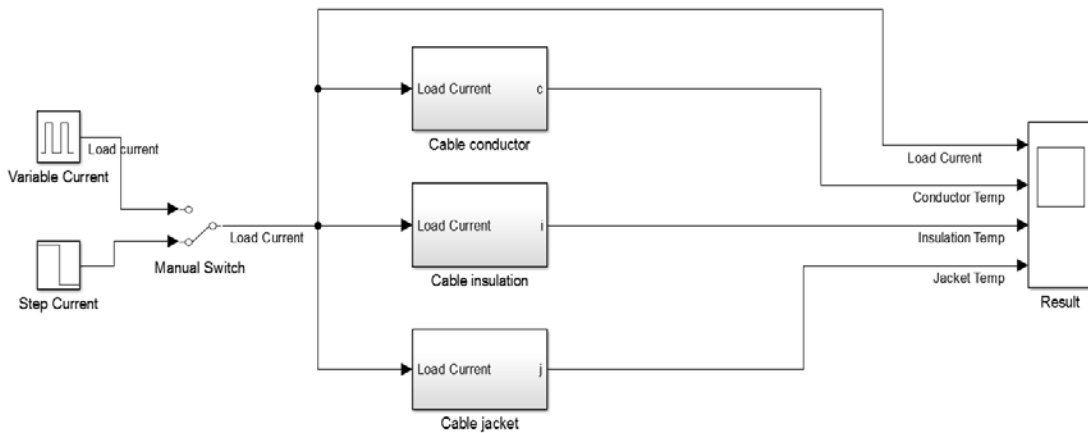


Figure 22: XLPE Cable model with current as input

Figure 21 shows the cable model with all the three core layers. This circuit represents the cable conductor, insulation, and jacket model. These boxes are the sub-circuits shown in Figures 18, 19 and 20. The simulation result of this circuit is shown in Figure 23 below. The switch in the circuit switches the current inputs from a step current input to a pulse or variable current input.

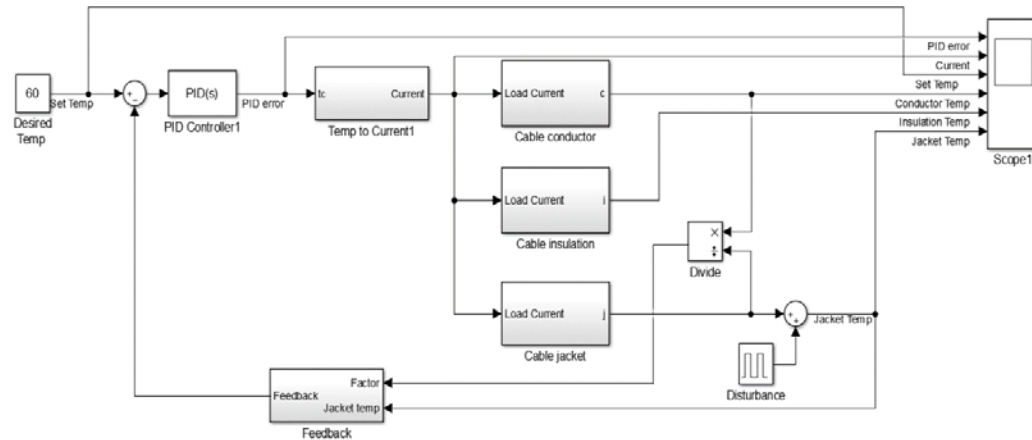


Figure 23: Conductor PID temperature control

Figure 22 is a closed loop control system; this circuit controls the conductor temperature to the desired temperature (set point) from the jacket temperature. In this circuit, the conductor temperature is specified, and the model will maintain this temperature by adjusting how much load current flow through the cable given the change in temperature on the jacket surface. This circuit automatically achieves and maintain the desired output conductor temperature by comparing it with the actual conductor and jacket temperature. In this model circuit, the output is the conductor temperature, but the feedback signal is the jacket temperature. Despite the change in temperature on the jacket surface the model automatically adjusts to maintain the conductor temperature.

5.5. Model Results

This section shows the results from Simulink model in Figures 21 and 22. The result shows the input and the output response. In these Figures, the input is a current source, and the outputs are the temperatures. Figure 23 illustrates the result of the circuit shown in Figure 21 when the switch is in the lower position. At this position, the current is a step input. The current is at 1530A for 695 minutes represented in green. The outputs are the lower curves in Figure 23. In these output graph, the yellow curve represents the conductor temperature while red curve is the jacket and blue is the jacket temperature.

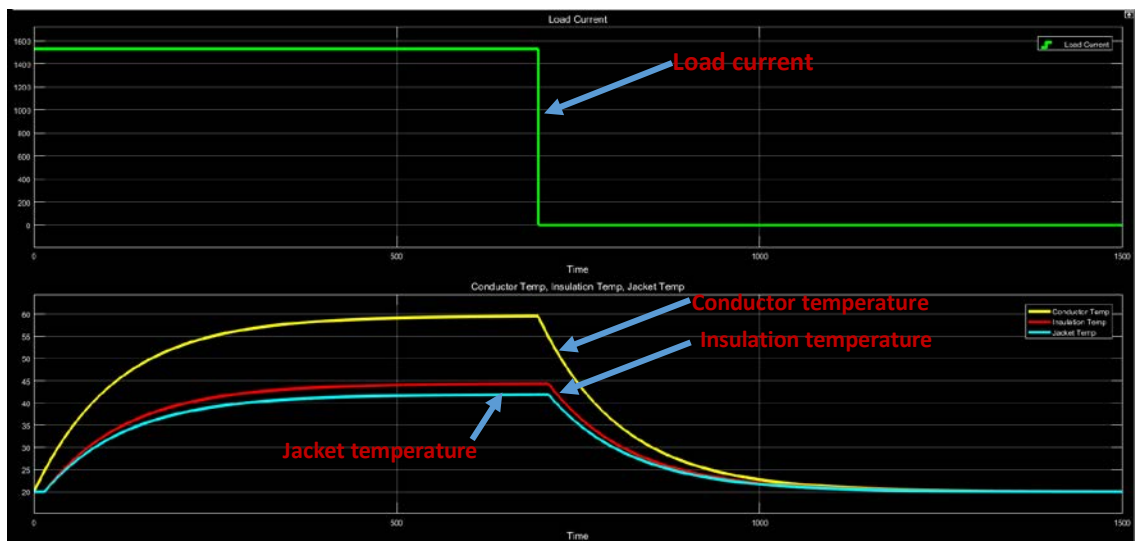


Figure 24: 1530A current step input response (temperature profile)

Figure 24 below shows the result of the cable modeling when the switch is in the upper position. At this position, the input current is a pulse signal. The current is on for four hours and off for the next four hours. This simulation was to test the model for a variable load input.

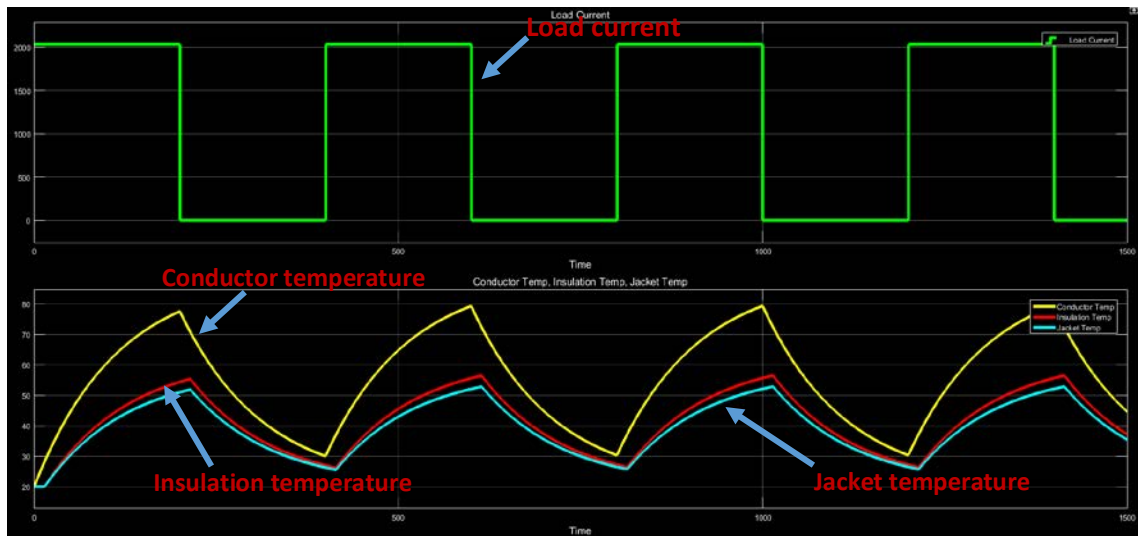


Figure 25: 2030A Pulse current input response

Figure 25 represents the result of the conductor temperature closed loop control circuit. In this Figure, the green curve is the error signal of the output and feedback. Yellow is the current required to maintain the conductor temperature to its desired set point. The red curve is the conductor set point; blue is the actual conductor temperature while orange and light green is the insulation and jacket temperature.

Figure 26 represents the result of the conductor temperature closed loop control circuit with a disturbance on the jacket. The disturbance was an impulse of amplitude five which represents 5°C . This disturbance impulse was applied to the jacket. With the increase in the jacket temperature, the PID controller drops the load current to reduce the system's error and bring the conductor temperature back to the desired value. From the graph, it can be seen the model responds automatically and corrects for the disturbance at the jacket. Note that the jacket and the conductor have an approx. 14 minutes' delay response time. With an increase in the jacket temperature, the PID controller drops the load current to

reduce the systems error and bring the conductor temperature back to the desired value. The PID controller was tuned to specific values to archives the system response. The Simulink tune tool was used to tune, and the following criteria were used. (1) The system should critically damped; (2) Rising time should not be greater than cable time constant; (3) System should not overshoot; (4) Desire temperature should $20 \leq t \leq 90$. Table 6 below shows the tuned values of the PID controller.

Table 6: PID Controller tuned parameters

Controller Parameters		
	Tuned	Block
P	1.2255	1.2255
I	0.01296	0.01296
D	9.2447	9.2447
N	0.026831	0.026831

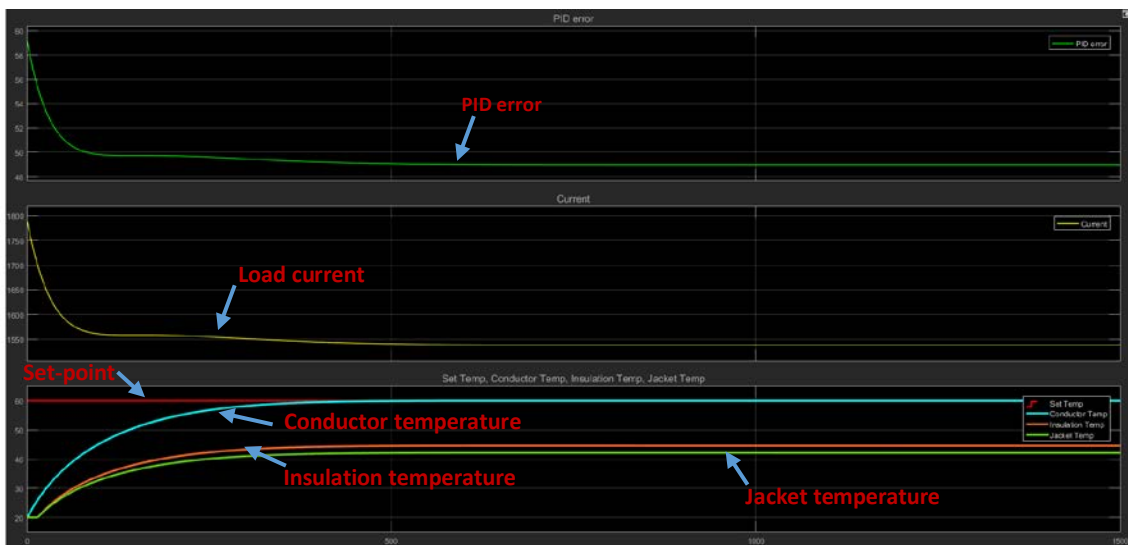


Figure 26: 60-degree desired conductor temperature response with PID control

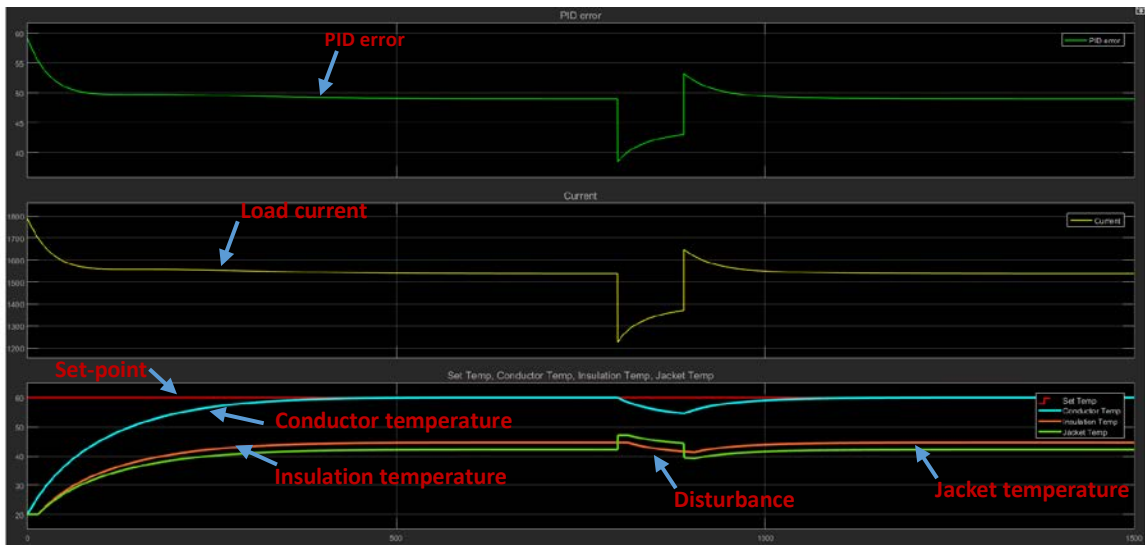
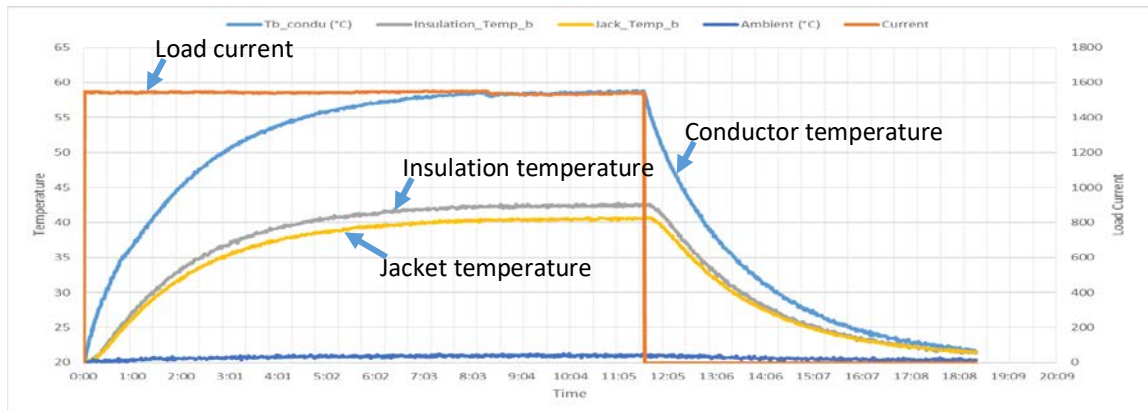


Figure 27: 60-degree desired conductor temperature response with PID control and disturbance verification.

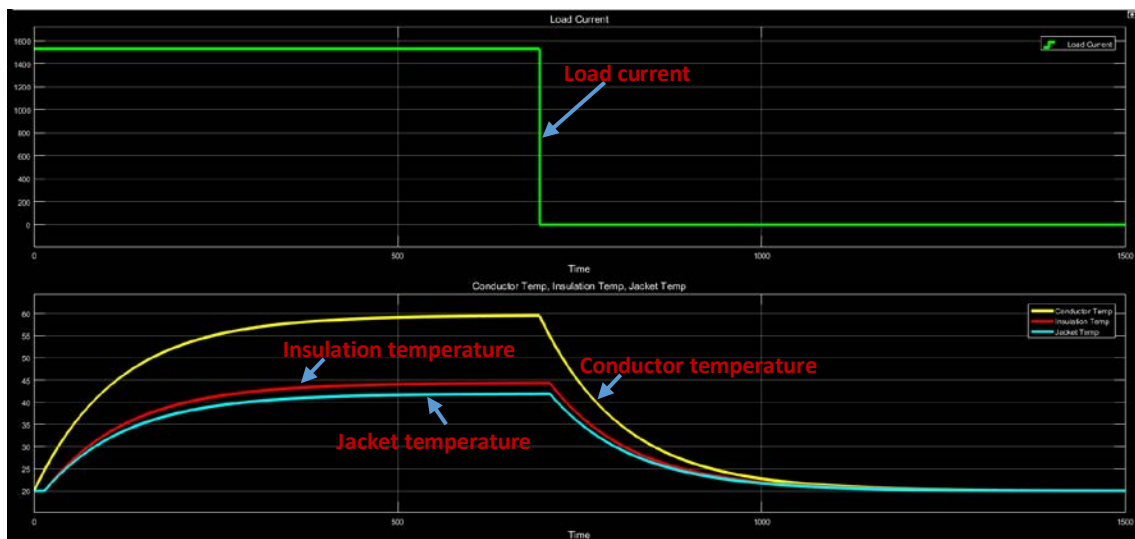
5.6. Measured vs. Model Results

One of the ways to verify the model was to compare its results to the experimental result obtained in the laboratory. The first comparison is that of the step load current.

5.6.1. Cable temperature profile @ 1530A step-load current



(a)



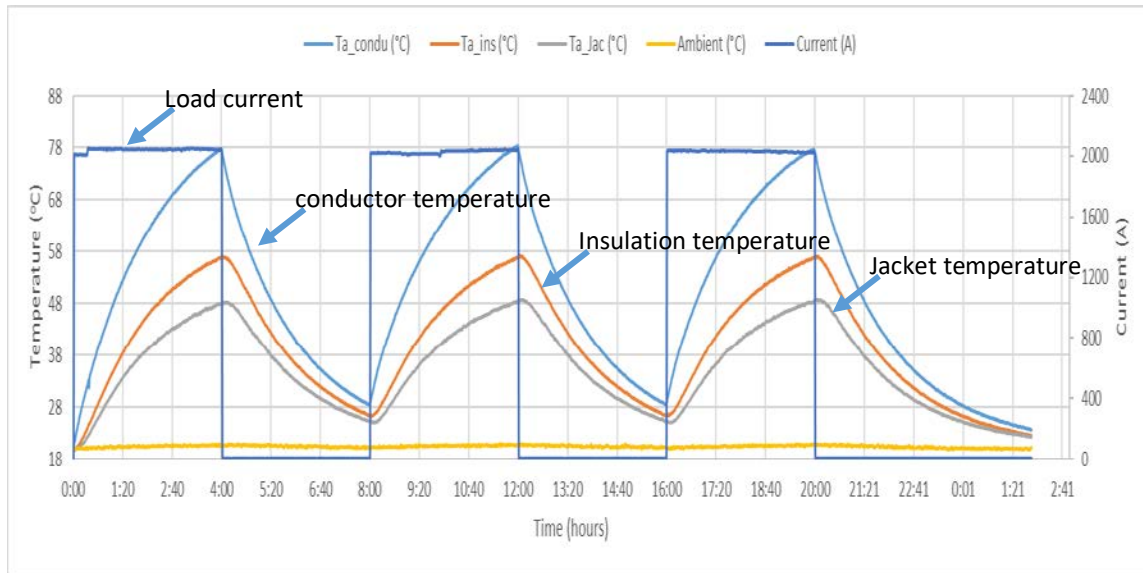
(b)

Figure 28: Cable temperature profile @ 1530A step-load current; (a) Measured result; (b) Model result

From Figure 27 above, the result in (a) is identical to that in (b). Figure 27 (a) is the laboratory result while (b) is the modeled result. The orange curve in Figure 27 (a)

represents the load current which is the green curve on the model result in Figure 27 (b). Figure 28 (a) and (b) shows the measured and the modeled result of a variable load current.

5.6.2. Cable temperature profile @ 2030A pulse load current



(a)

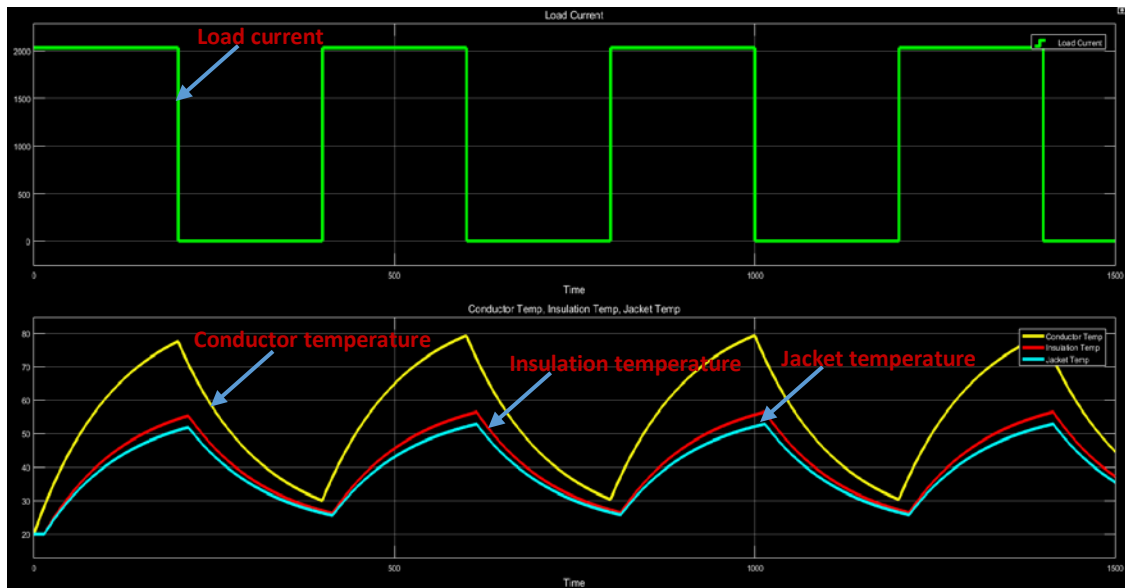


Figure 29: Cable temperature profile @ 2030A step load current; (a) Measured result;(b) Model result

CHAPTER 6: CONCLUSIONS

Underground cable current carrying capacity is limited due to the ability to withstand high temperature. High operating temperature affects the insulation of the cable. The estimated life of a cable depends on the operating temperature. This implies the maximum continuous operating temperature should never exceed that of the manufacturer's specification. This paper presents a model and algorithm to predict and control the temperature of the cable conductor, insulation, jacket and load current given of the following inputs jacket temperature, ambient temperature, bonding, load history, and cable surrounding.

A model was developed to predict the conductor temperature, from a load current and cable installation condition. The model predicts how much current is needed to produce a specified conductor temperature within the determined time. The second model was developed to predict load current profile from the desired conductor temperature. This model automatically achieves and maintains the desired conductor temperature by comparing it with the jacket temperature.

The developed algorithm and control system in this paper was verified with measured lab results from a laboratory environment. The accuracy of the model and algorithm is about $\pm 5\%$ given the conditions of the cable and installation

REFERENCES

- [1] EPRI, *Underground Transmission Systems Reference Book*, 2006 ed.: EPRI, Palo Alto, CA 2007 1014840.
- [2] A. N. Jahromi, Z. Li, J. Kuffel, M. Fenger, and J. Levine, "Load-cycling test of high-voltage cables and accessories," *IEEE Electrical Insulation Magazine*, vol. 27, pp. 14-28, 2011.
- [3] "Power Cables With Extruded Insulation and Their Accessories for Rated Voltages Above 30 kV ($U_m = 36$ kV) up to 150 kV ($U_m = 170$ kV)," *IEC 60840*, vol. ed 3rd, 2004.
- [4] "Power cables with extruded insulation and their accessories for rated voltages above 150 kV ($U_m = 170$ kV) up to 500 kV ($U_m = 550$ kV) – Test methods and requirements," *IEC 62067*, pp. 1-126, 2011.
- [5] "SPECIFICATION FOR EXTRUDED INSULATION POWER CABLES AND THEIR ACCESSORIES RATED ABOVE 46 kV THROUGH 345 kV_{ac}," *AEIC CS9-06*, 2006.
- [6] F. d. León, "Calculation of Underground Cable Ampacity," *CYME International T&D*, 2005.
- [7] J. H. Neher and M. H. McGrath, "The calculation of the temperature rise and load capability of cable systems," *Transactions of the American Institute of Electrical Engineers. Part III: Power Apparatus and Systems*, vol. 76, pp. 752-764, 1957.
- [8] IEC60287, "Electric cables - Calculation of the current rating - Part 2-1: Thermal resistance - Calculation of the thermal resistance," *IEC 60287 Part 2-1*, 2015.
- [9] ABB. (2004, April 6). *XLPE Land Cable Systems 2GM5007GB (Rev 5 ed.)*. Available:
<https://library.e.abb.com/public/ab02245fb5b5ec41c12575c4004a76d0/XLPE%20Land%20Cable%20Systems%202GM5007GB%20rev%205.pdf>
- [10] Southwire. (2010, April 6). *138 KV Power Cables (Section 4 ed.)*. Available:
<http://www.southwire.com/ProductCatalog/XTEInterfaceServlet?contentKey=prodatsheetHV4>

- [11] P. Castro, A. Arroyo, R. Martinez, M. Manana, R. Domingo, A. Laso, *et al.*, "Study of different mathematical approaches to determining the dynamic rating of overhead power lines and a comparison with real-time monitoring data," *Applied Thermal Engineering*, vol. 111, pp. 95-102, 1/25/ 2017.

- [12] J. P. Holman, *Heat Transfer*, 10 ed. New York: McGraw-Hill Companies, 2010.

- [13] N. S. Nise, *Control Systems Engineering*, 6 ed.: John Wiley & Sons, Incorporated, 2011.

APPENDIX A: Ampacity Calculation

This appendix is a summary of the exact wording of IEC-60287. According to IEC-60287 [8], the ampacity of an AC cable is derived from the expression for the conductor temperature rise above ambient.

$$\Delta\theta = (I^2R + \frac{1}{2}W_d)T_1 + [I^2R(1 + \lambda_1) + W_d]nT_2 + [I^2R(1 + \lambda_1 + \lambda_2) + W_d]n(T_3 + T_4) \quad (\text{A.1})$$

where

I is the current flowing in one conductor [A];

$\Delta\theta$ is the conductor temperature rise above the ambient temperature [K];

NOTE The ambient temperature is the temperature of the surrounding medium under normal conditions, at a situation in which cables are installed, or are to be installed, including the effect of any local source of heat, but not the increase of temperature in the immediate neighbourhood of the cables due to heat arising therefrom.

R is the alternating current resistance per unit length of the conductor at maximum operating temperature [Ω/m];

W_d is the dielectric loss per unit length for the insulation surrounding the conductor [W/m];

T_1 is the thermal resistance per unit length between one conductor and the sheath [Km/W];

T_2 is the thermal resistance per unit length of the bedding between sheath and armour [Km/W];

T_3 is the thermal resistance per unit length of the external serving of the cable [Km/W];

Skin effect factor y_s

The skin effect factor y_s is given by:

$$y_s = \frac{x_s^4}{192 + 0.8 \cdot x_s^4} \quad (\text{A.6})$$

where

$$x_s^2 = \frac{8\pi f}{R'} \cdot 10^{-7} \cdot k_s \quad (\text{A.7})$$

f is the supply frequency in hertz.

Proximity effect factor y_p (for three-core cables)

The proximity effect factor is given by:

$$y_p = \frac{x_p^4}{192 + 0.8x_p^4} \left(\frac{d_c}{s} \right)^2 \left[0.312 \cdot \left(\frac{d_c}{s} \right)^2 + \frac{1.18}{\frac{x_p^4}{192 + 0.8x_p^4} + 0.27} \right] \quad (\text{A.8})$$

where

$$x_p^2 = \frac{8\pi f}{R'} \cdot 10^{-7} \cdot k_p \quad (\text{A.9})$$

d_c is the diameter of conductor [mm];

s is the distance between conductor axes [mm].

A.1.2 Dielectric losses

The dielectric loss per unit length in each phase is given by:

$$W_d = \omega C U_0^2 \tan \delta \text{ [W/m]} \quad (\text{A.10})$$

where

$$\omega = 2\pi f;$$

C is the capacitance per unit length [F/m];

U_0 is the voltage to earth [V].

A.1. CALCULATION OF LOSSES

The capacitance for circular conductors is given by:

$$C = \frac{\varepsilon}{18 \ln \frac{D_i}{d_c}} \cdot 10^{-9} [F/m] \quad (\text{A.11})$$

where

ε is the relative permittivity of the insulation;

D_i is the external diameter of the insulation (excluding screen) [mm];

d_c is the diameter of conductor, including screen, if any [mm].

A.1.3 Loss factor for sheath and screen

The power loss in the sheath or screen (λ_1) consists of losses caused by circulating currents (λ_1') and eddy currents (λ_1''), thus:

$$\lambda_1 = \lambda_1' + \lambda_1'' \quad (\text{A.12})$$

The formulae given in this section express the loss in terms of the total power loss in the conductor(s).

$$R_S = R_{S0} [1 + \alpha_{20}(\theta_{SC} - 20)] [\Omega/m] \quad (\text{A.13})$$

where

R_{S0} is the resistance of the cable sheath or screen at 20 °C [Ω/m].

$$\lambda_1' = \frac{R_S}{R} \frac{1}{1 + \left(\frac{R_S}{X}\right)^2} \quad (\text{A.14})$$

where

R_S is the resistance of sheath or screen per unit length of cable at its maximum operating temperature [Ω/m];

X is the reactance per unit length of sheath or screen per unit length of cable = $2\omega \cdot 10^{-7} \ln \frac{2s}{d}$ [Ω/m];

ω = $2\pi f$ [1/s];

s is the distance between conductor axes in the electrical section being considered [mm];

d is the mean diameter of the sheath [mm];

$\lambda_1'' = 0$. The eddy-current loss is ignored according to IEC 60287-1-1 section 2.3.1 [1].

The eddy-current loss λ_1'' is ignored according to IEC 60287-1-1 section 2.3.1 [1].

A.2 Thermal resistance

A.2.1 Thermal resistance of constituent parts of a cable

Thermal resistance between one conductor and sheath T_1

For screened cables with circular conductors the thermal resistance T_1 is:

$$T_1 = \frac{\rho_T}{2\pi} G \quad (\text{A.15})$$

where

G is the geometric factor according to IEC60287 [2];

ρ_T is the thermal resistivity of insulation [Km/W];

Thermal resistance between sheath and armour T_2

AXKJ-F 3x95/25 does not contain armour nor metallic sheath. Hence T_2 is not considered.

Thermal resistance of outer covering (serving) T_3

$$T_3 = \frac{\rho_T}{2\pi} \cdot \ln \left(1 + \frac{2t_3}{D'_a} \right) \quad (\text{A.16})$$

where

t_3 is the thickness of serving [mm];

D'_a is the external diameter of the armour [mm];

A.2.2 External thermal resistance T_4

The external thermal resistance of a cable in a duct consists of three parts:

T'_4 is the thermal resistance of the air space between the cable surface and duct's internal surface;

T''_4 is the thermal resistance of the duct itself;

T'''_4 is the external thermal resistance of the duct.

$$T_4 = T'_4 + T''_4 + T'''_4 \quad (\text{A.17})$$

A.2. THERMAL RESISTANCE

Thermal resistance between cable and duct T'_4

$$T'_4 = \frac{U}{1 + 0.1(V + Y\theta_m)D_e} \quad (\text{A.18})$$

where

D_e is the external diameter of the cable [mm];

θ_m is the mean temperature of the medium filling the space between cable and duct. An assumed value has to be used initially and the calculation repeated with a modified value if necessary [$^{\circ}\text{C}$];

Thermal resistance of the duct T''_4

$$T''_4 = \frac{\rho_T}{2\pi} \cdot \ln\left(1 + \frac{D_0}{D_d}\right) \quad (\text{A.19})$$

where

D_0 is the outside diameter of the duct [mm];

D_d is the inside diameter of the duct [mm];

ρ_T is the thermal resistivity of duct material [K m/W]

External thermal resistance of the duct T'''_4

$$T'''_4 = \frac{1}{2\pi} \rho_T \cdot \ln(2u) \quad (\text{A.20})$$

where

ρ_T is the thermal resistivity of the soil [K m/W];

$u = \frac{2L}{D_0}$, L is the placement depth [mm];

APPENDIX B-1: ASD power Load Cycle Test System spec

Load Cycle Test System

Low Voltage, Current Test Set For Power Cable

Applications

Testing of insulating Cables

Current Transformers

ASD current transformer rated at 12 volts and 4000A is a standard building block of the test loop. As the loop size changes, the power level will change, requiring the addition or deletion of current transformers from the system in order to achieve the desired heating curve.

The K or other type thermocouples, isolated amplifier transmitter are mounted on a cart. A current transformer is also mounted on the cart, to monitor the current in the test loop.

Voltage Regulator

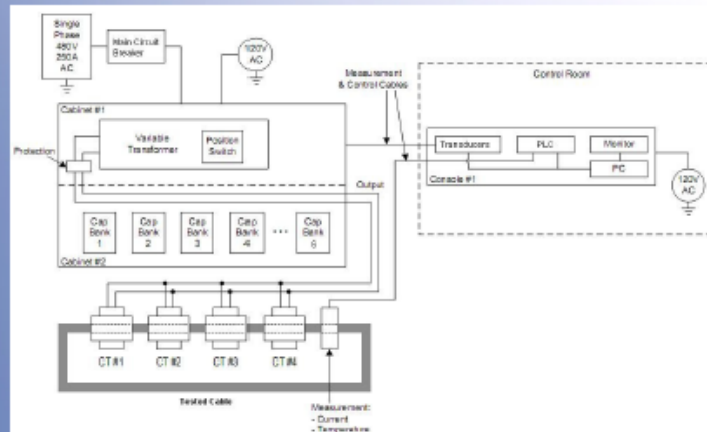
The motorized voltage regulator supplies the power to the primary winding (s) of the current transformers. Regulating Transformer adjust the input voltage of the transformer to achieve the proper required load.

Software

The system is equipped with user friendly software allowing you of:

- Performing measurements and taking readings automatically.
- Performing temperature corrections automatically.
- Showing real-time graphical and indicator value displays of current, voltage and temperature readings.
- Storing test results automatically.
- Viewing graphical analysis of current and previous test results.
- Generating extensive excel report for selected test's results. The report includes measured values, calculated values and graphical analysis for each connector.

The software offers a window to specify user configurable parameters that help control the system and perform the right test procedure regarding the cable's specifications.

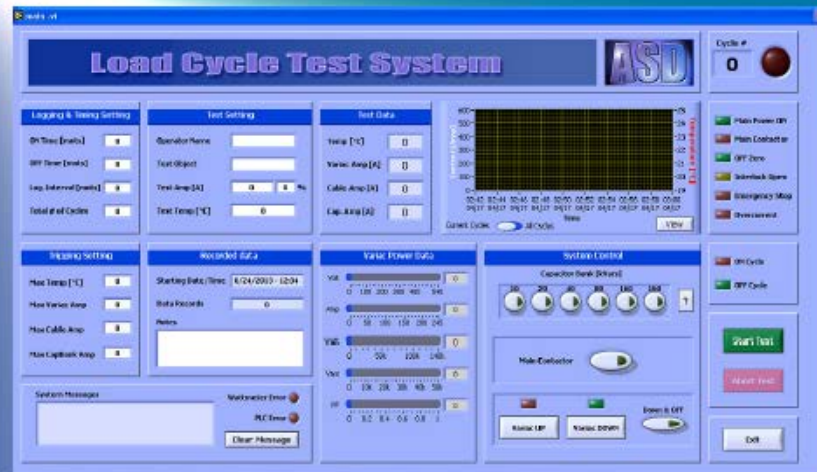


Automation Systems & Diagnostics, Inc
 1021 Davis Drive, Apex, NC 27523
 Phone: 919-842-2613, Fax: 919-380-1054
www.asdpower.com

APPENDIX B-2: ASD power Load Cycle Test System spec

Load Cycle Test System

Low Voltage, Current Test Set For Power Cable

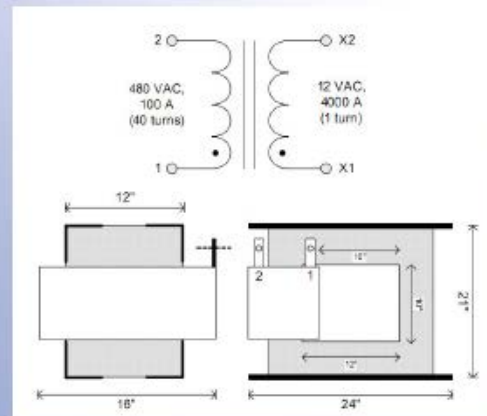


Technical Specifications

ASD reserves the right to change certain ratings or design parameters of individual components without affecting the overall system performance or guaranteed performance levels.

High current transformer assembly:

- Primary Winding: 480 VAC, 1 PH, 60 Hz
- Secondary Winding: 12 VAC, 4000 Amps, 1 turn
- Current transformer window is 10" x 10"
- One current transformers is installed on a platform with caster wheels (Note: Optional Two transformers can be installed on a platform)
- Platform dimensions: 16" x 24"
- Platform assembly can be wheeled around or forklift / crane liftable.



Automation Systems & Diagnostics, Inc
 1021 Davis Drive, Apex, NC 27523
 Phone: 919-842-2613, Fax: 919-380-1054
www.asdpower.com

APPENDIX C-1: Sample Cable Specification

138 kV Power Cables

138 kV XLPE - Copper Conductor

**TRADITIONAL WALL 850 MIL XLPE
COPPER NEUTRALS, COPPER COMPOSITE
LAMINATE SHEATH**

CABLE CONSTRUCTION

- Reverse Concentric Stranded Copper, Compressed Conductor or Milliken
- Super Smooth Conductor Shield
- Super Clean XLPE Insulation
- Traditional Wall – 850 mil XLPE
- True Triple Extrusion and Dry Cured
- Firmly Bonded Insulation Shield
- Copper Neutrals with Copper Composite Laminate Sheath
- Polyethylene Jacket with Extruded Semi-Conductive Outer Layer



CABLE DATA

Voltage Characteristics (kV)	
Max Voltage Rating	145
BIL Rating	650
Temperatures (°C)	
Nominal Conductor	90
Max. Emergency Conductor	105
Short Circuit Conductor	250
Minimum Installation	-10
Design Characteristics	
Design Standards	AEIC, IEC
Typical Test Voltages	240 kV / 15 min.
XLPE Loss Factor	0.0005
Relative Permittivity	2.3

APPENDIX C-2: Sample Cable Specification



Section 4

138 kV Power Cables

TRADITIONAL WALL 850 MIL XLPE COPPER NEUTRALS, COPPER COMPOSITE LAMINATE SHEATH



Conductor Size in kcmil ¹		750	1000	1250	1500	1750	2000	2500	3000	3500	4000	
Dimensional		Nominal										
Conductor Diameter	in	0.97	1.12	1.25	1.37	1.48	1.61	1.76	1.92	2.08	2.21	
	mm	24.7	28.5	31.8	34.8	37.6	40.9	44.7	48.8	52.8	56.1	
Diameter over Insulation	in	2.79	2.94	3.07	3.19	3.30	3.40	3.66	3.82	3.98	4.11	
	mm	70.8	74.6	78.0	81.0	83.8	86.4	93.0	97.1	101.0	104.4	
Diameter over Sheath	in	3.17	3.32	3.46	3.58	3.69	3.79	4.07	4.23	4.39	4.52	
	mm	80.6	84.4	87.8	90.8	93.6	96.2	103.4	107.5	111.4	114.8	
Overall Jacket Diameter	in	3.49	3.64	3.78	3.90	4.01	4.11	4.39	4.55	4.71	4.84	
	mm	88.7	92.5	95.9	98.9	101.7	104.3	111.5	115.6	119.5	123.0	
Total Weight	lbs/ft	6.8	7.8	8.8	9.7	10.7	11.6	13.8	15.6	17.5	19.3	
Min. Bending Radius (install/perm.)	in	70/52	73/55	76/57	78/58	80/60	82/62	88/66	91/68	94/71	97/73	
Maximum Pulling Tension	lbs	6,000	8,000	10,000	12,000	14,000	16,000	20,000	24,000	28,000	32,000	
Typical Shipping Reel Size												
Flange x Width	in	138x95	138x95	150x95	150x95	150x95	150x95	158x95	158x95	158x95	158x95	
Shipping Reel Capacity ²	ft	3,000	3,000	3,000	3,000	2,733	2,725	2,700	2,375	2,125	1,900	
Electrical												
Electrical Stress @ U₀												
Conductor Shield	kV/mm	6.1	5.9	5.7	5.5	5.4	5.3	5.1	5.0	4.9	4.9	
Insulation Shield	kV/mm	2.4	2.5	2.5	2.6	2.6	2.7	2.7	2.8	2.8	2.9	
Short Circuit for 0.5s³												
Conductor	kA	76.9	102.5	128.1	153.8	179.4	205.0	256.3	307.5	358.8	410.0	
Sheath	kA	43.9	44.2	44.6	44.9	45.2	45.5	46.2	46.6	47.0	47.4	
Conductor Resistance												
DC @ 20° C	Ω/kft	0.014	0.011	0.008	0.007	0.006	0.005	0.004	0.003	0.003	0.003	
DC @ 90° C	Ω/kft	0.018	0.014	0.011	0.009	0.008	0.007	0.005	0.005	0.004	0.003	
Capacitance	pF/ft	41.4	45.0	48.3	51.2	53.8	56.3	62.4	66.2	69.8	73.0	
Charging Current	Amps/kft	1.24	1.35	1.45	1.54	1.62	1.69	1.87	1.99	2.10	2.19	
Ampacity @ 90° C												
per circuit												
Typical Single Ductbank ⁴	Amps	750	870	970	1060	1140	1210	1455	1592	1714	1821	
Power Rating	MVA	180	208	232	254	273	290	348	381	410	436	
Typical Double Ductbank ⁴	Amps	640	740	820	890	950	1000	1206	1314	1410	1493	
Power Rating	MVA	153	177	196	213	228	240	289	315	338	357	

¹ 2500-4000 kcmil conductors are 5 segment Milliken conductors.
² Increased shipping reel capacity can be accommodated on request.
³ Declared values for 80 x 14 AWG copper wire screen with 6 mil copper tape shield. Larger wires can accommodate more current.
⁴ 4ft top of duct, 1°C-m/W native, 0.8°C-m/W ductbank backfill, 25°C Ambient, 75% if, 9" spacing, single-point or cross bonded

APPENDIX D-1: Thermocouple Specification



Thermocouple Probes
LS Series




TECHNICAL DATA

**Model TP-01 Beaded Thermocouple Wire Probe**

- Measurement range: -40 to 482°F (-40 to 250°C)
- For general purpose temperature applications
- Dimensions: Wire: 38" (96.5cm)

Model LS-181 Male Thermocouple Connector

- This type-k male thermocouple connector is constructed of glass-filled nylon for increased strength and wear resistance. The LS-181 is rated up 425°F (250°C) and is color coded according to ANSI thermocouple identification standards.

Model LS-182 Female Thermocouple Connector

- This type-k female thermocouple connector is constructed of glass-filled nylon for increased strength and wear resistance. The LS-182 is rated up 425°F (250°C) and is color coded according to ANSI thermocouple identification standards.

Model	Description
LS-103	Air/Gas Thermocouple Probe
LS-103-NIST	Air/Gas Thermocouple Probe & NIST
LS-104	Right Angle Thermocouple Surface Probe
LS-104-NIST	Right Angle TC Surface Probe & NIST
LS-107	Immersion Thermocouple Probe
LS-107-NIST	Immersion Thermocouple Probe & NIST
LS-109	Surface Thermocouple Probe
LS-109-NIST	Surface Thermocouple Probe & NIST
LS-134A	Needle Tip Thermocouple Probe
LS-134A-NIST	Needle Tip Thermocouple Probe & NIST
LS-139	Spring Loaded Surface Probe
LS-139-NIST	Spring Loaded Surface Probe & NIST
TP-01	Beaded Thermocouple Wire Probe
TP-01-NIST	Beaded Thermocouple Wire Probe & NIST
LS-181	Male Thermocouple Connector
LS-182	Female Thermocouple Connector

REED Instruments

1-877-849-2127 | info@reedinstruments.com | www.reedinstruments.com

APPENDIX E: Data logger Specification

USB-TEMP and USB-TC Series

Temperature Measurement Devices



The USB-TEMP Series provides temperature measurement flexibility as each channel can monitor any of the supported input types

Overview

All USB-TEMP and TC Series devices support thermocouple inputs. The USB-TEMP and USB-TEMP-AI also support RTD, thermistor, and semiconductor sensor measurements. In addition, voltage measurements are supported by the USB-TEMP-AI and USB-TC-AI. Each device also includes eight digital I/O lines.

The USB-TEMP and USB-TC Series offers the most accurate temperature measurement possible, since the internal measurement electronics accuracy exceeds the accuracy specifications of the temperature sensors.

The combination of the USB-TEMP and USB-TC Series and the Measurement Computing DAQ software suite gives you a complete data acquisition solution that will have you taking measurements in minutes.

Analog Input

The USB-TEMP and USB-TC each include eight thermocouple inputs. The USB-TEMP also supports RTD, thermistor, and semiconductor sensor measurements.

The USB-TEMP-AI and USB-TC-AI feature four thermocouple inputs plus four voltage inputs with ranges up to ± 10 V. The USB-TEMP-AI also supports RTD, thermistor, and semiconductor sensor measurements. The USB-TEMP-AI and USB-TC-AI also offer four voltage input channels with ranges from ± 1.25 V to ± 10 V.

A 24-bit analog-to-digital (A/D) converter is provided for each pair of analog inputs. Users can connect a different category of sensor to each temperature channel pair.

Open thermocouple detection (OTD) is provided to detect broken thermocouples. Cold junction compensation (CJC) sensors are provided for TC measurements, and built-in current excitation sources for resistive sensor measurements.

Sample Rate

Each channel can be sampled at up to two samples per second for a total device throughput of 16 samples per second.

Digital I/O

Eight independent, TTL-compatible digital I/O channels are used to monitor TTL-level inputs and communicate with external devices. The DIO lines on the USB-TEMP-AI and USB-TC-AI can also be used to generate alarms.

The digital I/O lines are software programmable for input or output.

Features

- Temperature and voltage measurements
- Thermocouples, RTDs, thermistors, semiconductor sensors
- 8 analog inputs
- 24-bit resolution
- 8 digital I/O
- 1 event counter

Supported Operating Systems

- Windows® 10/8/7/Vista®/XP, 32/64-bit
- Android™

Counter Input

USB-TEMP-AI and USB-TC-AI devices have a 32-bit event counter that accept frequency inputs up to 1 MHz. The internal counter increments when the TTL levels transition from low to high.

Calibration

USB-TEMP and USB-TC Series devices are factory-calibrated using a NIST-traceable calibration process. Specifications are guaranteed for one year.

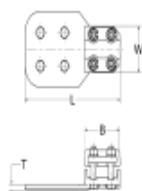
The USB-TEMP and USB-TC Series also supports field calibration for users to calibrate the device locally with the InstaCal utility.

InstaCal prompts you to run its calibration utility when you change from one sensor category to another. Allow the device to operate for at least 30 minutes before calibrating. This warm up time minimizes thermal drift and achieves the specified rated accuracy of measurements.

USB-TEMP and USB-TC Series Selection Chart

Model	Channels	Thermocouple Inputs	RTD, Thermistor, Semiconductor Sensor Inputs	Voltage Inputs
USB-TC	8	✓	—	—
USB-TEMP	8	✓	✓	—
USB-TC-AI	8	✓	—	✓
USB-TEMP-AI	8	✓	✓	✓

APPENDIX F: Cable termination specification


[On Line Catalog](#)


BURNDY Catalog Number	NAH4844N
UPC Number	7818100029577
Description	COPPER TERMINAL, 7.50 IN L
Status	Active

Web Use
BURNDY Product Line

Dimensional	
Pad Orientation	0A°
Width (in)	3.38
Length (in)	7.50
Thickness (in)	11/25
Height (in)	3.12
Size (Hex) or Size (Bolt)	1/2
Hole Size (Fraction)	9/16
Thickness	0.44
Size (Hex) or Size (Bolt) - in	0.50
B Length (in)	3.25
Pad Width (in)	4.00
E - in	1.75

General
Number of Conductors

1

Product Description

Cast Cu Alloy Terminal, 4 Holes,
500-2000 KCMIL, 230 kV, 1.75 IN
Stud Hole Spacing, Bolted, Cable
to Pad, 0.56 IN Hole Dia, 1/2 IN-
13 Bolt Dia

Copper Solid Size (Range)
Copper Stranded (Range)

Conductor(s)
N/A
500 kcmil-2000 kcmil

Type of Hardware
Pad Configuration
Type of Plating
Connector Type
Plated (Yes or No)
Product Material

Physical
DURIUMâ€¦ Silicon Bronze
4 x 4 - 4 holes
Unplated
Terminal
N
Copper Alloy

ROHS Compatible
Documentation

Approvals / Certifications
Exempt

For further technical assistance, please contact us

BURNDY LLC - USA
47, industrial Park Drive
Manchester NH03109

BURNDY Technical Services
47, industrial Park Drive
Manchester NH03109

Hours: 8.00 AM - 5.00 PM
Monday - Friday
Phone: 000-346-4175

APPENDIX G: 1530A at 19 hours Data

Sample	Date	Time	Time Interval	Time (minut)	Current	Tb_con							Temp_Jac (°C)	Ambient (°C)
						du (°C)	Tb_ins (°C)	Tb_jac (°C)	Ta_condu (%)	Ta_ins (°C)	Ta_Jac (°C)			
0	10/7/2016	9:48:45	0:00	0	0	19.88	19.87	20.11	20.31	19.67	20.04	20.68	20.07	
1	10/7/2016	9:49:45	0:01	1	1546	20.61	19.96	20.24	20.46	19.72	20.12	20.71	20.19	
2	10/7/2016	9:50:45	0:02	2	1546	20.72	20.18	20.17	20.88	19.76	20.3	20.67	20.09	
3	10/7/2016	9:51:45	0:03	3	1546	21.41	19.84	20.18	21.32	19.79	20.22	20.7	20.08	
4	10/7/2016	9:52:45	0:04	4	1546	22.03	20.06	20.29	21.77	19.88	20.09	20.91	20.11	
5	10/7/2016	9:53:45	0:05	5	1542	22.27	20.26	20.11	22.02	19.81	20.22	20.46	20.18	
6	10/7/2016	9:54:45	0:06	6	1542	22.89	20.05	20.2	22.33	19.85	20.25	20.76	20.12	
7	10/7/2016	9:55:45	0:07	7	1546	23.51	20.05	20.12	22.85	20.12	20.32	20.69	20.12	
8	10/7/2016	9:56:45	0:08	8	1546	23.8	20.19	20.3	23.27	20.11	20.29	20.89	20.2	
9	10/7/2016	9:57:45	0:09	9	1538	23.71	20.36	20.27	23.54	20.21	20.34	20.83	20.24	
10	10/7/2016	9:58:45	0:10	10	1542	24.79	20.28	20.31	23.81	20.36	20.37	20.76	20.22	
11	10/7/2016	9:59:45	0:11	11	1546	24.58	20.6	20.38	24.32	20.54	20.39	20.92	20.51	
12	10/7/2016	10:00:45	0:12	12	1538	25.36	20.41	20.5	24.49	20.67	20.48	20.92	20.21	
13	10/7/2016	10:01:45	0:13	13	1546	25.64	20.68	20.65	24.8	20.74	20.76	20.97	20.21	
14	10/7/2016	10:02:45	0:14	14	1546	26.2	20.35	20.54	24.99	20.8	20.61	21.29	20.31	
15	10/7/2016	10:03:45	0:15	15	1546	26.25	20.85	20.62	25.38	21.04	20.79	21.15	20.12	
16	10/7/2016	10:04:45	0:16	16	1546	26.78	20.73	20.71	25.78	21.19	20.92	21.43	20.32	
17	10/7/2016	10:05:45	0:17	17	1546	26.97	20.93	20.84	26.07	21.44	20.97	21.29	20.24	
18	10/7/2016	10:06:45	0:18	18	1546	27.59	21.09	21	26.34	21.47	21.19	21.32	20.27	
19	10/7/2016	10:07:45	0:19	19	1546	27.66	21.21	20.96	26.66	21.65	21.26	21.66	20.18	
20	10/7/2016	10:08:45	0:20	20	1538	28.03	21.19	21.15	26.93	21.68	21.25	21.7	20.23	
21	10/7/2016	10:09:45	0:21	21	1542	28.02	21.39	21.33	27.21	21.99	21.46	21.68	20.11	
22	10/7/2016	10:10:45	0:22	22	1546	28.81	21.43	21.42	27.41	22.14	21.69	21.75	20.2	
23	10/7/2016	10:11:45	0:23	23	1542	29.05	21.79	21.4	27.72	22.24	21.74	21.96	20.15	
24	10/7/2016	10:12:45	0:24	24	1542	29.52	21.83	21.58	27.82	22.55	21.88	22.15	19.94	
25	10/7/2016	10:13:45	0:25	25	1538	29.08	21.98	21.67	28.21	22.7	21.93	22.11	20.39	
26	10/7/2016	10:14:45	0:26	26	1542	29.56	22.22	21.86	28.41	22.86	22.08	22.58	20.38	
27	10/7/2016	10:15:45	0:27	27	1542	29.91	22.26	22.05	28.77	22.98	22.09	22.74	20.25	
28	10/7/2016	10:16:45	0:28	28	1542	30.32	22.51	22.05	29	23.11	22.45	22.65	20.33	
29	10/7/2016	10:17:45	0:29	29	1542	30.63	22.63	22.13	29.24	23.42	22.4	22.64	20.14	
30	10/7/2016	10:18:45	0:30	30	1538	30.41	22.79	22.35	29.52	23.47	22.67	22.88	20.36	
31	10/7/2016	10:19:45	0:31	31	1542	30.94	22.91	22.44	29.75	23.69	22.7	23.06	20.38	
32	10/7/2016	10:20:45	0:32	32	1542	31.16	23.21	22.6	30.09	23.81	22.88	23.16	20.26	
33	10/7/2016	10:21:45	0:33	33	1534	31.35	23.1	22.82	30.15	24.18	23.15	23.23	20.14	
34	10/7/2016	10:22:45	0:34	34	1538	32	23.31	22.82	30.46	24.15	23.31	23.32	20.25	
35	10/7/2016	10:23:45	0:35	35	1538	32.15	23.46	23.12	30.8	24.48	23.26	23.52	20.18	
36	10/7/2016	10:24:45	0:36	36	1538	32.04	23.48	23.15	30.84	24.61	23.45	23.62	20.32	
37	10/7/2016	10:25:45	0:37	37	1538	32.44	23.88	23.27	31.16	24.65	23.63	23.68	20.2	
38	10/7/2016	10:26:45	0:38	38	1542	32.72	24.01	23.39	31.41	25.04	23.72	24.02	20.33	
39	10/7/2016	10:27:45	0:39	39	1542	33.13	24.33	23.61	31.68	25.17	23.93	24.11	20.26	
40	10/7/2016	10:28:45	0:40	40	1542	33	24.24	23.8	31.9	25.32	24.03	24.23	20.32	
41	10/7/2016	10:29:45	0:41	41	1546	33.29	24.29	23.95	32.03	25.36	24.15	24.21	20.17	
42	10/7/2016	10:30:45	0:42	42	1546	33.69	24.58	23.99	32.29	25.7	24.26	24.4	20.65	
43	10/7/2016	10:31:45	0:43	43	1542	33.66	24.69	24.17	32.41	25.7	24.43	24.79	20.13	
44	10/7/2016	10:32:45	0:44	44	1546	34.13	24.94	24.29	32.81	25.88	24.61	24.61	20.47	
45	10/7/2016	10:33:45	0:45	45	1542	34.58	24.7	24.47	33.09	26.04	24.82	24.77	20.44	
46	10/7/2016	10:34:45	0:46	46	1538	34.68	25.19	24.48	33.22	26.25	24.89	24.9	20.27	
47	10/7/2016	10:35:45	0:47	47	1542	34.68	25.43	24.6	33.35	26.5	24.98	25.02	20.24	
48	10/7/2016	10:36:45	0:48	48	1542	35.08	25.26	24.75	33.61	26.67	25.14	25.12	20.36	
49	10/7/2016	10:37:45	0:49	49	1542	34.93	25.5	24.94	33.66	26.79	25.2	25.29	20.2	
50	10/7/2016	10:38:45	0:50	50	1542	35.31	25.75	24.92	33.95	26.96	25.33	25.38	20.37	
51	10/7/2016	10:39:45	0:51	51	1542	35.12	25.53	25.15	34.23	27.19	25.41	25.63	20.42	
52	10/7/2016	10:40:45	0:52	52	1542	35.57	25.74	25.28	34.2	27.43	25.78	25.65	20.99	
53	10/7/2016	10:41:45	0:53	53	1546	35.46	25.88	25.5	34.51	27.46	25.64	25.78	20.32	
54	10/7/2016	10:42:45	0:54	54	1538	35.62	26.14	25.58	34.7	27.65	25.87	26.04	20.35	
55	10/7/2016	10:43:45	0:55	55	1538	35.9	26.3	25.69	34.86	27.72	25.97	26.18	20.23	
56	10/7/2016	10:44:45	0:56	56	1542	35.85	26.23	25.72	35.17	28	26.15	26.21	20.35	
57	10/7/2016	10:45:45	0:57	57	1542	36.25	26.67	25.87	35.26	28.02	26.27	26.19	20.5	
58	10/7/2016	10:46:45	0:58	58	1546	36.29	26.65	25.96	35.56	28.21	26.42	26.49	20.33	
59	10/7/2016	10:47:45	0:59	59	1542	36.43	27.01	26.08	35.93	28.33	26.55	26.55	20.4	
60	10/7/2016	10:48:45	1:00	60	1542	36.51	27.19	26.18	35.99	28.45	26.8	26.61	20.55	
61	10/7/2016	10:49:45	1:01	61	1542	36.66	27.32	26.32	36.15	28.73	26.9	26.78	20.25	
62	10/7/2016	10:50:45	1:02	62	1542	36.92	27.04	26.51	36.31	28.68	26.86	26.77	20.38	
63	10/7/2016	10:51:45	1:03	63	1542	37.03	27.29	26.49	36.35	28.81	27.14	27.08	20.32	
64	10/7/2016	10:52:45	1:04	64	1534	37.52	27.47	26.75	36.69	28.99	27.22	27.11	20.49	
65	10/7/2016	10:53:45	1:05	65	1542	37.41	27.54	26.76	36.85	29.26	27.42	27.2	20.46	
66	10/7/2016	10:54:45	1:06	66	1534	37.29	27.78	26.92	37.03	29.32	27.54	27.23	20.38	
67	10/7/2016	10:55:45	1:07	67	1542	37.74	28.07	27.09	37.25	29.54	27.71	27.59	20.44	
68	10/7/2016	10:56:45	1:08	68	1538	37.86	27.93	27.09	37.42	29.45	27.64	27.48	20.47	
69	10/7/2016	10:57:45	1:09	69	1542	37.82	28.04	27.2	37.52	29.74	27.9	27.76	20.48	
70	10/7/2016	10:58:45	1:10	70	1538	38.06	28.09	27.37	37.63	29.94	27.91	27.73	20.7	
71	10/7/2016	10:59:45	1:11	71	1546	38.47	28.38	27.45	37.93	30.01	28.06	27.97	20.36	
72	10/7/2016	11:00:45	1:12	72	1538	38.63	28.65	27.81	37.98	30.03	28.09	27.98	20.46	
73	10/7/2016	11:01:45	1:13	73	1542	38.49	28.55	27.71	38.08	30.33	28.22	28.04	20.48	
74	10/7/2016	11:02:45	1:14	74	1542	38.88	28.74	27.84	38.47	30.41	28.45	28.16	20.39	
75	10/7/2016	11:03:45	1:15	75	1546	39.06	28.72	27.94	38.49	30.57	28.44	28.29	20.42	
76	10/7/2016	11:04:45	1:16	76	1542	39.09	28.93	28.12	38.81	30.63	28.54	28.35	20.69	
77	10/7/2016	11:05:45	1:17	77	1542	39.45	28.99	28.24	38.84	30.68	28.66	28.5	20.54	
78	10/7/2016	11:06:45	1:18	78	1542	39.2	29.36	28.34	39.16	30.85	28.88	28.65	20.42	
79	10/7/2016	11:07:45	1:19	79	1542	39.38	29.25	28.35	39.13	31.13	29.07	28.65	20.53	
80	10/7/2016	11:08:45	1:20	80	1546	39.85	29.49	28.39	39.39	31.07	29.13	28.85	20.47	
81	10/7/2016	11:09:45	1:21	81	1546	39.95	29.5	28.65	39.58	31.38	29.24	28.83	20.57	
82	10/7/2016	11:10:45	1:22	82	1546	39.92	29.68	28.63	39.83	31.47	29.18	29	20.44	
83	10/7/2016	11:11:45	1:23	83	1542	40.21	29.65	28.84	39.85	31.63	29.56	29.05	20.71	
84	10/7/2016	11:12:45	1:24	84	1546	40.15	29.9</							

104	10/7/2016	11:32:45	1:44	104	1538	42.99	31.84	30.7	42.9	34.04	31.4	31.14	20.71
105	10/7/2016	11:33:45	1:45	105	1542	43.27	32.06	30.8	43.08	34.12	31.47	31.16	20.55
106	10/7/2016	11:34:45	1:46	106	1542	43.38	32.05	30.86	43.26	34.04	31.46	30.96	20.52
107	10/7/2016	11:35:45	1:47	107	1546	43.38	32.11	30.99	43.41	34.35	31.77	31.33	20.64
108	10/7/2016	11:36:45	1:48	108	1546	43.67	32.15	31.08	43.58	34.39	31.9	31.36	20.41
109	10/7/2016	11:37:45	1:49	109	1546	43.79	32.33	31.15	43.74	34.44	31.82	31.29	20.87
110	10/7/2016	11:38:45	1:50	110	1546	43.85	32.24	31.08	43.85	34.64	32.01	31.4	20.55
111	10/7/2016	11:39:45	1:51	111	1542	44.05	32.42	31.27	43.99	34.58	32.01	31.44	20.59
112	10/7/2016	11:40:45	1:52	112	1546	44.04	32.52	31.37	44.09	34.75	32.18	31.6	20.37
113	10/7/2016	11:41:45	1:53	113	1542	44.15	32.72	31.42	44.11	34.94	32.18	31.71	20.67
114	10/7/2016	11:42:45	1:54	114	1546	44.36	32.69	31.56	44.43	35.06	32.34	31.94	20.56
115	10/7/2016	11:43:45	1:55	115	1546	44.59	32.81	31.56	44.44	35.09	32.31	31.64	20.55
116	10/7/2016	11:44:45	1:56	116	1542	44.73	32.89	31.68	44.51	35.18	32.41	32.04	20.55
117	10/7/2016	11:45:45	1:57	117	1546	44.66	32.9	31.8	44.66	35.49	32.6	31.78	20.68
118	10/7/2016	11:46:45	1:58	118	1542	44.94	32.99	31.56	44.82	35.25	32.64	31.94	20.6
119	10/7/2016	11:47:45	1:59	119	1546	44.92	32.85	31.77	44.77	35.44	32.78	32.13	20.59
120	10/7/2016	11:48:45	2:00	120	1546	45.01	33.38	31.89	45.05	35.62	32.78	32	20.53
121	10/7/2016	11:49:45	2:01	121	1542	45.27	33.22	32.12	45.06	35.63	32.79	32.31	20.59
122	10/7/2016	11:50:45	2:02	122	1538	45.14	33.26	31.97	45.3	35.68	32.91	32.33	20.48
123	10/7/2016	11:51:45	2:03	123	1542	45.3	33.38	32.02	45.31	35.85	33.12	32.52	20.71
124	10/7/2016	11:52:45	2:04	124	1542	45.46	33.68	32.06	45.48	35.93	33.29	32.37	20.68
125	10/7/2016	11:53:45	2:05	125	1542	45.68	33.62	32.39	45.54	36	33.12	32.62	20.65
126	10/7/2016	11:54:45	2:06	126	1542	45.73	33.59	32.31	45.63	36.08	33.22	32.84	20.5
127	10/7/2016	11:55:45	2:07	127	1542	45.65	33.66	32.34	45.96	36.19	33.37	32.68	20.68
128	10/7/2016	11:56:45	2:08	128	1542	46.04	33.75	32.53	45.95	36.26	33.57	32.83	20.59
129	10/7/2016	11:57:45	2:09	129	1542	46.08	34	32.58	46.02	36.38	33.54	32.75	20.58
130	10/7/2016	11:58:45	2:10	130	1542	46.29	33.94	32.83	46.21	36.47	33.65	32.91	20.7
131	10/7/2016	11:59:45	2:11	131	1542	46.32	34	32.77	46.2	36.52	33.67	33.1	20.74
132	10/7/2016	12:00:45	2:12	132	1542	46.26	33.97	32.84	46.47	36.44	33.78	33	20.64
133	10/7/2016	12:01:45	2:13	133	1542	46.45	34.25	32.86	46.47	36.71	34.04	32.99	20.62
134	10/7/2016	12:02:45	2:14	134	1542	46.34	34.07	32.96	46.62	36.79	33.85	33.15	20.64
135	10/7/2016	12:03:45	2:15	135	1542	46.62	34.22	32.92	46.78	36.76	34.05	33.18	20.67
136	10/7/2016	12:04:45	2:16	136	1546	46.79	34.29	33.05	46.76	36.96	34.19	33.48	20.68
137	10/7/2016	12:05:45	2:17	137	1542	46.79	34.53	33.08	46.99	36.96	34.26	33.41	20.49
138	10/7/2016	12:06:45	2:18	138	1546	47.29	34.76	33.21	47.08	37.08	34.23	33.54	20.43
139	10/7/2016	12:07:45	2:19	139	1546	47.03	34.7	33.19	47.14	37.02	34.23	33.41	20.53
140	10/7/2016	12:08:45	2:20	140	1546	47.04	34.76	33.21	47.15	37.44	34.38	33.32	20.59
141	10/7/2016	12:09:45	2:21	141	1546	47.18	34.79	33.34	47.37	37.3	34.45	33.54	20.59
142	10/7/2016	12:10:45	2:22	142	1546	47.3	34.67	33.49	47.44	37.41	34.61	33.61	20.74
143	10/7/2016	12:11:45	2:23	143	1546	47.63	34.79	33.55	47.4	37.41	34.53	33.63	20.8
144	10/7/2016	12:12:45	2:24	144	1546	47.53	34.82	33.49	47.56	37.66	34.58	33.73	20.68
145	10/7/2016	12:13:45	2:25	145	1542	47.69	34.92	33.62	47.8	37.58	34.54	33.7	20.5
146	10/7/2016	12:14:45	2:26	146	1546	47.73	35.02	33.66	47.79	37.71	34.61	33.94	20.65
147	10/7/2016	12:15:45	2:27	147	1546	47.84	34.91	33.71	48.02	37.68	34.9	33.81	20.58
148	10/7/2016	12:16:45	2:28	148	1542	47.84	35.22	33.78	48.12	37.88	34.96	34.01	20.65
149	10/7/2016	12:17:45	2:29	149	1542	47.95	35.22	33.84	48.14	37.84	34.89	33.83	20.7
150	10/7/2016	12:18:45	2:30	150	1546	48.11	35.54	34.01	48.2	37.99	34.96	34.2	20.68
151	10/7/2016	12:19:45	2:31	151	1546	48.15	35.35	33.94	48.3	38.13	35.01	34.17	20.53
152	10/7/2016	12:20:45	2:32	152	1542	48.05	35.41	34.01	48.24	37.98	35.09	34.2	20.45
153	10/7/2016	12:21:45	2:33	153	1542	48.27	35.39	33.96	48.44	38.03	35.2	34.3	20.59
154	10/7/2016	12:22:45	2:34	154	1542	48.57	35.26	34.13	48.6	38.32	35.15	34.19	20.6
155	10/7/2016	12:23:45	2:35	155	1546	48.6	35.38	34.18	48.6	38.39	35.33	34.42	20.64
156	10/7/2016	12:24:45	2:36	156	1546	48.72	35.6	34.35	48.79	38.3	35.39	34.43	20.8
157	10/7/2016	12:25:45	2:37	157	1542	48.65	35.71	34.21	48.96	38.47	35.27	34.61	20.55
158	10/7/2016	12:26:45	2:38	158	1542	48.78	35.8	34.2	49	38.54	35.36	34.48	20.6
159	10/7/2016	12:27:45	2:39	159	1546	48.95	35.92	34.32	49.02	38.75	35.49	34.75	20.79
160	10/7/2016	12:28:45	2:40	160	1542	49.02	35.79	34.48	49.15	38.76	35.52	34.64	20.66
161	10/7/2016	12:29:45	2:41	161	1546	49.15	35.96	34.49	49.21	38.72	35.52	34.6	20.57
162	10/7/2016	12:30:45	2:42	162	1546	49.09	36.03	34.57	49.31	38.67	35.48	34.83	20.72
163	10/7/2016	12:31:45	2:43	163	1538	49.21	36.05	34.6	49.44	38.94	35.71	34.85	20.73
164	10/7/2016	12:32:45	2:44	164	1542	49.22	36.15	34.64	49.47	39.02	35.71	34.8	20.66
165	10/7/2016	12:33:45	2:45	165	1542	49.52	36.2	34.7	49.48	39.18	35.91	34.99	20.82
166	10/7/2016	12:34:45	2:46	166	1542	49.56	36.16	34.91	49.63	39.01	35.86	34.83	20.58
167	10/7/2016	12:35:45	2:47	167	1542	49.46	36.4	34.82	49.67	39.08	36.05	34.92	20.63
168	10/7/2016	12:36:45	2:48	168	1542	49.48	36.46	34.95	49.76	39.13	36.06	35.01	20.66
169	10/7/2016	12:37:45	2:49	169	1542	49.77	36.24	34.82	49.8	39.14	36.02	35.02	20.57
170	10/7/2016	12:38:45	2:50	170	1542	49.7	36.59	34.98	49.97	39.23	36.13	35.17	20.75
171	10/7/2016	12:39:45	2:51	171	1542	49.69	36.25	34.94	50.05	39.24	36.19	35.24	20.55
172	10/7/2016	12:40:45	2:52	172	1542	49.9	36.54	34.97	50.16	39.49	36.28	35.34	20.66
173	10/7/2016	12:41:45	2:53	173	1542	49.98	36.56	35.22	50.1	39.46	36.34	35.43	20.72
174	10/7/2016	12:42:45	2:54	174	1542	50.06	36.6	34.92	50.23	39.51	36.44	35.25	20.74
175	10/7/2016	12:43:45	2:55	175	1542	49.93	36.68	35.02	50.06	39.69	36.52	35.3	20.53
176	10/7/2016	12:44:45	2:56	176	1542	50.28	36.6	35.23	50.35	39.72	36.5	35.53	20.82
177	10/7/2016	12:45:45	2:57	177	1546	50.21	36.77	35.28	50.25	39.75	36.61	35.43	20.76
178	10/7/2016	12:46:45	2:58	178	1542	50.21	36.72	35.26	50.51	39.76	36.58	35.37	20.65
179	10/7/2016	12:47:45	2:59	179	1546	50.5	36.62	35.39	50.87	39.76	36.57	35.47	20.73
180	10/7/2016	12:48:45	3:00	180	1546	50.34	36.63	35.39	50.67	39.91	36.48	35.6	20.74
181	10/7/2016	12:49:45	3:01	181	1546	50.54	36.87	35.54	50.78	40.14	36.51	35.5	20.73
182	10/7/2016	12:50:45	3:02	182	1542	50.61	36.81	35.38	50.78	40.1	36.75	35.58	20.85
183	10/7/2016	12:51:45	3:03	183	1542	50.7	37.26	35.5	50.91	39.94	36.81	35.68	20.55
184	10/7/2016	12:52:45	3:04	184	1546	50.89	37.15	35.45	51.02	40.07	36.73	35.81	20.86
185	10/7/2016	12:53:45	3:05	185	1542	50.74	37.18	35.83	51.03	40.13	36.83	35.8	20.63
186	10/7/2016	12:54:45	3:06	186	1542	50.99	37.25	35.66	51.13	40.42	36.98	36.03	20.64
187	10/7/2016	12:55:45	3:07	187	1542	51.03	37.35	35.57	51.25	40.25	37.22	36.06	20.88
188	10/7/2016	12:56:45	3:08	188	1542	50.99	37.54	35.69	51.39	40.32	37.07	35.9	

APPENDIX H: 2030A at 24 hours Data

Sample	Date	Time	Time Inter	Current (A)	Tb_condu (°C)	Tb_ins (°C)	Tb_jac (°C)	Ta_condu (°C)	Ta_ins (°C)	Ta_jac (°C)	Temp_jac (°C)	Ambient (°C)
0	10/14/2016	9:56:50	0:00	0	19.47	19.89	19.68	19.75	19.91	19.83	20.13	19.3
1	10/14/2016	9:57:50	0:01	0	19.58	19.73	19.89	19.91	20.12	20	20.25	19.4
2	10/14/2016	9:58:50	0:02	182	19.45	19.69	19.92	20.04	20.14	20.09	20.27	19.6
3	10/14/2016	9:59:50	0:03	2030	19.78	20.07	19.97	20.18	20.11	20.21	20.21	19.53
4	10/14/2016	10:00:50	0:04	2030	20.47	19.98	20.1	20.67	20.11	20.39	20.44	19.74
5	10/14/2016	10:01:50	0:05	2030	21.51	19.89	20.03	21.33	20.15	20.32	20.55	19.65
6	10/14/2016	10:02:50	0:06	2026	22.34	19.82	20.14	22.11	20.06	20.3	20.61	19.86
7	10/14/2016	10:03:50	0:07	2030	23.34	19.87	20.04	22.6	20.33	20.27	20.65	19.73
8	10/14/2016	10:04:50	0:08	2034	23.95	20.09	20.18	23.44	20.47	20.25	20.46	20.12
9	10/14/2016	10:05:50	0:09	2034	24.83	19.88	20.13	23.98	20.49	20.01	20.51	19.93
10	10/14/2016	10:06:50	0:10	2026	25.8	20.29	20.21	24.5	20.56	20.25	20.56	19.93
11	10/14/2016	10:07:50	0:11	2030	26.62	20.23	20.32	25.28	20.63	20.19	20.54	20.08
12	10/14/2016	10:08:50	0:12	2026	27.04	20.21	20.42	25.73	20.91	20.34	20.65	19.96
13	10/14/2016	10:09:50	0:13	2026	27.77	20.22	20.51	26.26	21.07	20.45	20.79	20.04
14	10/14/2016	10:10:50	0:14	2030	28.51	20.67	20.53	26.78	21.29	20.49	20.81	20.06
15	10/14/2016	10:11:50	0:15	2022	28.76	20.63	20.6	27.45	21.45	20.54	21.01	19.97
16	10/14/2016	10:12:50	0:16	2030	29.53	20.84	20.71	27.97	21.59	20.8	21.45	20.02
17	10/14/2016	10:13:50	0:17	2026	30.08	21.26	20.98	28.45	21.91	20.92	21.35	19.98
18	10/14/2016	10:14:50	0:18	2030	30.58	21.37	21.04	29.08	22.24	21.07	21.56	20.14
19	10/14/2016	10:15:50	0:19	2026	31.45	21.37	21.13	29.59	22.31	21.25	21.5	20.29
20	10/14/2016	10:16:50	0:20	2030	31.54	21.64	21.31	30	22.59	21.33	21.8	20.19
21	10/14/2016	10:17:50	0:21	2026	32.15	22.01	21.58	30.52	22.83	21.57	21.92	20.37
22	10/14/2016	10:18:50	0:22	2030	32.99	22.02	21.65	31.04	23.14	21.81	22.02	20.19
23	10/14/2016	10:19:50	0:23	2030	33.44	22.26	21.89	31.45	23.28	22.05	22.57	20.35
24	10/14/2016	10:20:50	0:24	2026	33.8	22.55	21.99	31.86	23.59	22.24	22.43	20.27
25	10/14/2016	10:21:50	0:25	2026	34.37	22.42	22.18	32.43	23.84	22.36	22.66	20.18
26	10/14/2016	10:22:50	0:26	2030	34.69	23.04	22.44	32.79	24.28	22.63	23.06	20.26
27	10/14/2016	10:23:50	0:27	2026	35.23	22.94	22.67	33.18	24.43	22.84	23.12	20.36
28	10/14/2016	10:24:50	0:28	2030	35.72	23.19	22.81	33.76	24.77	22.97	23.3	20.13
29	10/14/2016	10:25:50	0:29	2022	36.04	23.64	23.14	34.05	24.97	23.3	23.49	20.2
30	10/14/2016	10:26:50	0:30	2026	36.49	23.88	23.17	34.4	25.2	23.54	23.58	20.19
31	10/14/2016	10:27:50	0:31	2030	36.98	23.94	23.43	34.89	25.52	23.73	23.94	20.47
32	10/14/2016	10:28:50	0:32	2026	37.46	24.23	23.64	35.2	25.75	24.06	24.01	20.3
33	10/14/2016	10:29:50	0:33	2026	37.69	24.53	24.03	35.65	26.08	24.17	24.22	20.28
34	10/14/2016	10:30:50	0:34	2030	37.87	24.9	23.98	36.19	26.29	24.4	24.5	20.3
35	10/14/2016	10:31:50	0:35	2030	38.42	25.08	24.4	36.47	26.66	24.61	24.68	20.37
36	10/14/2016	10:32:50	0:36	2026	38.73	25.17	24.58	36.88	26.82	24.98	24.81	20.21
37	10/14/2016	10:33:50	0:37	2026	38.79	25.39	24.81	37.26	27.16	25.14	24.96	20.29
38	10/14/2016	10:34:50	0:38	2022	39.05	25.85	25.02	37.68	27.37	25.29	25.27	20.47
39	10/14/2016	10:35:50	0:39	2022	39.23	26.19	25.21	37.92	27.74	25.57	25.57	20.5
40	10/14/2016	10:36:50	0:40	2022	39.64	26.38	25.36	38.33	27.93	25.76	25.75	20.5
41	10/14/2016	10:37:50	0:41	2026	40.08	26.59	25.64	38.76	28.21	26.04	26.03	20.35
42	10/14/2016	10:38:50	0:42	2026	40.06	26.72	25.82	39.06	28.43	26.28	26.07	20.32
43	10/14/2016	10:39:50	0:43	2026	40.63	27.03	26.13	39.6	28.78	26.44	26.13	20.22
44	10/14/2016	10:40:50	0:44	2030	40.84	27.15	26.4	40.06	29.06	26.71	26.77	20.34
45	10/14/2016	10:41:50	0:45	2022	41.08	27.46	26.38	40.34	29.28	26.93	26.75	20.59
46	10/14/2016	10:42:50	0:46	2022	41.48	27.74	26.81	40.63	29.65	27.05	26.99	20.59
47	10/14/2016	10:43:50	0:47	2022	41.9	27.9	26.96	40.99	29.77	27.4	27.18	20.33
48	10/14/2016	10:44:50	0:48	2022	42.19	28.17	27.11	41.42	30.04	27.71	27.43	20.4
49	10/14/2016	10:45:50	0:49	2026	42.29	28.51	27.43	41.67	30.31	27.78	27.68	20.67
50	10/14/2016	10:46:50	0:50	2022	42.7	28.48	27.53	42.12	30.56	28.08	27.79	20.49
51	10/14/2016	10:47:50	0:51	2026	43.02	28.71	27.8	42.45	30.65	28.3	28.06	20.34
52	10/14/2016	10:48:50	0:52	2030	43.29	29.17	27.95	42.74	31.17	28.45	28.21	20.44
53	10/14/2016	10:49:50	0:53	2022	43.87	29.32	28.23	43.12	31.37	28.71	28.52	20.34
54	10/14/2016	10:50:50	0:54	2026	43.82	29.45	28.34	43.44	31.66	28.9	28.52	20.62
55	10/14/2016	10:51:50	0:55	2026	44.28	29.76	28.46	43.81	31.95	29.24	28.77	20.37
56	10/14/2016	10:52:50	0:56	2022	44.66	29.86	28.76	44.12	32.21	29.33	28.8	20.7
57	10/14/2016	10:53:50	0:57	2022	44.78	30.26	29.05	44.53	32.44	29.58	29.27	20.28
58	10/14/2016	10:54:50	0:58	2026	45.33	30.26	29.16	44.83	32.74	29.79	29.45	20.37
59	10/14/2016	10:55:50	0:59	2018	45.59	30.73	29.38	45.17	33.1	30.01	29.71	20.48
60	10/14/2016	10:56:50	1:00	2022	46.1	30.82	29.54	45.57	33.27	30.25	29.94	20.39
61	10/14/2016	10:57:50	1:01	2026	46.24	31.21	29.9	45.89	33.4	30.48	30.14	20.46
62	10/14/2016	10:58:50	1:02	2022	46.53	31.29	30.01	46.11	33.68	30.64	30.29	20.58
63	10/14/2016	10:59:50	1:03	2022	46.8	31.46	30.13	46.54	33.88	30.82	30.48	20.33
64	10/14/2016	11:00:50	1:04	2022	47.07	31.84	30.35	46.79	34.32	31.06	30.49	20.53
65	10/14/2016	11:01:50	1:05	2022	47.4	31.91	30.61	47.07	34.35	31.4	30.8	20.53
66	10/14/2016	11:02:50	1:06	2026	47.76	31.92	30.83	47.43	34.71	31.56	30.85	20.36
67	10/14/2016	11:03:50	1:07	2026	48.15	32.53	30.83	47.64	34.96	31.45	31.23	20.55
68	10/14/2016	11:04:50	1:08	2022	48.18	32.56	31.13	48.03	35.11	31.76	31.23	20.36
69	10/14/2016	11:05:50	1:09	2022	48.5	32.71	31.44	48.09	35.2	31.93	31.44	20.72
70	10/14/2016	11:06:50	1:10	2026	48.7	32.87	31.46	48.66	35.49	32.21	31.73	20.55
71	10/14/2016	11:07:50	1:11	2022	49.27	33	31.7	48.76	35.83	32.39	31.86	20.61
72	10/14/2016	11:08:50	1:12	2026	49.6	33.25	31.89	49.12	36.08	32.67	31.95	20.58
73	10/14/2016	11:09:50	1:13	2022	49.61	33.47	32.11	49.6	36.18	32.9	32.36	20.51
74	10/14/2016	11:10:50	1:14	2026	49.93	33.47	32.33	49.67	36.57	32.87	32.46	20.42
75	10/14/2016	11:11:50	1:15	2026	50.28	34.05	32.52	50.12	36.72	33.15	32.74	20.55
76	10/14/2016	11:12:50	1:16	2022	50.67	33.87	32.74	50.32	36.91	33.36	32.71	20.72
77	10/14/2016	11:13:50	1:17	2026	50.99	34.22	32.7	50.36	37.07	33.62	32.96	20.72
78	10/14/2016	11:14:50	1:18	2022	51.14	34.28	33.02	50.93	37.45	33.77	33.3	20.72
79	10/14/2016	11:15:50	1:19	2026	51.35	34.54	33.12	51.19	37.61	33.87	33.31	20.67
80	10/14/2016	11:16:50	1:20	2022	51.72	34.89	33.24	51.45	37.72	34.07	33.63	20.45
81	10/14/2016	11:17:50	1:21	2022	52	34.88	33.52	51.63	37.99	34.35	33.69	20.67
82	10/14/2016	11:18:50	1:22	2026	52.26	35.2	33.74	52.05	38.34	34.59	33.85	20.6
83	10/14/2016	11:19:50	1:23	2026	52.43	35.35	33.69	52.25	38.46	34.48	33.91	20.48
84	10/14/2016	11:20:50	1:24	2026	52.8	35.44	34	52.59	38.91	34.82	34.13	20.59

85	10/14/2016	11:21:50	1:25	2026	52.86	35.64	34.11	52.82	38.92	34.87	34.28	20.3
86	10/14/2016	11:22:50	1:26	2026	53.41	36.14	34.25	52.99	39.1	35.19	34.43	20.6
87	10/14/2016	11:23:50	1:27	2026	53.37	35.73	34.4	53.34	39.23	35.38	34.6	20.41
88	10/14/2016	11:24:50	1:28	2018	53.99	36.17	34.63	53.61	39.45	35.41	34.97	20.62
89	10/14/2016	11:25:50	1:29	2022	53.82	36.34	34.76	53.84	39.7	35.71	34.94	20.62
90	10/14/2016	11:26:50	1:30	2022	54.18	36.37	34.87	54.12	39.86	35.72	34.98	20.66
91	10/14/2016	11:27:50	1:31	2022	54.62	36.74	35.1	54.35	39.9	36.01	35.26	20.66
92	10/14/2016	11:28:50	1:32	2026	54.81	36.87	35.14	54.58	40.26	36.18	35.42	20.48
93	10/14/2016	11:29:50	1:33	2018	55.1	36.99	35.38	54.79	40.38	36.34	35.5	20.69
94	10/14/2016	11:30:50	1:34	2018	55.26	37.22	35.5	54.94	40.74	36.56	35.73	20.66
95	10/14/2016	11:31:50	1:35	2018	55.36	37.22	35.73	55.47	40.86	36.65	35.92	20.59
96	10/14/2016	11:32:50	1:36	2018	55.83	37.53	35.74	55.61	40.89	36.79	36.21	20.5
97	10/14/2016	11:33:50	1:37	2026	55.78	37.72	35.79	55.72	41.08	37.12	36.46	20.62
98	10/14/2016	11:34:50	1:38	2018	56.08	37.98	36.02	56.06	41.46	37.16	36.38	20.55
99	10/14/2016	11:35:50	1:39	2026	56.24	37.88	36.33	56.32	41.55	37.53	36.42	20.65
100	10/14/2016	11:36:50	1:40	2022	56.54	38.14	36.36	56.48	41.66	37.42	36.69	20.48
101	10/14/2016	11:37:50	1:41	2022	56.78	38.1	36.58	56.62	41.84	37.56	36.86	20.43
102	10/14/2016	11:38:50	1:42	2018	56.97	38.37	36.84	56.89	42.01	37.75	37.06	20.83
103	10/14/2016	11:39:50	1:43	2022	57.13	38.63	36.91	57.21	42.33	38.08	37.13	20.75
104	10/14/2016	11:40:50	1:44	2018	57.5	38.78	37.01	57.37	42.35	38.32	37.34	20.6
105	10/14/2016	11:41:50	1:45	2018	57.79	38.77	36.99	57.71	42.51	38.34	37.37	20.6
106	10/14/2016	11:42:50	1:46	2022	57.83	39.14	37.06	57.76	42.7	38.58	37.51	20.52
107	10/14/2016	11:43:50	1:47	2022	58.11	39.17	37.26	58.22	42.98	38.39	37.54	20.68
108	10/14/2016	11:44:50	1:48	2018	58.34	39.2	37.57	58.38	43.29	38.39	37.8	20.91
109	10/14/2016	11:45:50	1:49	2018	58.6	39.42	37.48	58.49	43.14	38.76	38.02	20.81
110	10/14/2016	11:46:50	1:50	2022	58.78	39.55	37.8	58.76	43.42	38.93	37.96	20.78
111	10/14/2016	11:47:50	1:51	2018	58.95	39.69	37.82	58.89	43.52	38.99	38.17	20.69
112	10/14/2016	11:48:50	1:52	2018	59.11	39.89	37.98	59.18	43.74	39.19	38.21	20.66
113	10/14/2016	11:49:50	1:53	2014	59.2	40.09	38.1	59.58	44.07	39.28	38.2	20.58
114	10/14/2016	11:50:50	1:54	2014	59.49	39.93	38.27	59.54	44.13	39.33	38.45	20.57
115	10/14/2016	11:51:50	1:55	2014	59.88	40.28	38.39	59.89	44.33	39.49	38.43	20.66
116	10/14/2016	11:52:50	1:56	2014	59.93	40.49	38.43	59.97	44.52	39.64	38.65	20.74
117	10/14/2016	11:53:50	1:57	2014	60.19	40.53	38.55	60.06	44.52	39.85	38.88	20.77
118	10/14/2016	11:54:50	1:58	2014	60.45	40.49	38.87	60.55	44.62	39.87	39.06	20.71
119	10/14/2016	11:55:50	1:59	2014	60.39	40.78	38.81	60.76	44.92	40.18	39.26	20.59
120	10/14/2016	11:56:50	2:00	2014	60.71	41	38.83	60.76	45.02	39.48	39.1	20.87
121	10/14/2016	11:57:50	2:01	2014	60.84	40.96	38.97	61.05	44.84	39.07	39.31	20.81
122	10/14/2016	11:58:50	2:02	2018	61	41.08	39.07	61.25	44.87	39.19	39.32	20.75
123	10/14/2016	11:59:50	2:03	2018	61.1	41.29	39.25	61.51	45.16	38.93	39.75	20.67
124	10/14/2016	12:00:50	2:04	2018	61.33	41.2	39.45	61.52	45.31	39.15	39.85	20.83
125	10/14/2016	12:01:50	2:05	2022	61.7	41.55	39.45	61.72	45.3	39.16	39.97	20.86
126	10/14/2016	12:02:50	2:06	2018	61.66	41.52	39.64	62.11	45.51	39.25	39.92	20.58
127	10/14/2016	12:03:50	2:07	2014	61.96	41.83	39.69	62.27	45.55	39.35	40.05	20.67
128	10/14/2016	12:04:50	2:08	2014	62.22	42.01	39.93	62.34	45.86	39.45	40.08	20.71
129	10/14/2016	12:05:50	2:09	2014	62.17	41.99	40.04	62.63	45.82	39.5	40.26	20.71
130	10/14/2016	12:06:50	2:10	2014	62.36	42.13	40.11	62.67	45.97	39.63	40.5	20.65
131	10/14/2016	12:07:50	2:11	2014	62.68	41.96	40.14	62.89	46.24	39.99	40.74	20.71
132	10/14/2016	12:08:50	2:12	2014	62.83	42.26	40.24	63.03	46.29	40.02	40.66	20.76
133	10/14/2016	12:09:50	2:13	2014	62.85	42.15	40.43	63.32	46.57	40.07	40.61	20.88
134	10/14/2016	12:10:50	2:14	2014	63.28	42.65	40.3	63.39	46.61	40.18	40.91	20.73
135	10/14/2016	12:11:50	2:15	2014	63.39	42.71	40.6	63.72	46.69	40.05	40.99	20.83
136	10/14/2016	12:12:50	2:16	2014	63.52	42.63	40.75	63.78	46.67	40.47	40.95	20.71
137	10/14/2016	12:13:50	2:17	2014	63.62	42.81	40.94	63.86	46.73	40.34	41.03	20.76
138	10/14/2016	12:14:50	2:18	2014	63.85	42.9	40.94	63.89	46.89	40.51	41.22	20.83
139	10/14/2016	12:15:50	2:19	2014	64.11	43.19	41.24	64.24	47.14	40.48	41.35	20.78
140	10/14/2016	12:16:50	2:20	2022	64.24	43.21	41.1	64.43	47.18	40.49	41.28	20.75
141	10/14/2016	12:17:50	2:21	2014	64.53	43.25	41.13	64.56	47.31	40.8	41.57	20.82
142	10/14/2016	12:18:50	2:22	2014	64.42	43.43	41.29	64.77	47.24	40.85	41.61	20.76
143	10/14/2016	12:19:50	2:23	2014	64.69	43.57	41.38	64.76	47.56	40.81	41.74	20.89
144	10/14/2016	12:20:50	2:24	2014	64.93	43.51	41.62	64.99	47.66	40.84	41.68	20.86
145	10/14/2016	12:21:50	2:25	2014	65.15	43.67	41.64	65.32	47.7	40.99	41.92	20.95
146	10/14/2016	12:22:50	2:26	2014	65.2	43.75	41.9	65.39	48.01	41.31	42.15	20.86
147	10/14/2016	12:23:50	2:27	2018	65.3	43.92	41.78	65.59	47.88	41.12	42.19	20.75
148	10/14/2016	12:24:50	2:28	2014	65.68	44.14	41.78	65.73	48.43	41.26	42.02	20.82
149	10/14/2016	12:25:50	2:29	2014	65.59	43.89	41.96	65.69	48.17	41.28	42.09	20.69
150	10/14/2016	12:26:50	2:30	2014	65.71	44.24	42.07	66.06	48.37	41.42	42.34	20.72
151	10/14/2016	12:27:50	2:31	2018	65.94	44.31	42.19	66.23	48.33	41.58	42.33	20.91
152	10/14/2016	12:28:50	2:32	2014	66.06	44.31	42.29	66.43	48.56	41.82	42.3	20.75
153	10/14/2016	12:29:50	2:33	2014	66.15	44.53	42.39	66.55	48.72	41.76	42.53	20.78
154	10/14/2016	12:30:50	2:34	2014	66.27	44.52	42.54	66.59	48.88	41.96	42.63	20.93
155	10/14/2016	12:31:50	2:35	2014	66.42	44.69	42.51	66.69	48.82	41.99	42.79	20.9
156	10/14/2016	12:32:50	2:36	2014	66.61	44.79	42.54	66.95	48.98	42.14	42.89	20.91
157	10/14/2016	12:33:50	2:37	2014	66.91	44.98	42.79	66.96	49.15	42.22	42.98	20.83
158	10/14/2016	12:34:50	2:38	2014	66.81	45.01	42.73	67.39	49.09	42.34	42.92	20.93
159	10/14/2016	12:35:50	2:39	2014	66.95	45.02	42.95	67.29	49.22	42.31	43.04	20.73
160	10/14/2016	12:36:50	2:40	2014	67.08	45.14	42.83	67.55	49.35	42.34	43.32	20.96
161	10/14/2016	12:37:50	2:41	2014	67.37	45.08	43.14	67.72	49.44	42.44	43.27	20.81
162	10/14/2016	12:38:50	2:42	2014	67.41	45.24	43.29	67.74	49.5	42.46	43.42	20.87
163	10/14/2016	12:39:50	2:43	2014	67.45	45.17	43.24	67.88	49.7	42.75	43.55	21.02
164	10/14/2016	12:40:50	2:44	2014	67.76	45.37	43.22	68.1	49.77	42.76	43.8	20.85
165	10/14/2016	12:41:50	2:45	2014	67.94	45.57	43.24	68.12	49.9	42.76	43.55	20.72
166	10/14/2016	12:42:50	2:46	2014	68.07	45.52	43.41	68.41	50.02	42.97	43.75	20.96
167	10/14/2016	12:43:50	2:47	2014	68.26	45.69	43.46	68.63	50.03	43.04	43.87	20.88
168	10/14/2016	12:44:50	2:48	2014	68.36	45.85	43.62	68.53	50.09	42.94	43.66	21.08
169	10/14/2016	12:45:50	2:49	2014	68.56	45.72	43.69	68.78	50.15	43.05	43.84	20.87
170	10/14/2016	12:46:50	2:50	2006	68.37	45.88	43.7	69.03	50.26	43.24	44.16	20.88
171	10/14/2016	12:47:50	2:51	2014	68.72	46.05	43.79	68.96	50.38	43.19	44.09	21.06
172	10/14/2016	12:48:50	2:52	2014	68.73	45.91	43.76	69.14	50.5	43.17	44.13	20.93

APPENDIX I: 2030A at 1 day 2 hours Data

Sample	Date	Time	Time Int.	Time (h)	Current	Cycle	Tb_conc	Tb_ins (°C)	Tb_jac (°C)	Ta_conc	Ta_ins (°C)	Ta_jac (°C)	Temp_j	Ambient (°C)
0	10/21/2016	9:57:32	0:00	0	0	1	19.82	19.85	20.41	20.31	19.77	20.42	20.97	20.13
1	10/21/2016	9:58:32	0:01	1	0	1	20.33	20.16	20.36	20.37	19.83	20.31	20.81	20.03
2	10/21/2016	9:59:32	0:02	2	2010	1	20.74	19.91	20.22	21.08	19.83	20.25	20.86	20.12
3	10/21/2016	10:00:32	0:03	3	2014	1	21.9	19.93	20.16	21.48	19.76	20.28	20.77	20.15
4	10/21/2016	10:01:32	0:04	4	2006	1	22.74	19.99	20.28	22.15	19.94	20.25	20.87	20.04
5	10/21/2016	10:02:32	0:05	5	2010	1	23.63	19.98	20.34	22.8	20.01	20.2	20.74	20.14
6	10/21/2016	10:03:32	0:06	6	2010	1	24.41	19.91	20.19	23.39	20.16	20.11	21.02	20.07
7	10/21/2016	10:04:32	0:07	7	2010	1	25.19	20.13	20.24	23.89	20.37	20.17	20.94	20.11
8	10/21/2016	10:05:32	0:08	8	2006	1	25.43	20.26	20.32	24.64	20.5	20.25	20.89	20.23
9	10/21/2016	10:06:32	0:09	9	2006	1	26.37	20.43	20.41	24.98	20.56	20.37	20.79	20.22
10	10/21/2016	10:07:32	0:10	10	2010	1	27.73	20.58	20.41	25.66	20.71	20.4	20.96	20.17
11	10/21/2016	10:08:32	0:11	11	2010	1	27.61	20.8	20.46	26.31	20.97	20.47	20.97	20.14
12	10/21/2016	10:09:32	0:12	12	2010	1	28.79	20.89	20.4	26.68	21.12	20.54	21.08	20.07
13	10/21/2016	10:10:32	0:13	13	2010	1	29.14	20.78	20.68	27.36	21.34	20.66	21.27	20.13
14	10/21/2016	10:11:32	0:14	14	2006	1	29.73	20.96	20.63	27.81	21.7	20.88	21.39	20.19
15	10/21/2016	10:12:32	0:15	15	2006	1	30.29	21.26	20.93	28.2	21.89	21.07	21.53	20.26
16	10/21/2016	10:13:32	0:16	16	2010	1	30.93	21.49	21.12	28.9	22.01	21.02	21.39	20.19
17	10/21/2016	10:14:32	0:17	17	2010	1	31.27	21.55	21.21	29.26	22.26	21.19	21.58	20.04
18	10/21/2016	10:15:32	0:18	18	2006	1	32.07	21.7	21.35	29.73	22.45	21.22	21.86	20.15
19	10/21/2016	10:16:32	0:19	19	2006	1	32.46	21.95	21.57	30.18	22.65	21.52	22.04	19.98
20	10/21/2016	10:17:32	0:20	20	2006	1	32.65	22.41	21.76	30.68	23.06	21.62	22.42	20.29
21	10/21/2016	10:18:32	0:21	21	2010	1	33.32	22.48	21.85	31.03	23.22	21.19	22.29	20.1
22	10/21/2016	10:19:32	0:22	22	2006	1	33.66	22.63	22.14	31.68	23.59	22.02	22.47	20.42
23	10/21/2016	10:20:32	0:23	23	2010	1	34.62	22.93	22.17	31.98	23.69	22.35	22.78	20.16
24	10/21/2016	10:21:32	0:24	24	2050	1	34.99	23.06	22.48	32.41	24.03	22.38	22.97	19.99
25	10/21/2016	10:22:32	0:25	25	2050	1	35.53	23.12	22.67	33.1	24.55	22.61	23.09	20.17
26	10/21/2016	10:23:32	0:26	26	2046	1	35.73	23.34	22.81	31.65	24.59	22.91	23.26	20.26
27	10/21/2016	10:24:32	0:27	27	2050	1	36.48	23.68	23.11	33.9	24.93	22.92	23.4	20.24
28	10/21/2016	10:25:32	0:28	28	2050	1	36.76	23.93	23.25	34.23	24.98	23.19	23.77	20.38
29	10/21/2016	10:26:32	0:29	29	2046	1	37.48	24.3	23.47	34.72	25.3	23.44	23.74	20.14
30	10/21/2016	10:27:32	0:30	30	2046	1	37.73	24.58	23.68	34.99	25.63	23.68	24	20.1
31	10/21/2016	10:28:32	0:31	31	2046	1	38.23	24.64	23.86	35.47	25.89	23.94	24.27	20.35
32	10/21/2016	10:29:32	0:32	32	2050	1	38.56	25	24.08	35.94	26.13	24.15	24.48	20.23
33	10/21/2016	10:30:32	0:33	33	2046	1	38.83	25.29	24.29	36.3	26.36	24.37	24.79	20.22
34	10/21/2016	10:31:32	0:34	34	2046	1	39.48	25.48	24.57	36.84	26.78	24.56	24.96	20.41
35	10/21/2016	10:32:32	0:35	35	2046	1	39.64	25.66	24.78	37.08	27.01	24.65	25.12	20.26
36	10/21/2016	10:33:32	0:36	36	2050	1	40.2	25.78	24.89	37.49	27.25	25.02	25.21	20.2
37	10/21/2016	10:34:33	0:37	37	2046	1	40.47	26.15	25.22	37.86	27.74	25.17	25.57	20.14
38	10/21/2016	10:35:33	0:38	38	2046	1	41.24	26.28	25.44	38.4	27.74	25.39	25.76	20.3
39	10/21/2016	10:36:33	0:39	39	2046	1	41.67	26.92	25.57	38.18	28.16	25.67	26.01	20.5
40	10/21/2016	10:37:33	0:40	40	2046	1	42.12	26.93	25.85	39.21	28.32	25.83	26.25	20.22
41	10/21/2016	10:38:33	0:41	41	2046	1	42.35	26.96	26.06	39.48	28.6	25.91	26.63	20.38
42	10/21/2016	10:39:33	0:42	42	2050	1	42.73	27.51	26.19	39.88	28.94	26.2	26.73	20.45
43	10/21/2016	10:40:33	0:43	43	2050	1	42.73	27.61	26.34	40.38	29.16	26.47	26.84	20.38
44	10/21/2016	10:41:33	0:44	44	2046	1	43.44	27.84	26.62	40.62	29.45	26.45	27.04	20.2
45	10/21/2016	10:42:33	0:45	45	2046	1	43.29	28.01	26.86	40.82	29.65	26.88	27.34	20.23
46	10/21/2016	10:43:33	0:46	46	2050	1	43.45	28.39	27.05	41.4	30.04	27	27.42	20.23
47	10/21/2016	10:44:33	0:47	47	2050	1	43.54	28.51	27.28	41.75	30.12	27.19	27.75	20.05
48	10/21/2016	10:45:33	0:48	48	2046	1	43.95	28.56	27.55	42	30.48	27.45	27.78	20.3
49	10/21/2016	10:46:33	0:49	49	2042	1	44.25	28.84	27.61	42.36	30.79	27.66	28	20.3
50	10/21/2016	10:47:33	0:50	50	2050	1	44.29	29.28	27.93	42.77	30.94	27.78	28.12	20.12
51	10/21/2016	10:48:33	0:51	51	2046	1	44.83	29.46	28.12	42.99	31.32	28.15	28.57	20.59
52	10/21/2016	10:49:33	0:52	52	2050	1	44.83	29.55	28.45	43.47	31.44	28.4	28.68	20.23
53	10/21/2016	10:50:33	0:53	53	2046	1	45.24	30.07	28.61	43.72	31.73	28.54	28.79	20.42
54	10/21/2016	10:51:33	0:54	54	2038	1	45.59	30.26	28.8	44.09	32.1	28.74	28.96	20.47
55	10/21/2016	10:52:33	0:55	55	2050	1	45.76	30.3	28.95	44.57	32.3	28.99	29.29	20.38
56	10/21/2016	10:53:33	0:56	56	2042	1	46.01	30.56	29.2	44.76	32.64	29.15	29.53	20.48
57	10/21/2016	10:54:33	0:57	57	2050	1	46.24	30.83	29.48	45.26	32.7	29.22	29.75	20.5
58	10/21/2016	10:55:33	0:58	58	2046	1	46.88	31.04	29.64	45.43	33.13	29.5	29.77	20.29
59	10/21/2016	10:56:33	0:59	59	2050	1	46.83	31.32	29.85	45.83	33.32	29.68	30.17	20.5
60	10/21/2016	10:57:33	1:00	60	2042	1	47.21	31.65	29.99	46.25	33.6	29.99	30.22	20.62
61	10/21/2016	10:58:33	1:01	61	2050	1	47.49	31.61	30.17	46.46	33.79	30.06	30.33	20.62
62	10/21/2016	10:59:33	1:02	62	2042	1	47.7	31.89	30.54	46.92	34.17	30.29	30.64	20.62
63	10/21/2016	11:00:33	1:03	63	2046	1	48.07	32.11	30.67	47.23	34.18	30.25	30.84	20.23
64	10/21/2016	11:01:33	1:04	64	2046	1	48.49	32.36	30.83	47.57	34.55	30.68	30.99	20.12
65	10/21/2016	11:02:33	1:05	65	2042	1	48.67	32.71	31.04	47.7	34.67	30.86	31.19	20.43
66	10/21/2016	11:03:33	1:06	66	2046	1	49.02	32.76	31.13	48.25	35	30.95	31.43	20.28
67	10/21/2016	11:04:33	1:07	67	2050	1	49.24	32.92	31.29	48.6	35.25	31.17	31.43	20.47
68	10/21/2016	11:05:33	1:08	68	2042	1	49.61	33.24	31.6	48.67	35.5	31.48	31.77	20.21
69	10/21/2016	11:06:33	1:09	69	2050	1	49.87	33.4	31.89	49.15	35.65	31.52	31.93	20.39
70	10/21/2016	11:07:33	1:10	70	2050	1	50.08	33.59	31.85	49.48	35.87	31.86	32.06	20.24
71	10/21/2016	11:08:33	1:11	71	2050	1	50.29	33.88	32.05	49.7	36.18	31.93	32.4	20.43
72	10/21/2016	11:09:33	1:12	72	2046	1	50.71	33.94	32.2	50.03	36.35	32.14	32.44	20.61
73	10/21/2016	11:10:33	1:13	73	2046	1	50.96	34.31	32.35	50.19	36.61	32.34	32.71	20.52
74	10/21/2016	11:11:33	1:14	74	2046	1	51.16	34.43	32.62	50.54	36.86	32.47	32.94	20.59
75	10/21/2016	11:12:33	1:15	75	2050	1	51.55	34.44	32.65	50.88	36.95	32.59	33.04	20.42
76	10/21/2016	11:13:33	1:16	76	2050	1	51.69	34.84	33.05	51.07	37.39	32.81	33.06	20.74
77	10/21/2016	11:14:33	1:17	77	2050	1	52.04	34.95	33.24	51.36	37.47	33.03	33.4	20.55
78	10/21/2016	11:15:33	1:18	78	2046	1	52.33	35.29	33.21	51.88	37.84	33.19	33.88	20.46
79	10/21/2016	11:16:33	1:19	79	2050	1	52.57	35.25	33.59	51.94	37.94	33.4	33.68	20.2
80	10/21/2016	11:17:33	1:20	80	2042	1	52.92	35.46	33.68	52.23	38.23	33.5	33.94	

107	10/21/2016	11:44:33	1:47	107	2046	1	59.4	39.98	37.72	59.02	43.4	37.51	37.97	20.45
108	10/21/2016	11:45:33	1:48	108	2046	1	59.6	40.27	38.04	59.17	43.4	37.58	38.19	20.63
109	10/21/2016	11:46:33	1:49	109	2042	1	59.98	40.12	38.07	59.36	43.58	37.77	38.33	20.56
110	10/21/2016	11:47:33	1:50	110	2042	1	60.09	40.23	38.16	59.67	43.86	37.83	38.54	20.51
111	10/21/2016	11:48:33	1:51	111	2042	1	60.32	40.47	38.33	59.82	44.04	38.06	38.3	20.45
112	10/21/2016	11:49:33	1:52	112	2046	1	60.44	40.63	38.33	60.05	44.17	38.08	38.63	20.42
113	10/21/2016	11:50:33	1:53	113	2046	1	60.72	40.75	38.45	60.35	44.39	38.34	38.69	20.69
114	10/21/2016	11:51:33	1:54	114	2042	1	60.87	40.71	38.78	60.51	44.55	38.37	38.79	20.63
115	10/21/2016	11:52:33	1:55	115	2042	1	61.1	41.06	38.64	60.71	44.68	38.47	39.08	20.6
116	10/21/2016	11:53:33	1:56	116	2042	1	61.3	41.19	38.96	60.92	44.91	38.51	39.07	20.29
117	10/21/2016	11:54:33	1:57	117	2046	1	61.57	41.21	39.2	61.22	44.98	38.65	39.32	20.54
118	10/21/2016	11:55:33	1:58	118	2046	1	61.83	41.24	39.35	61.21	45.22	38.78	39.48	20.42
119	10/21/2016	11:56:33	1:59	119	2046	1	61.79	41.51	39.22	61.51	45.19	38.94	39.51	20.56
120	10/21/2016	11:57:33	2:00	120	2046	1	62.04	41.67	39.35	61.81	45.56	38.95	39.68	20.53
121	10/21/2016	11:58:33	2:01	121	2042	1	62.26	41.85	39.32	61.93	45.65	39.2	39.68	20.63
122	10/21/2016	11:59:33	2:02	122	2042	1	62.45	41.97	39.64	62.03	45.82	39.32	39.77	20.54
123	10/21/2016	12:00:33	2:03	123	2046	1	62.49	42.03	39.69	62.43	45.88	39.32	40.24	20.39
124	10/21/2016	12:01:33	2:04	124	2042	1	62.79	42.12	39.92	62.44	46.14	39.4	40.07	20.57
125	10/21/2016	12:02:33	2:05	125	2046	1	62.99	42.26	39.89	62.67	46.19	39.69	40.09	20.54
126	10/21/2016	12:03:33	2:06	126	2046	1	63.31	42.29	40.09	62.84	46.33	39.74	40.25	20.57
127	10/21/2016	12:04:33	2:07	127	2042	1	63.32	42.39	40.17	63.29	46.68	39.78	40.45	20.54
128	10/21/2016	12:05:33	2:08	128	2042	1	63.64	42.61	40.46	63.25	46.75	39.87	40.43	20.61
129	10/21/2016	12:06:33	2:09	129	2046	1	63.88	42.48	40.4	63.55	46.72	40	40.75	20.77
130	10/21/2016	12:07:33	2:10	130	2042	1	63.91	42.97	40.56	63.73	46.96	40.14	40.91	20.72
131	10/21/2016	12:08:33	2:11	131	2046	1	64.23	42.81	40.75	63.79	47.06	40.43	40.81	20.5
132	10/21/2016	12:09:33	2:12	132	2042	1	64.47	42.97	40.76	64.18	47.26	40.41	41.08	20.56
133	10/21/2016	12:10:33	2:13	133	2046	1	64.61	43.08	40.89	64.34	47.26	40.22	40.98	20.55
134	10/21/2016	12:11:33	2:14	134	2046	1	64.8	43.22	41	64.4	47.45	40.46	41.1	20.62
135	10/21/2016	12:12:33	2:15	135	2042	1	64.8	43.43	41.19	64.61	47.61	40.54	41.42	20.68
136	10/21/2016	12:13:33	2:16	136	2042	1	65.03	43.67	41.3	64.91	47.78	40.79	41.5	20.61
137	10/21/2016	12:14:33	2:17	137	2046	1	65.35	43.46	41.3	64.86	47.65	40.76	41.59	20.56
138	10/21/2016	12:15:33	2:18	138	2046	1	65.36	43.78	41.51	65.43	47.84	41.27	41.68	20.62
139	10/21/2016	12:16:33	2:19	139	2042	1	65.75	44.07	41.46	65.37	47.81	41.05	41.81	20.83
140	10/21/2016	12:17:33	2:20	140	2042	1	65.78	44.18	41.64	65.67	48.09	41.13	41.77	20.5
141	10/21/2016	12:18:33	2:21	141	2042	1	65.95	44.03	41.61	65.54	48.46	41.23	41.84	20.65
142	10/21/2016	12:19:33	2:22	142	2042	1	66.12	44.22	41.64	65.76	48.41	41.39	41.86	20.73
143	10/21/2016	12:20:33	2:23	143	2046	1	66.15	44.28	41.84	66.03	48.54	41.41	41.91	20.59
144	10/21/2016	12:21:33	2:24	144	2046	1	66.38	44.48	42.17	66.29	48.69	41.53	42.26	20.65
145	10/21/2016	12:22:33	2:25	145	2042	1	66.74	44.6	42.19	66.3	48.79	41.71	42.41	20.56
146	10/21/2016	12:23:33	2:26	146	2038	1	66.55	44.6	42.22	66.39	48.71	41.78	42.35	20.55
147	10/21/2016	12:24:33	2:27	147	2046	1	66.74	44.86	42.26	66.83	49.08	41.75	42.51	20.68
148	10/21/2016	12:25:33	2:28	148	2042	1	67.15	44.86	42.45	66.91	49.16	41.92	42.72	20.53
149	10/21/2016	12:26:33	2:29	149	2042	1	67.14	44.96	42.39	67.02	49.3	42.09	42.65	20.78
150	10/21/2016	12:27:33	2:30	150	2046	1	67.1	45.18	42.48	67.14	49.4	42.23	42.87	20.82
151	10/21/2016	12:28:33	2:31	151	2042	1	67.4	45.25	42.76	67.39	49.68	42.3	42.9	20.77
152	10/21/2016	12:29:33	2:32	152	2046	1	67.67	45.17	42.7	67.54	49.72	42.51	42.93	20.85
153	10/21/2016	12:30:33	2:33	153	2042	1	67.63	45.46	42.93	67.71	49.71	42.44	42.89	20.74
154	10/21/2016	12:31:33	2:34	154	2046	1	68.01	45.7	43.11	67.85	49.91	42.55	43.06	20.68
155	10/21/2016	12:32:33	2:35	155	2046	1	68.07	45.41	43.02	67.95	49.95	42.39	43.2	20.66
156	10/21/2016	12:33:33	2:36	156	2046	1	68.29	45.66	43.12	68.16	50.05	42.65	43.23	20.7
157	10/21/2016	12:34:33	2:37	157	2046	1	68.55	45.89	43.28	68.33	50.14	42.8	43.42	20.61
158	10/21/2016	12:35:33	2:38	158	2046	1	68.5	45.92	43.34	68.36	50.37	42.78	43.55	20.71
159	10/21/2016	12:36:33	2:39	159	2046	1	68.68	45.91	43.41	68.7	50.27	43.04	43.32	20.75
160	10/21/2016	12:37:33	2:40	160	2042	1	68.76	46.01	43.57	68.86	50.39	43.16	43.64	20.53
161	10/21/2016	12:38:33	2:41	161	2038	1	68.92	46.11	43.62	69.01	50.78	43.06	43.83	20.46
162	10/21/2016	12:39:33	2:42	162	2042	1	69.13	46.11	43.63	69.16	50.71	43.16	43.82	20.92
163	10/21/2016	12:40:33	2:43	163	2046	1	69.22	46.33	43.54	69.34	50.76	43.34	43.93	20.68
164	10/21/2016	12:41:33	2:44	164	2042	1	69.45	46.33	43.82	69.34	50.83	43.12	43.89	20.64
165	10/21/2016	12:42:33	2:45	165	2042	1	69.45	46.37	43.89	69.56	50.96	43.35	43.96	20.62
166	10/21/2016	12:43:33	2:46	166	2046	1	69.69	46.43	43.9	69.54	51.04	43.24	43.92	20.8
167	10/21/2016	12:44:33	2:47	167	2042	1	69.95	46.47	44.01	69.83	51.05	43.57	43.93	20.77
168	10/21/2016	12:45:33	2:48	168	2042	1	69.85	46.83	44.01	69.93	51.47	43.7	44.28	20.68
169	10/21/2016	12:46:33	2:49	169	2046	1	70.18	46.76	43.93	69.99	51.34	43.56	44.48	20.67
170	10/21/2016	12:47:33	2:50	170	2046	1	70.28	46.83	44.3	70.3	51.48	43.57	44.67	20.7
171	10/21/2016	12:48:33	2:51	171	2046	1	70.36	46.94	44.33	70.23	51.47	43.82	44.37	20.73
172	10/21/2016	12:49:33	2:52	172	2046	1	70.61	47.08	44.5	70.42	51.57	43.79	44.57	20.63
173	10/21/2016	12:50:33	2:53	173	2042	1	70.46	47.09	44.54	70.65	51.88	44.07	44.4	20.64
174	10/21/2016	12:51:33	2:54	174	2042	1	70.72	47.27	44.6	70.66	51.66	43.86	44.75	20.76
175	10/21/2016	12:52:33	2:55	175	2042	1	70.96	47.41	44.62	70.92	51.83	44.11	44.63	20.54
176	10/21/2016	12:53:33	2:56	176	2034	1	71.01	47.44	44.56	71	52.02	44.12	44.95	20.52
177	10/21/2016	12:54:33	2:57	177	2046	1	71.14	47.54	44.7	71.29	52.11	44.39	44.94	20.57
178	10/21/2016	12:55:33	2:58	178	2046	1	71.22	47.46	45.08	71.28	52.25	44.44	44.99	20.63
179	10/21/2016	12:56:33	2:59	179	2046	1	71.19	47.72	44.9	71.49	52.41	44.43	45.14	20.89
180	10/21/2016	12:57:33	3:00	180	2046	1	71.51	47.62	45.01	71.51	52.28	44.6	45.21	20.67
181	10/21/2016	12:58:33	3:01	181	2042	1	71.81	47.76	45.15	71.58	52.53	44.43	45.26	20.79
182	10/21/2016	12:59:33	3:02	182	2050	1	71.85	47.92	45.08	71.84	52.5	44.5	45.36	20.8
183	10/21/2016	13:00:33	3:03	183	2046	1	71.77	47.94	45.15	71.85	52.71	44.83	45.44	20.79
184	10/21/2016	13:01:33	3:04	184	2050	1	71.86	48.01	45.39	72.24	52.9	44.79	45.34	20.61
185	10/21/2016	13:02:33	3:05	185	2050	1	72.29	47.99	45.29	72.27	52.79	44.78	45.46	20.52
186	10/21/2016	13:03:33	3:06	186	2050	1	72.19	48.14	45.4	72.31	53.06	44.83	45.73	20.69
187	10/21/2016	13:04:33	3:07	187	2050	1	72.5	48.1	45.68	72.5	53.12	45.04	45.63	

APPENDIX J: MATLAB Code

```

% This program Calculate the transient ampacity parament of an XLPE cable
%
% Date                Programmer                Revisions
% ----                -
% 05/01/2017          Ansovinus Akumawah          1.0

clear all;
clc;
close all;

U = 138e3;    % Phase voltage
f = 60;      % operating frequency
Uo = U/sqrt(3);    % phase to netural voltage
w = 2*pi*f;
TanP = 0.004;
E = 2.3; % relative permitivity of insulation

% Ambient temperteure
Ta = 20;    % Ambient temperature

% Conductor inital temperature
Cond_Ti = 20;    % Ambient temperature
%-----%
%Copper conductor
A=0.001;    % cross-sectional area(m^2)
Amm=1000;    % cross-sectional area(mm^2)
P_20= 1.7241e-8; %resistivity of copper @ 20oc (ohm.m)
apha_20=3.93e-3; %temp coef @ 20
thetal= 90; %conductor operating temp (oC)
L= 15.25; % Cable length (m)
Cond_OD = 1.610; % Conducctor diameter (inch)
Cond_ODmm = 40.9; % Conducctor diameter (mm)
Cond_iDmm = 0.01; % Conducctor diameter (mm)
Ins_thk = 0.591; % insulation thickness (inch)
Ins_thkmm = 15.0114; % insulation thickness (mm)
Ins_ID = 2.81; % insulation inner diameter (inch)
Ins_IDmm = 71.39; % insulation inner diameter (mm)
Ins_IDm = Ins_IDmm/1000; % insulation inner diameter (m)
Ins_OD = 3.402; % insulation Outter diameter (inch)
Ins_ODmm = 86.4; % insulation Outter diameter (mm)
Ins_ODm = Ins_ODmm/1000; % insulation Outter diameter (m)
jac_ID = 3.79; % Jack inner diameter (inch)
jac_IDmm = 96.2; % Jack inner diameter (mm)
jac_IDm = jac_IDmm/1000; % Jack inner diameter (m)
jac_OD = 4.1; % Jack Outter diameter (inch)
jac_ODmm = 104.3; % Jack Outter diameter (mm)
jac_ODm = jac_ODmm/1000; % Jack Outter diameter (m)

%-----%

% Cable Capacitance (F)

C= E*1e-9/(18*log(Ins_ODmm/Cond_ODmm)); % capacitance

```

```

%-----
%Cable Resistance

Rdc = (1.02e6*P_20*L/Amm)*(1+apha_20*(thetal-20)); %DC resistance @ L

%skin effect
ks=1; % conductor type (rounnd,stranded)
xs= sqrt((8*pi*f*ks*1e-7/Rdc));
xs_4= xs^4;
ys= xs_4/(192+0.8*xs_4); %skin effect factor

%proximity effect
kp=1; % conductor type (rounnd,stranded)
xp=sqrt((8*pi*f*kp*1e-7/Rdc));
xp_4= xp^4;

s= Cond_ODmm+Ins_thkmm; %distance between conductor axes (mm)
d = 103.3; % mean diameter of the sheath
yp= (xp_4/(192+0.8*xp_4))*(Cond_ODmm/s)^2*2.9; %proximity effect factor

% AC resistance
Rac = Rdc*(1+ys+yp); % AC resistance

%cross-sectional area of sheath
Asl=(pi/4)*(jac_IDmm^2-Ins_ODmm^2); %cross-sectional area of sheath wires

% sheath AC resistance
Rsl = (1.02e6*P_20/Asl)*(1+apha_20*(thetal-20))*L; % sheath AC resistance

% Mutual reactance of sheath wires (trefoil)

Xsl = (2*w*1e-7)*log((2*s)/d); % Mutual reactance of sheath wires (trefoil)

%Loss Factor

lamdal = (Rsl/Rac)*(1/(1+(Rsl/Xsl)^2)); % loss factor

%-----
% Thermal Capacitance of conductor Cth_c (J/oC)
V_c=A*L; %Volum of the whole cable length (m^3)
Cp_c=390; %Specific Heat of copper (J/kg.oC)
Den_cp=8900; %Density of copper (kg/m^3)

Cth_c =V_c*Cp_c*Den_cp; % (J/oC)

% Thermal Capacitance of insulation Cth_in (J/oC)
V_in=(pi/4)*(Ins_ODm^2-Ins_IDm^2)*L; %Volum of the whole insulation length (m^3)
Cp_in=2.4e+6; %Specific Heat of XLPE (J/kg.oC)
Den_in=922; %Density of XLPE (kg/m^3)

Cth_in =V_in*Cp_in*Den_in; % (J/oC)

% Thermal Capacitance of Jacket Cth_j (J/oC)
V_j=(pi/4)*(jac_ODm^2-jac_IDm^2)*L; %Volum of the whole jacket length (m^3)
Cp_j=2.4e+6; %Specific Heat of jacket (J/kg.oC)

```

```

Den_ja=962; %Density of jacket (kg/m^3)

Cth_j =V_j*Cp_j*Den_ja; %(J/oC)
%-----
%Thermal Resistance Rth (oC/W)

%Thermal Resistance condutor T0 %(oC/W)
k_c=400; %thermal conductivity of copper (W/oC.m)

Rth_c1 = L/(k_c*A); %(oC/W)

Rth_c = 0.0295;

% Rth_c2 = (log(Cond_ODmm/Cond_IDmm)/(2*pi*k_c*L));

T0 = Rth_c1;

%Thermal Resistance Insulation T1, Rth_in (oC/W)

k_ins=3.5; %Thermal Resistivity of the insulation (oC m/W)

Rth_in = (log(Ins_ODmm/Cond_ODmm)*k_ins/(2*pi*L));

T1 = Rth_in;

%Thermal Resistance Insulation T2, Rth_sl (oC/W)

Rth_sl = 0;

T2 = Rth_sl;

%Thermal Resistance jack T3, Rth_j (oC/W)

k_jac= 3.5; %Thermal resistivity of the Jack (oC m/W)

Rth_j = (log(jac_ODmm/jac_IDmm)*k_jac/(2*pi*L));%

T3 = Rth_j;

% Thermal Resistance of Air @ raduis 2.43m
%Heat transfer coeff.of air (W/oC m^2)
h = 10;
Aair = L^2/(4*pi);

T4_air= 1/(h*18.55);

T4= T4_air;
%-----
% Define the Load currennt
% I = 900;
I = 1530;
% I = 2030;
% I = 2070;

% Define the time lapse that we're going to explore
% Test duration in munite (m)

```

```

% Define Load Current Duration in munite (m)
% I_on = 60;
% I_on = 200;
I_on = 695;
% I_on = 750;
% I_on = 813;
% I_on = 900;
% I_on = 1000;

t_max = I_on*2;

% Defining current vector
I1 = zeros(1,t_max+2);
I1(2:I_on)=I;
%I1(700:1000)=I;
%I1(1100:1200)=I;

% Ic=I.^2;
%-----
t1 = 0:I_on;
t2 = 1:(t_max-I_on+1);
t = [t1 I_on+t2];
%-----
% Conductor copper losses

Wc= I.^2*Rac;

% Dielectric Losses
Wd = w*C*Uo^2*TanP;

%Time constant

tau_c = ((T0+T1+T3+T4)*(Cth_c+Cth_in+Cth_j))*1e-4/3600;

%Measured tau
% tau_c1 = 114;
% tau_in = 113;
%-----
% insulation time delay

i_delay = tau_c/8;
%-----

% calculate the temperature on the conductor

tc = (Wc+(0.5*Wd))*T1 + ((Wc*(1+lamda1+Wd))*(T3+T4));% conductor temperature at ss

Tc = tc.*(1 - exp(-t1/tau_c))+ Cond_Ti; % Cond temp in f(t)

Tc1 = tc.*(1 - exp(-t1/tau_c));

%conductor cooling
Tc2 = Tc1(end);

Tco = Tc2.*exp(-t2/tau_c)+Cond_Ti;

Tcond = [Tc Tco];

```

```

%-----
% Insulation temperature rise
t_in = (Wc*(1+lamdal)+Wd)*(T1+T3);
tin = t_in; %
Tin= tin.*(1-exp(-t1/tau_c))+ Cond_Ti;
% Tin(1:10)=Cond_Ti;
Tin1 = tin.*(1-exp(-t1/tau_c));
%Insulation cooling
Tin2 = Tin1(end);
Tin_cool = Tin2.*exp(-t2/tau_c)+ Cond_Ti;
Tinsulation = [Tin Tin_cool];
%-----
% Jack temperature rise
t_j = (Wc+(0.5*Wd))*T1;
tj= t_j;
Tj= tj.*(1-exp(-t1/tau_c))+Cond_Ti;
Tj1= tj.*(1-exp(-t1/tau_c));
%Jacket cooling
Tj2 = Tj1(end);
Tj_cool = (Tj2.*exp(-t2/tau_c))+ Cond_Ti;
Tjacket = [Tj Tj_cool];

```